

*Life and dreams are leaves of the same book, reading them in order is living, skimming through
them is dreaming
(Arthur Schopenhauer)*

*Non t'ama chi amor ti dice ma t'ama chi guarda e tace
(W. Shakespeare).*



**Università
degli Studi
di Ferrara**

DOCTORAL COURSE IN CHEMISTRY

CYCLE XXXII

DIRECTOR Prof. Alberto Cavazzini

**Design, synthesis, characterization and investigation of structure-activity
relationships on antioxidants and/or uv filtering properties of new potential
sunscreen molecules**

Scientific/Disciplinary Sector (SDS) CHIM/08

Candidate

Dott. Serra Elena

Supervisor

Prof. Manfredini Stefano

Co-Supervisor

Dr. Andreotti Daniele

Years 2016/2020

Table of contents

1. Introduction	5
1.1 The Electromagnetic Spectrum	6
1.2 Effect of UV radiation on the skin	8
2. Antioxidant and Sunscreen	12
2.1 Skin UV photodamage: causes & consequences.....	13
2.2 Endogenous antioxidant	14
2.2.1 Antioxidant Defense Enzymes	15
2.2.3 Non-enzymatic antioxidants.....	16
2.2.4 Vitamin E and Its Derivatives	17
2.2.5 Vitamin C and Its Derivatives.....	18
2.2.6 Carotenoids	19
2.2.7 Polyphenols	20
3. UV filters	22
3.1. Mechanism of Sunscreen Action.....	23
3.1.1. The Chemistry and characteristics of organic Ultraviolet Filters	25
3.1.2 Organic Ultraviolet Filters	28
3.1.2.1 UVB filters	28
3.1.2.2 UVA filters	33
3.1.2.3 Organic Broad UV filters	36
3.2. Properties of UV filters	39
3.3 The regulatory frameworks	44
3.4 Safety of the UV absorbers	45
4. Aim	47
4.1 PBSA derivatives	50
4.1.1. Chemistry: Design and Synthesis	50
4.1.2 Group 1: Structures without a linker.....	54
4.1.3. Group 2: Structures with a hydrazone linker	59
4.1.4. Group 3: Tinosorb S derivatives	66
5. Biological discussion.....	71
5.1 Antioxidant capability	71
5.1.1 DPPH Test.....	71
5.1.2 FRAP Test.....	72

5.2 Results	73
6. Conclusions	81
7. Experimental Section.....	82
7.1 General Methods	82
7.2 Synthetic Procedures	85
7.3 Antibiotic susceptibility testing protocol	114
7.3.1. Antimicrobial agents preparation	114
7.3.2. Medium	114
7.3.3. Inoculum preparation	115
7.3.4. Determination of MIC End Points	115
7.4 Antioxidant Assays	116
7.4.1 DPPH (1,1-diphenyl-2-picrylhydrazyl) test	116
7.4.2 Ferric Reducing Antioxidant Power (FRAP) assay	116
7.4.3 Evaluation of filtering parameters of compounds in solution.....	116
7.5 Antiproliferative assay	117
Acknowledgements	118
References	119

Abbreviations

AcOEt: Ethyl acetate

APX: Ascorbate Peroxidase

BLQ: Below limit of quantitation

CAT: Catalase

CPD: Cyclobutane Pyrimidine Dimers

Cy: cyclohexane

DCM: Dichloromethane

2,3-DHP: 2,3-Dihydro-4H-pyran

DMSO: Dimethylsulfoxide

DPPH : 2,2-Diphenyl-1-picryl Hydrazyl

DNA: DeoxyriboNucleic Acid;

DPDT: Disodium Phenyl dibenzimidazole tetrasulfonate

ϵ : molar extinction coefficient (values are expressed in $M^{-1}cm^{-1}$)

Et₂O: Diethyl ether

EtOH: Ethanol

FDA: Food and Drug Administration

Fe₂O₃: Iron Oxide

FRAP: Ferric Reducing Antioxidant Power

GPx: Glutathione Peroxidase

GR: Glutathione Reductase

HCl: Hydrochloric acid

H₃PO₄: Phosphoric acid

LDA: Lithium diisopropylamide

MDA: Malondialdehyde

MED: Minimal Erythematol Dose

NADPH: Nicotinamide Adenine Dinucleotide Phosphate

MeOH: Methanol

NaOH: Sodium Hydroxide

POCl₃: Phosphoryl Chloride

PBSA: 2-Phenyl-1H-Benzimidazole-5-Sulfonic Acid

RNA: RiboNucleic Acid

RNS: Reactive Nitrogen Species

ROS: Reactive Oxygen Species
SOD: Superoxide Dismutase
SPF: Sun Protection Factor
RSS: Reactive Sulfur Species
r.t.: Room temperature
TBDMS-Cl: tert-Butyldimethylsilyl chloride
TiO₂: Titanium Dioxide
TPTZ: 2,4,6-Tris(2-pyridyl)-*s*-Triazine
TsOH: p-Toluenesulfonic acid
UV: Ultraviolet
UVAPF: UVA Protection Factor
ZnO: Zinc oxide

1. Introduction

The sun has always been of vital importance for life on earth. It gives light, warmth, and energy. All vegetation on which life on earth depends is dependent on the sun for carbon and water. Life would be impossible without the sun, but the wrong exposition could reserve undesired surprises. The known negative effects of human exposure to ultraviolet (UV) radiation can be immediate, due mainly to UVB as in the case of sunburn, or long-term, due to UVA causing, in most cases, the formation of oxidizing species responsible for photo-aging, immunosuppression and chronic effects such as photo carcinogenicity. Ultraviolet radiation of sunlight consists of UVA (315–400 nm), UVB (280–315 nm) and UVC (100–280 nm) radiations, depending on the wavelength. Whereas the stratospheric ozone layer completely blocks UVC radiation and UVB wavelengths below 295 nm, 90–95% of the UV radiation that reaches the earth's surface is UVA, with UVB accounting for most of the remainder. At longer wavelengths UVA penetrates deeply into human skin, reaching the basal layer of the epidermis and the inner dermis, interacting with endogenous and exogenous photosensitizers and generating reactive oxygen species (ROS). These ROS are responsible for the onset of DNA mutations related to skin cancer development, of the acceleration of collagen breakdown and of the decrease of collagen synthesis, with consequent appearance of skin fragility and wrinkles.¹ Sunscreens are the most common products used for skin protection against the harmful effects of ultraviolet radiation; they should provide broad-spectrum UV protection due to the presence of active ingredients, which attenuate the transmission of UV radiation onto the skin by absorbing, reflecting or scattering the incident radiation. It is not infrequent to see mixtures of different types of molecules present in commercially available formulations - such combinations are utilised as none of the constituents are individually able to provide broad spectrum UVA-UVB protection. The active molecules can be classified as either “chemical” or “physical” based on their mechanism of action. As the site of action of sunscreens is restricted to the skin surface or to the uppermost part of the stratum corneum, they should not penetrate into the viable epidermis, the dermis and into the systemic circulation. Furthermore, the follicular uptake should be avoided, to prevent penetration into human cells where they can cause deleterious modifications to DNA. The degree of penetration depends strongly on the physico-chemical properties of the active compound, the nature of the vehicle in which the sunscreen is formulated and several factors related to the skin, and indeed, both molecular weight and lipophilicity of the molecule play an important role in cutaneous penetration. It

has also been demonstrated that skin permeation and retention from topical products can differ significantly with the formulation used.¹ Recently, combinations of UV filters with antioxidant agents have been introduced in order to improve photoprotection.

1.1 The Electromagnetic Spectrum

Human skin and hair are constantly subjected to solar radiation.² In order from shorter to longer wavelength the electromagnetic spectrum of the sun is composed of: cosmic rays, gamma rays, X rays, UV radiation (UVC, UVB, UVA), visible light, infrared rays, microwaves and radio waves (Fig.1). Fortunately higher energy rays, such as cosmic rays (below 10^{-16} m) gamma rays (10^{-16} - 10^{-11} m), X rays (10^{-11} - 10^{-8} m) and UVC rays (100-280 nm), are filtered by the stratospheric ozone layer, while the earth's surface is constantly irradiated by the lower frequency light coming from the sun, comprised of 56% infrared waves (wavelength, 780-5000 nm), 39% of visible light (400-780 nm), 4.9% of UVA rays (315-400 nm) and 0.1% of UVB rays (280-315nm).³

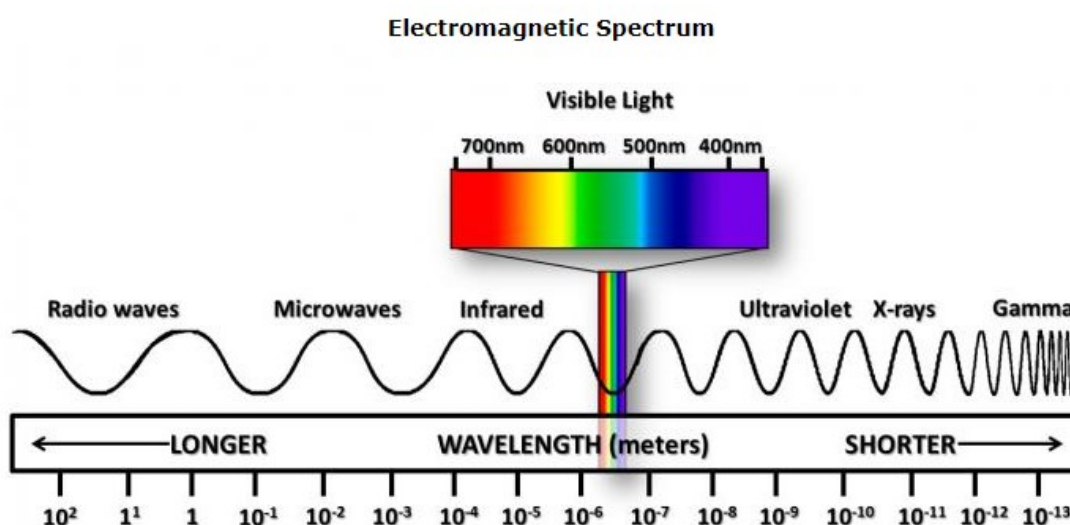


Figure 1.1 The electromagnetic spectrum of radiant energy.

The radiation emitted by the sun is of an electromagnetic character and differs from other forms of electromagnetic radiant energy in its spectrum, as described by its energy (E), Wavelength (λ), or the frequency (ν). The energy of electromagnetic radiation is governed by the following relationship:

$$E=h\nu$$

Where E = energy (ergs), h = Planck's constant = 6.62×10^{-27} erg/s, and ν = frequency (cycles per second [cps] or Hertz [Hz]).

An important physical relationship governing the properties of electromagnetic waves is described by the following equation:

$$\nu = c/\lambda$$

Where c = speed of light = 3.0×10^{10} cm/s and λ = wavelength (cm).

By substituting the second equation into the first, we arrive at the all important equation governing the action of sunlight on humans where the energy (E) and the wavelength (λ) have a reciprocal relationship as shown below:

$$E = hc/\lambda$$

The above relationship reveals that the wavelength increases as the energy associated with it decreases and vice versa. Thus, the UVB region of the spectrum (280-315 nm) will have higher energies associated with it than the UVA region (315-400 nm). The significance of this relationship between energy and wavelength will become more evident when effects of UV radiation on the skin are discussed. The UVA and UVB regions that are not completely filtered out by the ozone layer are sufficiently energetic to cause damage to the skin and hair.⁴ The UVB rays, also called *the burning or erythematous rays*, with wavelengths ranging from 280 to 315 nm, are responsible for most of the immediate damage to the skin, resulting in erythema or sunburn, and subsequent long-term damage if the skin is left unprotected.

The UVA region extends from 315 to 400 nm and is further subdivided into UVA I from 340 to 400 nm and UVA II from 315 to 340 nm. Parish et al.⁵ list many reasons why the UVA rays are extremely important and should be dealt with:

- The amount of solar UVA reaching the earth's surface is enormously greater than that of UVB.
- Photosensitivity reactions (phototoxicity and photoallergy) are mostly mediated by UVA.
- High doses of UVA can cause redness to human skin; moreover, UVA may potentiate or add to the biological effects of UVB.
- The development of sunscreens that effectively block or diminish the highly erythemogenic UVB permits prolonged sun exposures; however, many of these sunscreens do not significantly alter the amount of UVA reaching the skin.

- UVA is transmitted by most window glass and many plastics that do not transmit UVB.
- Recent studies suggest that UVA can affect cells and microorganisms.
- There is experimental and epidemiological evidence to suggest that solar UVA is one of the possible etiological agents for certain kinds of cataracts in humans.

For these and more reasons protection from UVA rays is crucial in any photoprotection regimen.

1.2 Effect of UV radiation on the skin

Human skin is the largest organ of the body. It has different functions, such as the regulation of body temperature and protection from the environment, and it is also associated with biochemical functions such as melanin formation, epinephrine stimulation of the sweat glands and the regeneration of viable epidermal cells.⁶ Skin is composed of three layers: the epidermis, including the stratum corneum, the dermis, and the hypodermis (see Figure 1.2)

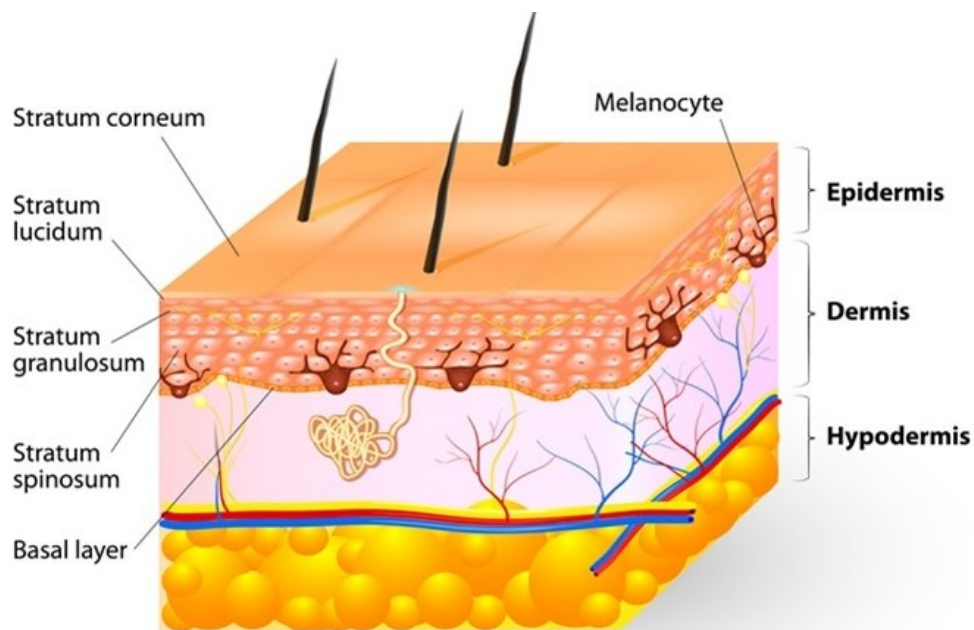


Figure 1.2 The layers of human skin.

The dermis contains melanocytes, which generate the melanin pigment responsible for the colour of the skin. Exposure to rays with wavelengths in the UVA region stimulates the

formation of melanin, which acts as a protective layer on the skin. Radiation with wavelengths longer than 350 nm starts penetrating the dermis thereby stimulating the formation of melanin and producing a tan that protects the skin from immediate sunburn. Although UVA rays are of lower energy than the UVB rays, the fact that they can penetrate further into the hypodermis, causes elastosis (loss of structural support and elasticity of the skin) and other skin damage, potentially leading to the skin cancers we observe rising in epidemic proportions today. UV radiation near 300 nm (UVB) penetrates both the stratum corneum and the epidermis and is sufficiently energetic to cause severe burning or erythema. The incidence of melanoma and non-melanoma skin cancers has continued to rise over the past few decades. The etiology is multifactorial with discrete genetic pathways and environmental factors. Although genetic factors may contribute significantly, environmental factors can be modified to potentially decrease the risk of developing deadly diseases such as melanoma. Exposure to UVR from sunlight is well established as a significant risk factor for melanoma development. A history of sunburn in childhood and continued unprotected exposure to UVR through adolescence and adulthood contribute to skin cancer risk. UVR directly targets macromolecules in the skin such as proteins, lipids, and nucleic acids, with the latter resulting in signature mutations characteristically found in melanomas and other skin cancers. When these mutations occur within genes regulating apoptosis, cell cycle progression, and genetic repair machinery, they may initiate oncogenic transformation.⁷ UVR photoexcitation of the direct chromophore DNA produces excited electron states and toxic by-products, leading to direct and indirect DNA damage (see Figure 1.3).

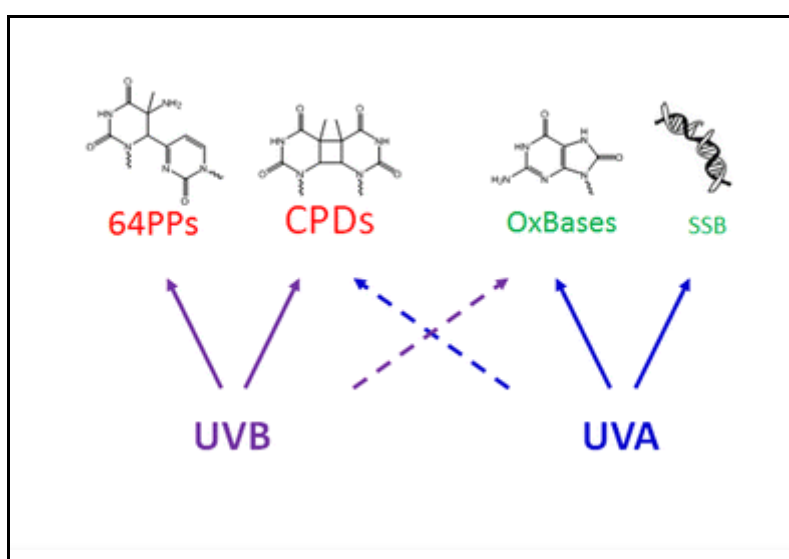


Figure 1.3 UV A/B effects on DNA

This often produces signature mutations dependent on the insult and mechanism of damage. The most energetic part of the solar spectrum at the earth's surface (UVB, 280–315 nm) leads to the formation of cyclobutane pyrimidine dimers (CPDs) (see Figure 1.4) and pyrimidine(6–4)pyrimidone photoproducts (64PPs) (see Figure 1.5).

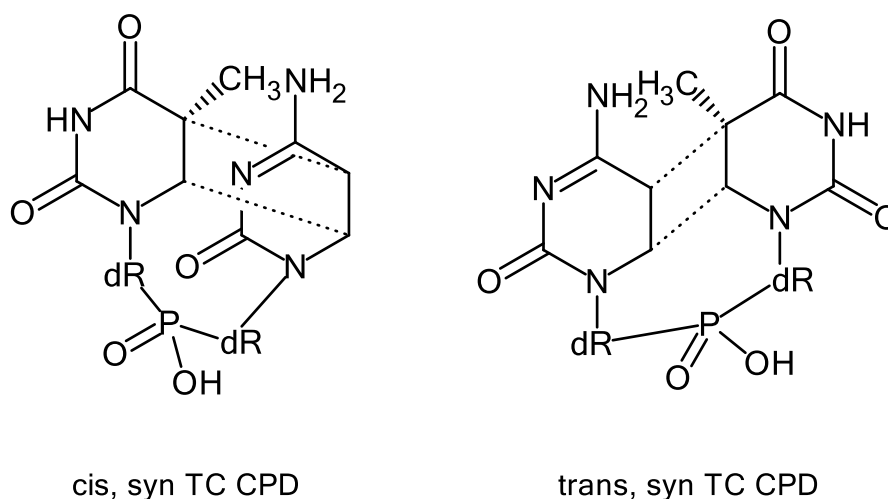


Figure 1.4 Chemical structure of the two isomers of thymine-cytosine cyclobutane pyrimidine dimer (TC CPD) found in DNA. The trans, syn isomer is formed only in single-stranded and destabilized double-stranded DNA dR:2-deoxyribose, P: phosphate.

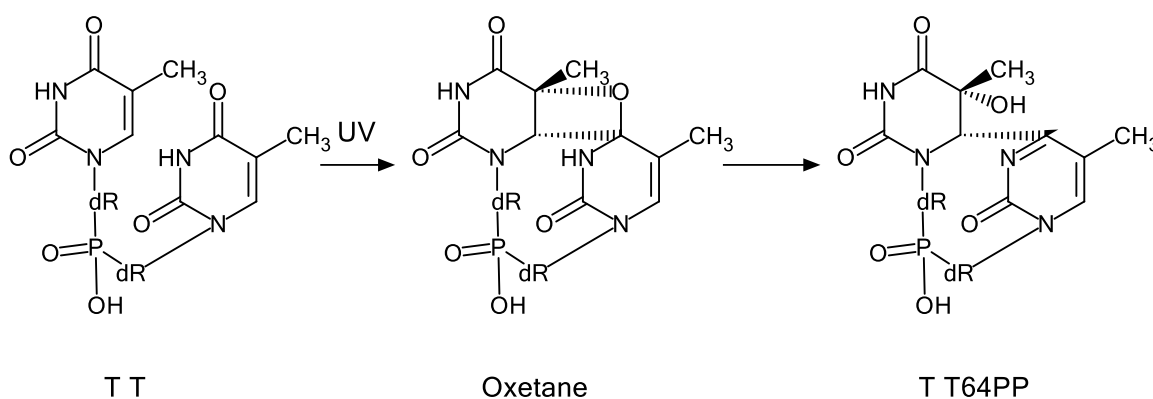


Figure 1.5 Formation of thymine-thymine (TT)64PP with involvement of an oxetane intermediate. In the case of thymine-cytosine (TC) or cytosine-cytosine (CC) 64PPs the oxygen atom of the four-membered ring is replaced by a NH group and the intermediate is an azetidene. dR:2-deoxyribose, P:phosphate.

Less energetic but 20-times more intense UVA (315–400 nm) also induces the formation of CPDs together with a wide variety of oxidatively generated lesions such as single strand

breaks and oxidized bases.⁸ Among those, 8-oxo-7,8-dihydroguanine (8-oxoGua) (see Figure 1.6) is the most frequent since it can be produced via several mechanisms. Efficient repair of DNA damage before replication is a requisite to prevent carcinogenesis to occur. Data available on the respective yield of DNA photoproducts in cells and skin show that exposure to sunlight mostly induces pyrimidine dimers, which explains the mutational signature found in skin tumors, with lower amounts of 8-oxoGua and strand breaks.⁹

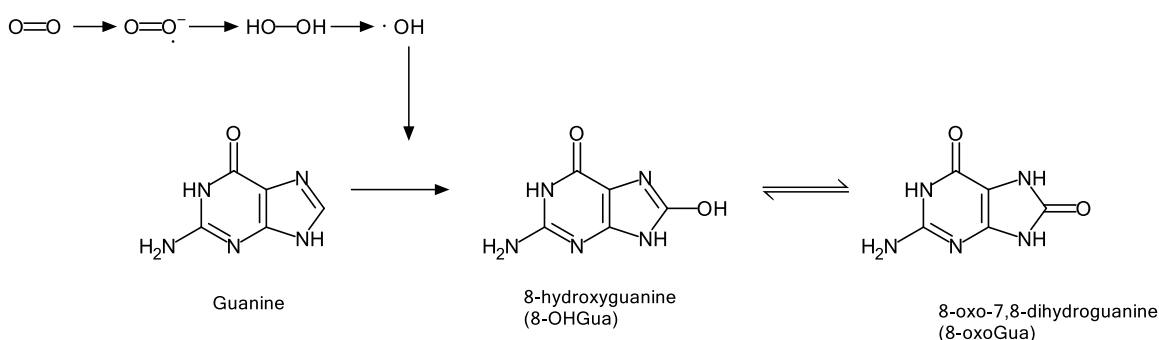


Figure 1.6 Synthesis of 8-oxoGua

Although UVA rays are of lower energy than the UVB rays, the fact that they can penetrate further into the hypodermis, causes elastosis (loss of structural support and elasticity of the skin) and other skin damage, potentially leading to the skin cancers we observe rising in epidemic proportions today.⁴

2. Antioxidant and Sunscreen

Sunlight has an important role as an initiator of photochemical reactions, which give energy that sustains plant life and maintains human health. The relationship that humans have with the sun's exposure is delicately balanced between the positive effects that solar energy provides and the negative aspects that overexposure produces. The benefits of sun exposure include its positive physiological actions, the role it plays in vitamin D metabolism, and the value it has as a therapeutic agent in cutaneous and systemic disease. The negative consequences of overexposure include acute UV-induced erythema (e.g. sunburn), non-melanoma skin cancer (cutaneous squamous cell and basal cell carcinoma), melanoma, photoaging of the skin and UV-induced immunosuppression. The incidence of melanoma of the skin has risen rapidly over the past 30 years, although current trends differ by age. From 2006 to 2015, the rate increased by 3% per year among men and women ages 50 and older, but was stable among those younger than age 50. Every year, more than 100,000 new cases of melanoma are diagnosed in Europe and more than 22,000 European citizens lose their lives to the disease.¹⁰ Although there are many ways in which the adverse effects of overexposure to ultraviolet (UV) radiation can be successfully treated, a much more effective method of handling this problem is through preventive measures. Besides the use of physical protective measures, such as protective clothing and shields, various sunscreens which provide a barrier between the sun and the skin have been developed. In addition, the data that are available suggest that sunscreens are effective at preventing at least some forms of skin cancer and its precursor. Unfortunately, none of the currently available sunscreens have an effect on UV side effects and all of them are inadequate to protect against UVA-induced free radicals in the skin. Thus our interest is to identify new sunscreens which provide broad protection against UVA and UVB and quench the possible formation of reactive oxygen species (ROS) and other free radicals responsible for causing skin cancer and also less severe photoaging changes such as wrinkling, scaling, dryness and hyper-hypopigmentation.

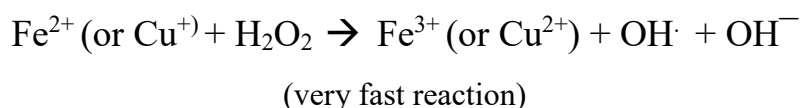
2.1 Skin UV photodamage: causes & consequences

Free radicals are continuously produced in the human organism as a result of cellular metabolism. They play an important role providing a signalling function between the cells and the destruction of viruses and bacteria. Free radicals are also produced in human skin subsequent to its irradiation with UV light, visible light (VIS) and IR light at different efficacies. The ROS are produced following irradiation with UVA and UVB via the absorption of photons by endogenous photosensitive molecules. There are many endogenous chromophores in human skin, which in the presence of UVA radiation can generate ROS. Porphyrins (protoporphyrin, coproporphyrin, and uroporphyrin), flavins (riboflavin), quinone (ubiquinone), and the pyrimidine nicotinamide cofactors (nicotinamide adenine dinucleotide, NADH; and nicotinamide adenine dinucleotide phosphate, NADPH) are examples of common photosensitizers in mammalian cells. Recently, the absorbing chromophore trans-urocanic acid was identified in the epidermises.¹¹ The excited photosensitizer subsequently reacts with oxygen resulting in the generation of ROS including superoxide anion radical and singlet oxygen. Superoxide anion radical and singlet oxygen are also produced by neutrophils that are present in increased quantities in photodamaged skin, and contribute to the overall pro-oxidant state. Superoxide dismutase (SOD) converts superoxide anion radical to hydrogen peroxide. Hydrogen peroxide is able to cross cell membranes easily and, in conjunction with Fe^{2+} , generates highly toxic hydroxyl radicals. Both singlet oxygen and hydroxyl radical can initiate lipid peroxidation (see Figure 2.1).

As a consequence of their high reactivity, ROS react non-specifically with nearly every cellular target and may damage DNA, proteins, lipids, and carbohydrates.

Both UVA and UVB contribute to the deleterious effects on the skin, but it appears that UVB is more associated with autoimmune diseases than UVA. Somewhere, there is a balance between too much sun and melanoma risk or too little sun and autoimmune disease.⁴

Presence of Iron (or Copper) and H_2O_2



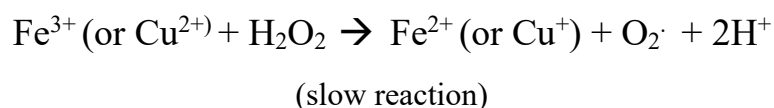


Figure 2.1 The chemistry involved in iron/copper-induced ROS formation

Another important endogenous target for UV are MMPs (matrix metalloproteases). Matrix metalloproteases (MMPs) constitute a family of structurally similar zinc-containing metalloproteases, which are involved in the remodelling and degradation of extracellular matrix (ECM) proteins, such as collagens, elastins, fibronectin, and proteoglycans, both as part of normal physiological processes and in pathological conditions. At this time over 20 different MMPs have been identified and classified. Several studies carried out by Scharffetter-Kochanek's group using dermal fibroblast cells show that both UVA and UVB cause a four- to five fold increase in the production of MMP-1 and MMP-3.^{12,13} Brennan et al. have shown by punch biopsies of human skin after UV irradiation that MMP-1 rather than MMP-13 is the major collagenolytic enzyme responsible for collagen damage in photoaging. In contrast, the synthesis of tissue inhibitory metalloprotease-1 (TIMP-1), the natural inhibitor of matrix metalloprotease, increases only marginally. This imbalance is one of the causes of severe connective tissue damage resulting in photoaging of the skin.

2.2 Endogenous antioxidant

The human organism has developed a protection strategy against the destructive action of the free radicals, in the form of an "antioxidative network". Typical antioxidant substances in the organism include vitamins (A, C, E and D) as well as carotenoids (β -carotene, lycopene and lutein), different enzymes and others. Most of these antioxidants cannot be synthesized by the human organism entirely or in sufficient amounts and the body must be supplemented via consumption of nutritionally rich foods, for instance, fruit and vegetables, cacao, green tea and plant extracts. Interaction of antioxidants with free radicals gives rise to the destruction of the antioxidants and neutralization of the free radicals.

The antioxidative network is responsible for maintaining the equilibrium between pro-oxidants and antioxidants. However, the antioxidant defence can be submerged by

increased exposure to exogenous sources of ROS. The skin has developed a complex system in order to protect itself from oxidative stress that consists of enzymes and non-enzymatic antioxidants. The best endogenous protection of our skin is melanin. Melanin, the pigment deposited by melanocytes, is the first line of defence against DNA damage at the surface of the skin, but it cannot totally prevent skin damage. Additional UV protection includes avoidance of sun exposure, usage of sunscreens, protective clothes, and antioxidant supplements.

2.2.1 Antioxidant Defence Enzymes

Superoxide dismutase (SOD) converts superoxide to hydrogen peroxide and oxygen and minimizes production of the hydroxyl radical that causes so much damage (it is the most potent of the oxygen free radicals). This system is nearly always the antioxidant defence in cells exposed to oxygen. It is extremely quick and can more than match the production of superoxide when working properly.¹⁴

There are three forms of SOD in the human body: copper- and zinc-containing isoform (CuZn-SOD, a cytosolic enzyme), manganese-containing isoform (Mn-SOD, a mitochondrial enzyme), and extracellular SOD (EC-SOD, a tetrameric glycoprotein which contains Cu and Zn). SOD is thought to protect from free radicals produced by the ageing process and ischaemic tissue damage. It also has an effect on inflammation. Mutations in SOD have been linked to familial amyotrophic lateral sclerosis (ALS).¹⁴ As compared to other body tissues, SOD activity is relatively low in the skin. Glutathione peroxidase (GSH-Px) is a selenoenzyme consisting of four identical subunits, each of which contains a selenocysteine residue in its active site. GSH-Px is localized mainly in the cytosol and to a lesser extent in mitochondria.

It converts hydrogen peroxide to water and oxygen and reduces lipid hydroperoxides using glutathione.¹⁵ The baseline levels of GSH-Px measured in epidermis and dermis vary considerably and therefore do not point to a clear preferential distribution in skin.

2.2.3 Non-enzymatic antioxidants

Antioxidants can be subdivided into two groups: endogenous (synthesized in the body) and exogenous (derived from food). Human skin contains both lipophilic antioxidants such as vitamin E (tocopherols and tocotrienols), ubiquinones (coenzyme Q) and carotenoids, and hydrophilic antioxidants such as vitamin C (ascorbate), glutathione (GSH) and uric acid (urate).

Vitamin E, vitamin C, and carotenoids are derived from the diet whereas the other three are synthesized endogenously.⁴ Vitamin C is the predominant antioxidant in skin; its concentration is 15-fold higher than glutathione, 200-fold higher than vitamin E, and 1000-fold higher than ubiquinones.¹⁶ Concentrations of antioxidants are higher in epidermis than dermis; six-fold for vitamin C and glutathione, and two-fold for vitamin E and ubiquinones. Some antioxidants are also present in the stratum corneum, such as vitamin E, which is the predominant antioxidant in the human stratum corneum.¹⁷ The antioxidants present in the stratum corneum are quite susceptible to UV radiation. For example, a single suberythemal dose of UV radiation depleted vitamin E by about 50% while dermal and epidermal vitamin E depletion required much higher doses.¹⁷ Vitamin C is present in human stratum corneum at very low levels, hence it is not available to recycle photo-oxidized vitamin E. Ubiquinones seem to be absent in human stratum corneum.⁴ When the endogenous antioxidants are not present in sufficient quantities to contrast the ROS an exogenous support could help avoid undesirable effects. Direct application of antioxidants onto skin has an advantage over oral administration because targeting antioxidants to the area of skin requiring protection is easier to achieve. It seems desirable to add low molecular weight antioxidants to the skin reservoir by applying antioxidants topically as they protect the skin against oxidative stress. The stratum corneum may particularly benefit from topical application of antioxidants to increase its antioxidant capacity because cutaneous antioxidants undergo depletion significantly under radiation induced oxidative stress. To protect deeper layers of the skin, antioxidants need to be formulated in a way that delivers them into the skin, but it requires an adequate formulation because antioxidants are often hydrolytically and photo-chemically unstable compounds (see Figure 2.2), which is why they function in redox reactions.

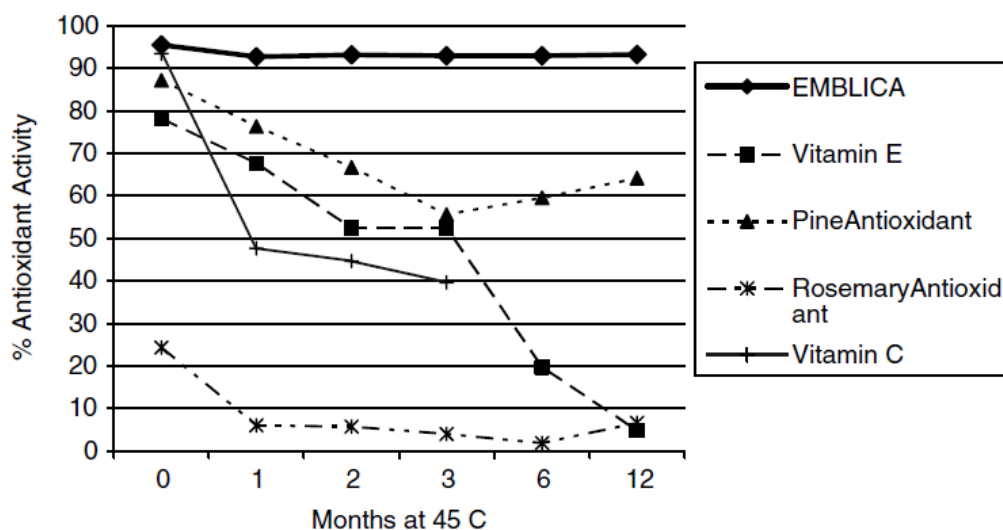


Figure 2.2 Comparison between stability of Emblica and other antioxidants. All antioxidant activities were derived from optical density measurements at 517 nm in an ethanol-water mixture using diphenylpicrylhydrazide method.

2.2.4 Vitamin E and Its Derivatives

Vitamin E is a mixture of four lipid-soluble tocopherols (α , β , γ and δ) and four lipid-soluble tocotrienols (α , β , γ and δ). Tocopherols and tocotrienols differ only in their prenyl side chain (see Figure 2.3). The chromanol head of each is identical with α , β , γ and δ isomers, each containing an essential hydroxyl group necessary for antioxidant activity.

Vitamin E is depleted during oxidative stress and it cannot be regenerated in the absence of a co-antioxidant. Vitamin E is important for protecting the lipid structures of the stratum corneum proteins from oxidation. However, topically applied α -tocopherol is rapidly depleted by UVB radiation in a dose-dependent manner.

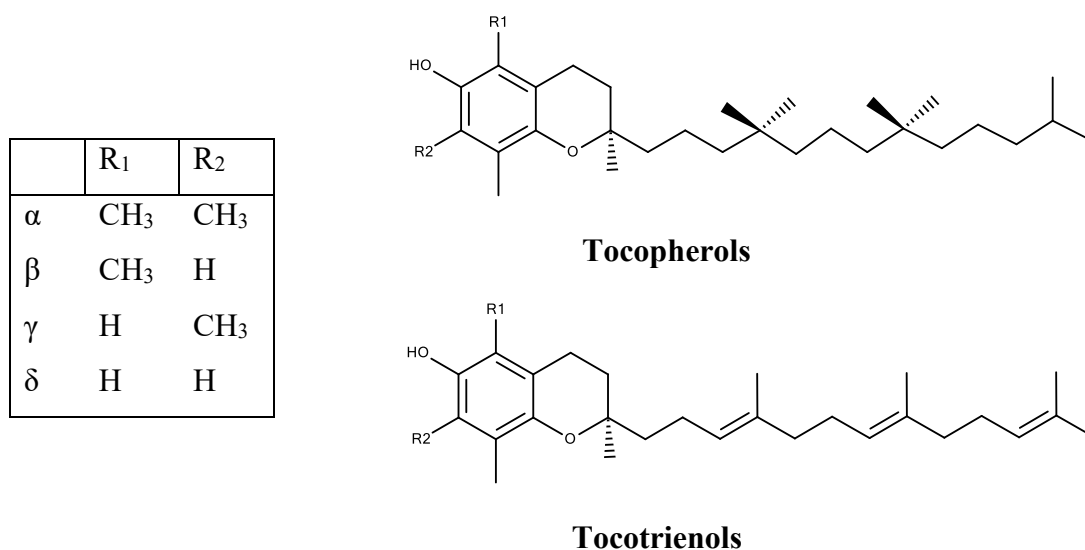


Figure 2.3 Structures of tocopherols and tocotrienols.

The photoprotective effect of Vitamin E and its esters have been studied extensively and the topical application of Vitamin E has shown significant reduction in the acute response after UV-radiation exposure.⁴

2.2.5 Vitamin C and Its Derivatives

Vitamin C¹⁸ (L-ascorbic acid) is a water-soluble micronutrient required for multiple biological functions. It is necessary for normal growth and development, and is an essential enzyme cofactor for several enzymes in the post-translational hydroxylation of collagen, the biosynthesis of carnitine, the conversion of the neurotransmitter dopamine to norepinephrine, peptide amidation, and in tyrosine metabolism. Vitamin C is a potent reducing agent and scavenger of free radicals in biological systems, working as a scavenger of oxidizing free radicals and harmful oxygen-derived species, such as hydroxyl radical, hydrogen peroxide (H₂O₂), and singlet oxygen. A negative aspect of vitamin C is its instability in aqueous solutions, even at neutral pH at room temperature (~25°C). To overcome this problem, a number of stable synthetic derivatives of vitamin C have been developed such as sodium ascorbyl phosphate (SAP) and magnesium ascorbyl phosphate (MAP) but unfortunately both these forms have to be formulated at basic pH due to their instability in acidic media. A chelating agent needs to be included in the formulation to prevent degradation of MAP and SAP; most commercial products do contain EDTA as a

chelating agent. Recently, several clinical studies have been reported on the use of vitamin C at high percentage levels (>5%) and its beneficial effect on skin.¹⁹ Aside from its antiaging and photoprotective effects, vitamin C is also known to be the primary replenisher of vitamin E. Several clinical studies have proved the synergistic antioxidant effect of vitamins C and E in photoprotection. Vitamin C is sensitive to light and is degraded to form dehydroascorbic acid and 2,3-diketogulonic acid upon UV irradiation by photooxidation and subsequent hydrolysis²⁰ (see Figure 2.4).

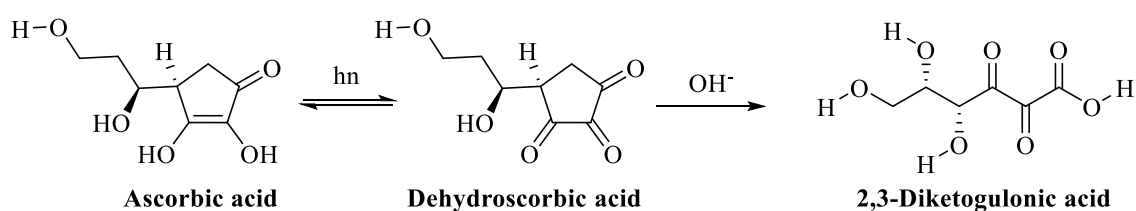


Figure 2.4 Structure of ascorbic acid and its degradation products.

Topical application of 5% vitamin C cream was an effective and well tolerated treatment. It led to a clinically apparent improvement of the photodamaged skin and induced modifications of skin relief and ultrastructure, suggesting a positive influence of topical vitamin C on parameters characteristic for sun-induced skin ageing.¹⁹

2.2.6 Carotenoids

Carotenoids are a class of lipophilic compounds of plant origin that contain an extended system of conjugated double bonds. Currently, 1178 natural carotenoids have been characterized and reported in the literature, which present huge diversity in both structure and physicochemical properties. This number comprises a wide distribution of these biomolecules in approximately 700 source organisms including plants, bacteria, fungi, and algae.

β -Carotene, α -carotene, lycopene, β -cryptoxanthine, lutein, and zeaxanthine are major carotenoids in human skin and their levels differ between various skin areas.²¹ It was demonstrated that a single exposure to solar simulated UV light lowers the skin lycopene level by 31– 46%, whereas the same UV dose has very little effect on the β -carotene level.²² However, repeated exposure to UV light also depletes the β -carotene level.²³

Carotenoids have been reported to react with virtually any radical species. Carotenoids are among the most efficient scavengers of singlet oxygen, either by physical or by chemical quenching.²⁴ The products of such reactions are generally short-lived radical species. The most potent antioxidant product of carotenoid oxidation is retinoic acid (RA), formed during the enzymatic cleavage of β -carotene.²⁵ There is some clinical evidence of increased skin cancer incidence in smokers supplemented with β -carotene. In fact, cigarette smoke is a complex mixture of literally thousands of compounds, many of which are known or suspected human carcinogens. β -Carotene oxidation products formed by smoke may be responsible for pro-carcinogenic effects in human. It has recently been shown that 4-nitro- β -carotene is the major product of the reaction between nitrogen oxide in smoke and β -carotene.²⁶(see Figure 2.5).

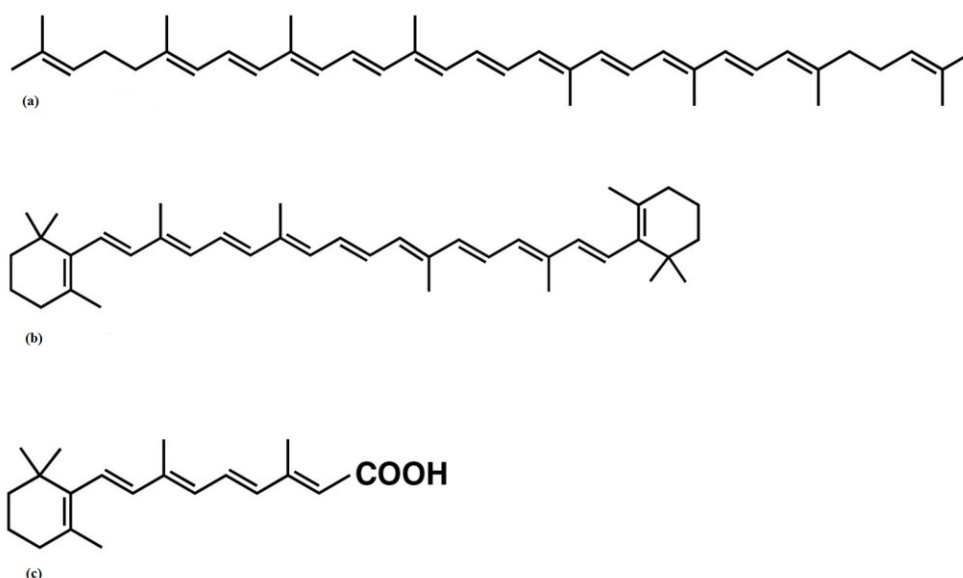


Figure 2.5 Structure of lycopene (a), β -carotene (b), and retinoic acid (c)

2.2.7 Polyphenols

The polyphenol family contains one of the most abundant and extensively studied molecules that naturally occur in the plant kingdom, and innumerable phenolic structures have already been characterised. Polyphenols can be found in fruits, vegetables, nuts, seeds, flowers and tree barks. These components are minor metabolites of the vegetable kingdom and are generally involved in the attraction of pollinators, the execution of structural functions, the defence against ultraviolet radiation and the protection of plants

against microbial invasion and herbivores. Polyphenolics comprise a wide variety of natural products of plant origin.²⁷ Almost all of them exhibit a marked antioxidant activity. Typical examples are oligomeric catechols, flavonoids, monomeric and oligomeric flavan-3-ols (condensed tannins), and gallo- and ellagitannins (hydrolyzable tannins). The tannins are considered superior antioxidants as their eventual oxidation may lead to oligomerization via phenolic coupling and enlargement of the number of reactive sites, a reaction which has never been observed with flavonoids themselves. Many of these plant polyphenolics are consumed in the diet and are believed to have beneficial health effects for human beings. Recently, some polyphenolics have been demonstrated to have significant photoprotective properties when used topically. Administration of different plant extracts, particularly flavonoids (see Figure 2.6), has been reported to reduce acute and chronic skin damage after UV radiation exposure. The antioxidant activity of phenolic compounds depends on the number and the positions of the hydroxyl groups. Polyphenolics are inherently unstable compounds due to aerial oxidation; this allows them to function in redox reactions. In addition, many polyphenolics are deeply coloured, adding to the complexity of producing an aesthetically acceptable product for topical applications.⁴

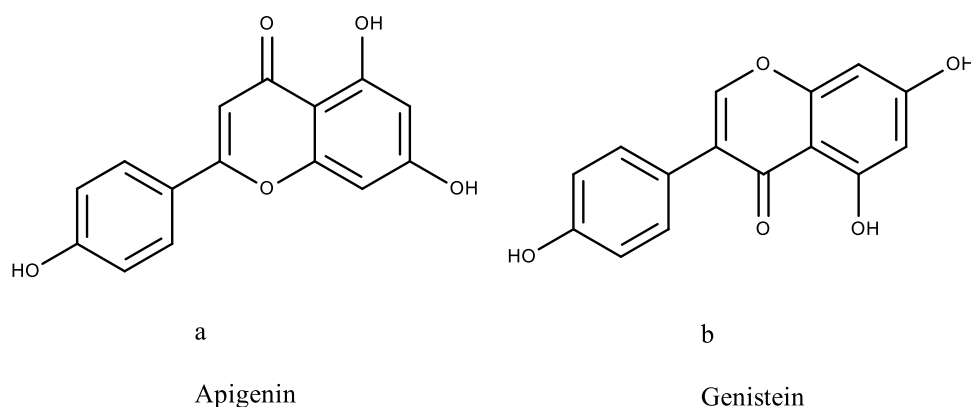


Figure 2.6 Structure of an example of flavonoid (a) and isoflavonoid (b)

The effect of topical antioxidants applied after UV radiation is not obvious whereas the photoprotective effect of topical antioxidants applied before UV exposure has been well recognized. Co-application of vitamins E and C provided a much more pronounced photoprotective effect as compared to the application of a single antioxidant.²⁸

3. UV filters

The human skin is the largest organ of the body with a surface area of approximately 1.5–2.0 m². Skin acts as an effective barrier against the harmful effects of environmental and xenobiotic agents. Among all factors chronic exposure to UV radiation is the key factor in the instigation of skin problems like cracks, burns, immune suppression, wrinkles, dermatitis, urticaria, ageing, hypopigmentation, hyperpigmentation and most complicated skin cancers.

In the Cosmetics Directive 76/768/EEC, Annex VII, the council of the European communities defines UV filters as substances, which are contained in cosmetic sunscreen products and are specifically intended to filter certain UV rays in order to protect the skin from certain harmful effects of these rays.²⁹ Ultraviolet filters can be classified into two types: UV organic and inorganic filters. There are only two approved inorganic particulates: zinc oxide and titanium dioxide. Both ingredients are considered broad spectrum since they absorb, scatter, and reflect UVB and UVA rays depending on their particle size. The remaining UV Absorbing molecules are classified as either UVB or UVA filters or both. Many new UV filters have been introduced in the last decade, particularly UVA filters, with improved efficacy and safety. There are about 55 UV filters that are approved for use in sunscreen products globally but that are not available, however, in some countries, such as the USA, for regulatory reasons. For example, 26 UV filters are accepted by Therapeutic Goods Administration in Australia and 31 UV filters are allowed in Japan. In Europe, Annex VII of the Cosmetics Directive lists 26 UV filters, whereas the sunscreen monograph in the USA mentions only 16, including only 10 in common with the EU. Each filter is approved or rejected according to regional requirements. Sunscreens appeared in commerce in the 1920s in the USA and in the 1930s in Europe. During the Second World War, red petrolatum was used as a sunscreen by US armed forces. The varieties and uses of sunscreens proliferated after that time with changes in fashion, increased leisure time and greater awareness of health issues. Ideal sun screening agents should be safe, chemically inert, non-irritating, non-toxic, photostable, and able to provide complete protection to the skin against damage from solar radiation. They should be formulated in a cosmetically acceptable form and ingredients should remain on the upper layers of the skin even after sweating and swimming. Sun screening agents should provide efficient scavenging activities against singlet oxygen and other reactive oxygen species.³⁰ They should also effectively block both UVB and UVA rays, which is possible with an

agent that has an SPF (sun protection factor) of 30 or greater. Sunscreens with an SPF of 30 or greater that incorporate photostable or photostabilized UVA filters (labelled as “broad spectrum” in the US) are usually ideal.³¹ Sunscreens should not only protect the skin from the sun, but also minimize the cumulative health hazards from sun damage caused over time.³²

3.1. Mechanism of Sunscreen Action

Electromagnetic rays interact with UV filters by either absorbing or scattering of their energy. When an organic filter absorbs a UV photon, the electrons in its highest occupied molecular orbital (HOMO) are promoted to its lowest unoccupied molecular orbital (LUMO) as shown in Figure 3.1.

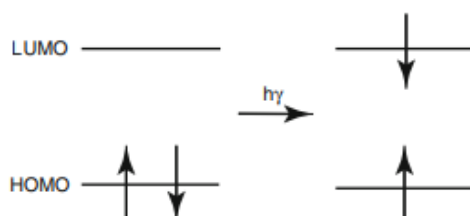


Figure 3.1 Absorption of energy by an organic UV filter

This singlet excited state can be deactivated by a simple vibrational relaxation back to the ground state, through fluorescence of the molecule, or by undergoing photochemical reactions. On the other hand, under certain conditions, the singlet excited state can undergo an intersystem crossing that leads to a triplet excited state. The energy in the triplet state may be dissipated in a number of ways,⁴ with emission of a photon (phosphorescence), energy transfer to other receptor molecules (T-T transfer), or photochemical reactions as shown in Figure 3.2.

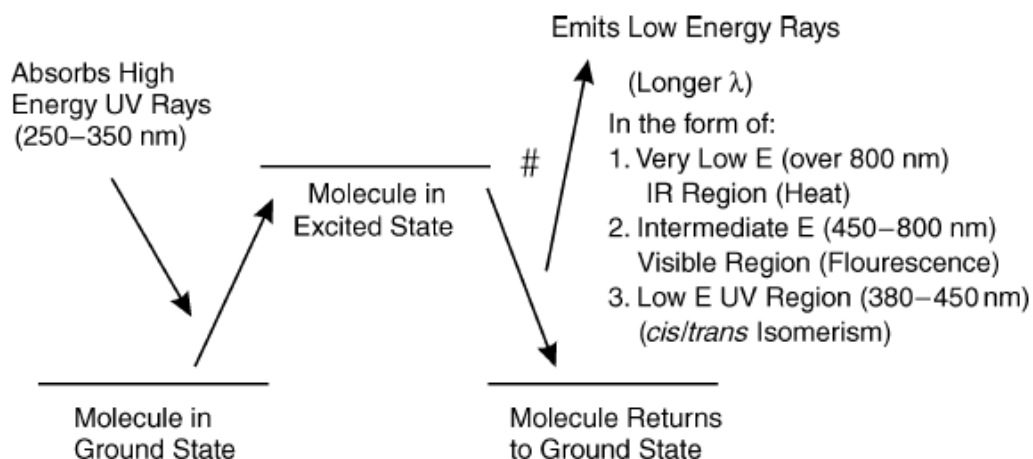


Figure 3.2 Energy release pathways

The inorganic particulates, on the other hand, act by scattering or absorbing solar radiation. The factors which affect the effectiveness of inorganic sunscreens are their reflective index, particle size, dispersion in base and film thickness. These particulates are semiconductors with high bandgap energy between the valence and conduction band (between 380 and 420 nm) as shown in Figure 3.3.

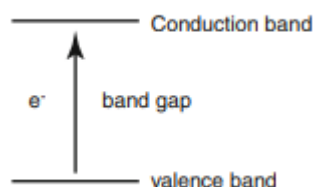


Figure 3.3 The bandgap energy in inorganic particulates between valence and conduction bands

The wavelength of absorption varies with the particle size of the inorganic particulates. The smaller the primary particulate size is the higher the bandgap energy is, but there can be safety implications when the particle size is too small so a suitable compromise must be reached between positive and negative effects. The inorganic UV filters offer some highly relevant advantages over the organic ones: they give broader spectrum protection (covering UVA and UVB), they are photostable while some organic UV filters (for example, avobenzone) are not photostable, and they have low tendency to provoke allergenicity and sensitization. This last factor justifies their widespread use in sunscreens for children as they tend to cause less skin irritation than the organic UV filters.³³ Their opaque nature and

“whitening effect” is an inherent disadvantage, which may be minimized by the use of micronized or ultrafine particles. Various types of inorganic sunscreen agents have been described in the literature including: zinc oxide (ZnO), titanium dioxide (TiO₂), iron oxide, red veterinary petrolatum, kaolin, calamine, ichthammol, and talc. ZnO and TiO₂ are by far the two most common physical, with microfine ZnO being a better blocker than TiO₂.

3.1.1. The Chemistry and characteristics of organic Ultraviolet Filters

Organic UV filters are generally aromatic compounds substituted directly or conjugated with a double bond (R₁) to an electron-accepting group (e.g., a carbonyl group) and an electron-donating group (R₂)⁴ (an amine, a hydroxyl, or a methoxy group) that is substituted in the ortho or para position of the aromatic ring as indicated in Figure 3.4.

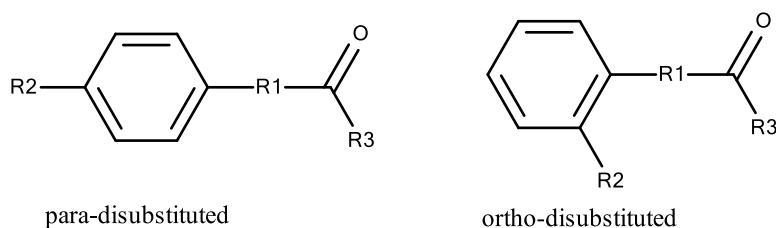


Figure 3.4 General Structures of organic UV filters.

Compounds of this configuration absorb the harmful short-wave (high-energy) UV rays (200–400 nm) and convert the absorbed energy is released in the form of innocuous longer-wave (lower-energy) radiation (>400 nm). Thus, the energy absorbed from the UV radiation corresponds to the energy required to cause a “photochemical excitation” in the sunscreen molecule. In other words, the sunscreen chemical is excited to a higher energy state from its ground state by absorbing the UV radiation. As the excited molecule returns to the ground state, energy is emitted that is lower in magnitude than the energy initially absorbed to cause the excitation (longer wavelengths).⁴ The longer wavelength radiation is emitted in one of several ways (see Figure 3.2). If the loss in energy is quite large, that is, if the wavelength of the emitted radiation is of sufficient length that it lies in the infrared region, then it may be perceived as a mild heat radiation on the skin. This minuscule heat effect is undetected because the skin receives a much larger heat effect by being directly

exposed to the sun's heat. If the emitted energy lies in the visible region, then it may be perceived as either a fluorescent or a phosphorescent effect. This is common in the imidazoline-type sunscreens.

In extreme cases, the emitted radiation is sufficiently energetic (lower wavelength) that it may cause a fraction of the sunscreen molecule to react photochemically. *Cis-trans* or *keto-enol* photochemical isomerization has been observed in some organic molecules, causing a mild shift in the λ_{max} of the chemical.³⁴

Cosmetic vehicles may have a profound effect on the efficacy of UV filters and their formulation. The pH, λ_{max} and extinction coefficient (ϵ) directly influence the SPF and characteristics of the cosmetic formulations. The UV absorption spectra of acidic and basic compounds may be affected by pH. With acidic compounds, the use of alkaline conditions (pH > 9) will assist in the formation of anions that tend to increase delocalization of electrons.³⁵ This electron delocalization decreases the energy required for the electronic transition in the UV spectrum; therefore, a bathochromic shift is observed (longer wavelength or λ_{max}). For example, phenols in an alkaline environment will experience this anticipated bathochromic shift owing to the formation of the phenolate anion, which will participate in resonance delocalization of electrons. Conversely, acidic conditions (pH < 4) will assist in the formation of cations in compounds containing aromatic amines. A hypsochromic shift towards a shorter wavelength occurs because the protonation of the unbound lone pair of electrons by acid would prevent any resonance delocalization of the electrons. Thus aniline, for example, forms the anilinium cation at low pH and a considerable hypsochromic shift occurs in its acidic formulations.⁴

Solvent shifts of sunscreen chemicals can be observed due to the combination of chemicals with a variety of emollients (such as petrolatum, lanolin, mineral oil and dimethicone). The shifts in the UV spectrum are due to the relative degrees of solvation by the emollient in the ground state and the excited state of the compounds. To predict the effect of the emollient on a particular chemical, the interaction (mostly hydrogen bonding) between the emollient and the sunscreen chemical must be understood. The solvation of polar sunscreens (e.g para-aminobenzoic acid) with polar solvents such as water or ethanol will be extensive. This extensive solvation stabilizes the ground state, thereby inhibiting electron delocalization, which in consequence results in a hypsochromic shift to lower wavelength. For less polar compounds, such as padimate-O (4-dimethylamino-benzoic acid 2-ethyl-hexyl ester), the nature of the solvent-solute interaction is different because the excited state is more polar than the ground state. The net result is greater stabilization

of the excited state by polar solvents, which lowers the energy requirements for the electronic transition; hence, a higher λ_{max} would be expected, and a bathochromic shift occurs.⁴

Another important parameter that can influence the efficacy of UV filters is the extinction coefficient (ϵ).

The value of the extinction coefficient (ϵ) is the basis of how the effectiveness of the sunscreen chemical is assessed. Therefore, chemicals with a high extinction coefficient are more efficient in absorbing the energy of the harmful UV radiation than chemicals with a lower extinction coefficient. All of the electronic transitions for any compound may be characterized as *symmetry-allowed* or *symmetry-forbidden*.³⁶ *Symmetry-allowed transitions* generally have high extinction coefficients, and *symmetry-forbidden transitions* have lower extinction coefficients. The degree of resonance delocalization in a molecule gives a clear indication as to its λ_{max} and a qualitative prediction of its extinction coefficient is possible. The more efficient the electron delocalization in a molecule, the higher its extinction coefficient. Compare, for example, padimate-O and homosalate (3,3,5-trimethylcyclohexyl 2-hydroxybenzoate) (see Figure 3.5).

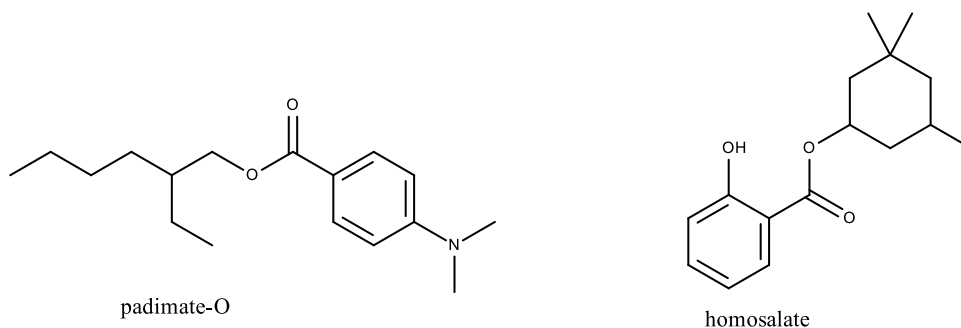


Figure 3.5 Structures of padimate-O and homosalate.

In padimate-O, the two substituents on the benzene ring are in a para orientation, whereas the two substituents in homosalate are in a sterically hindered ortho arrangement. In ortho-disubstituted aromatic compounds, the two groups are close to one another, which can cause a deviation from planarity. The slightest deviation from coplanarity will significantly reduce resonance delocalization; hence, a lower extinction coefficient is observed in homosalate compared to padimate-O. For the same reason, octisalate and homosalate (both ortho disubstituted) have lower extinction coefficients than para-disubstituted compounds

such as padimate-O. Increased conjugation, allowing for more efficient resonance delocalization, will also result in higher extinction coefficients. For example, the extinction coefficient of ethylene is 15,000, that of 1,3-butadiene is 21,000, that of 1,3,5-hexatriene is 35,000, and that for the highly conjugated molecule β carotene is 152,000.¹⁸ The new UV filters originating in Europe have multiple chromophores and therefore increased conjugation resulting in extinction coefficients exceeding 40,000, as is the case for the broad UV filter Tinosorb S (2,2'-[6-(4-Methoxyphenyl)-1,3,5-triazine-2,4-diyl] bis{5-[(2-ethylhexyl)oxy]phenol}), which will be described in detail below.

3.1.2 Organic Ultraviolet Filters

Organic filters absorb radiation energy within a specific range of wavelengths, depending on their chemical structure, then on the basis of their lambda maxima and of the bandwidth of absorption they can be divided into UVB, UVA and broad-spectrum filters.

3.1.2.1 UVB filters

UVB filters are compounds that absorb radiation in the region between 280 nm and 315 nm. Several different chemotypes belong to this category:

PABA and p-Aminobenzoates

Para-aminobenzoic acid (PABA) has an absorption maxima at 290 nm and a moderate molar extinction coefficient of 14,000. Its chemical structure reveals the presence of two functional groups, an amino group and a carboxylic acid moiety, substituted in a para orientation on the benzene nucleus as illustrated in Figure 3.6.

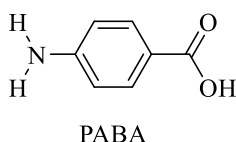


Figure 3.6 Structure of PABA

This particular configuration of an electron-donating group ($-NR_2$) substituted para to an electron acceptor group ($-COOH$) allows for efficient electron delocalization (see Figure 3.7).

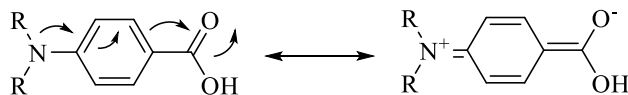


Figure 3.7 PABA derivative delocalization

Unfortunately, the presence of these two extremely polar groups contributes to a number of problems, for example the amine tends to oxidize rapidly in air and thereby produce off-colours. Also, the presence of these two extremely polar groups induces some hydrogen bonds either intermolecularly or with polar solvents promoting the aqueous solubility of the sunscreen chemical in the finished cosmetic formulation but an excessive hydrogen bonding between PABA and polar emollients also leads to a dramatic solvent effect.⁷ This solvent effect shifts the λ_{max} ~ 27 nm from 293 nm in non-polar solvents to 266 nm in polar solvents. The carboxylic acid and amine substituents cause the molecule to be sensitive to pH changes in the formulation. In addition, some doubts have been raised about the safety of PABA as several recent reports cite some cases of sensitization.⁴ In fact, PABA binds to the proteins of keratinocytes forming strong hydrogen bonds such that it clings to skin cells; this quality makes it an ideal water resistant UV filter but leads to some photoallergic reactions.³⁷

The sunscreen padimate-O (4-dimethylamino-benzoic acid 2-ethyl-hexyl ester (see Figure 3.5) was designed to overcome the issues related to the amino and carboxylic acid groups in PABA. The change in structure resulted in a UV filter that is a liquid instead of a crystalline solid and also decreased the problems associated with the primary amine and the carboxylic acid group that were described above. Its molar extinction coefficient is one of the highest found in a USA approved UVB filter, reaching 27,300. The extinction coefficient is double that of PABA. Unfortunately, some reports declare cases of its photoinstability and its commercial use worldwide has decreased significantly.³⁸

Salicylates

Salicylates were the first UVR filters used in sunscreen preparations.³⁹ Several of these derivatives have registered sizeable sales worldwide including octisalate (2-ethylhexyl 2-hydroxybenzoate, S-13 in Europe), homosalate (3,3,5-trimethylcyclohexyl 2-hydroxybenzoate, S12 in Europe), and the water-soluble trolamine salicylate (tris(2-hydroxyethyl)ammonium 2-hydroxybenzoate, S9 in Europe) (see Figure 3.8). This class consists of ortho-disubstituted compounds, which allows the formation of internal hydrogen bonds and thus decreases the propensity of electrons to interact with other ingredients or solvents or biological substrates. Although they are relatively weak UVR absorbers, they have excellent safety records and, because they are easily incorporated into cosmetic formulations, some are used to aid solubilisation of other, usually insoluble, cosmetic ingredients such as benzophenones. Of the salicylates on the market today, homosalate and octisalate are the most widely used in sunscreen preparations.

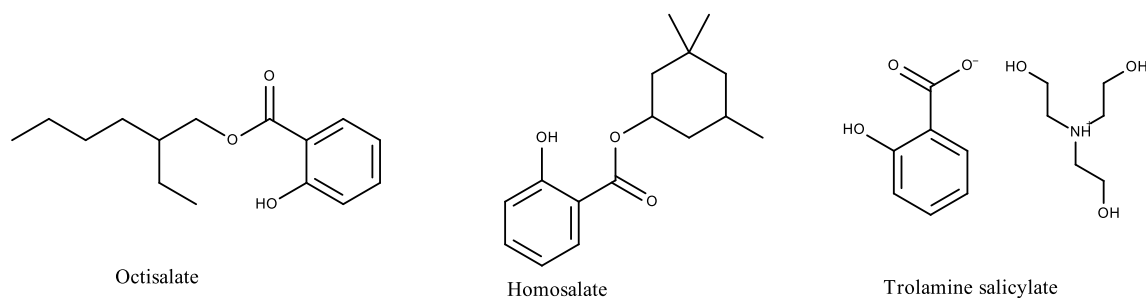


Figure 3.8 Salicylates

Cinnamates

Cinnamates, most notably octinoxate (2-ethylhexyl-*p*-methoxycinnamate) (see Figure 3.9), are currently the most popular sunscreens to protect against UVB rays of the electromagnetic spectrum. There are over a dozen cinnamate derivatives on the European list and there are three derivatives approved for use in the USA. Their chemical structure is characterized by an extra unsaturation conjugated to both the aromatic ring and the carbonyl portion of the carboxylic ester. This configuration permits the electron delocalization to occur throughout the cinnamate moiety. The energy corresponding to the

electronic transition in cinnamates has a wavelength of about 310 nm and they exhibit fairly strong molar extinction coefficients (>23,000). For practical purposes, this molecule is insoluble in water, making it suitable for most water resistant sunscreen formulations.

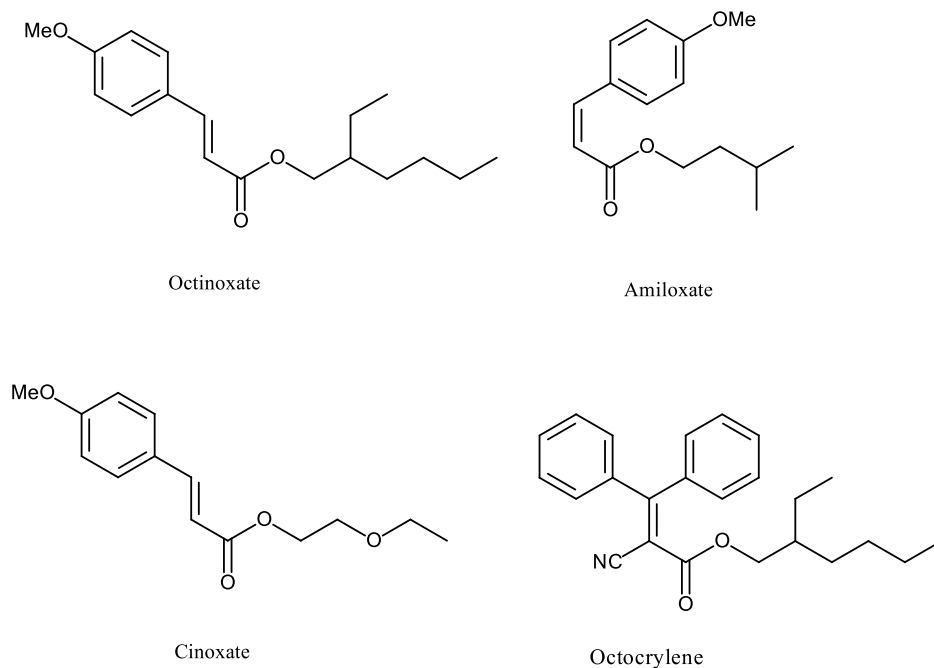
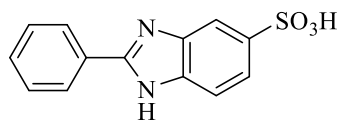


Figure 3.9 Cinnamates

Octinoxate is subject to *cis-trans* isomerism and it is known to lose some of its efficacy due to this photoinstability. Nevertheless it has an excellent safety record and remains the most popular UV filter in use worldwide. Another cinnamate approved for use today is octocrylene (2-ethylhexyl 2-cyano-3,3-diphenylacrylate) with a λ_{\max} of 303 nm and an extinction coefficient of 12,600. Due to this modest value it is used in association with other UV filters to increase the SPF value. Octocrylene is approved for use in the USA at levels up to 10%. Cinoxate has had limited use in cosmetic formulations in the USA.⁴

Ensulizole (PBSA)

2-Phenyl-1H-benzimidazole-5-sulfonic acid (PBSA, ensulizole) (see Figure 3.10) has some water solubility, is a high melting white powder, is affected by pH changes and is used in limited quantities in the USA. It has a moderate to high extinction coefficient of 26,000 and its λ_{\max} is about 310 nm.



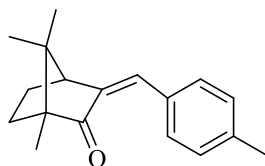
Ensulizole

Figure 3.10 Ensulizole

Camphor derivatives

Condensation of camphor with aromatic aldehydes provides $\alpha\beta$ -unsaturated camphor derivatives that contain a cinnamate-like substructure. Most of this class of bicyclic derivatives are solids and have a high molar extinction coefficient, generally $>20,000$, and absorb in the UVB range between 290–300 nm. In Europe six camphor derivatives, including Enzacamene, are approved for use in sunscreen formulations.

Enzacamene (4-methylbenzylidene camphor) (see Figure 3.11) is not approved for use in the United States by the Food and Drug Administration and it is not permitted in Japan.



Enzacamene

Figure 3.11 Enzacamene

Studies have raised the issue that enzacamene acts as an endocrine disruptor. There is, however, some controversy about the estrogenic effects of enzacamene and while one study showed only a relatively minor effect, a study in Switzerland showed significant uterine growth in immature rodents.⁴⁰ In addition, there is some evidence that enzacamene may suppress the pituitary-thyroid axis, leading to hypothyroidism.⁴¹

All camphor-derived sunscreens show high photostability to resonance delocalization in the molecule and they all dissipate the photon energy by *cis-trans isomerisation* (see Figure 3.12).

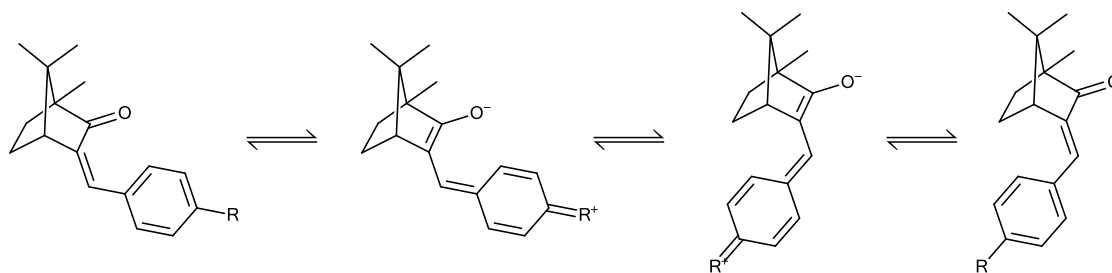


Figure 3.12 Camphor derivatives resonance delocalization

3.1.2.2 UVA filters

UVA filters are compounds that absorb wavelengths between 315 and 400 nm; the majority of these filters absorb in the UVA II range (315-340 nm) and only a few molecules provide protection in the UVA I range (340-400 nm).⁴²

Several different chemotypes belong to this category:

Benzophenone derivatives

The benzophenones are the only class of sunscreens that belong to the aromatic ketone category. Resonance delocalization in benzophenones, as in all the other classes of compounds discussed previously, is aided by the presence of an electron-donating group in either the ortho or para position, or both, relative to the ketone (see Figure 3.13).

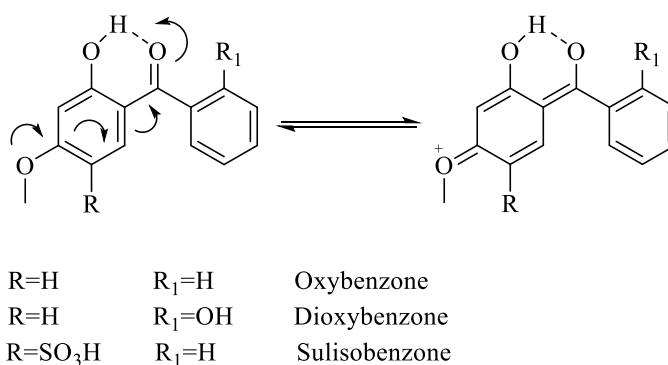


Figure 3.13 Benzophenone derivatives resonance delocalization

In this case, the electron-accepting group in the resonance delocalized structure is further stabilised by participation in an internal hydrogen-bond. Aromatic ketones, unlike the

esters encountered earlier, will resonate more easily, thereby requiring a lower quantum of energy for the electronic transition resulting in a longer wavelength (exceeding 320 nm) hence their use as UVA filters. There are various drawbacks associated with the use of benzophenones as UV filters. For example aromatic ketones are not as readily metabolised as ester containing UV filters, which slows the detoxification mechanism. Furthermore, they are difficult to manage solids and can exhibit unusually large λ_{\max} shifts. It has also been reported that patients developed statistically more allergic reactions to oxybenzone than to PABA.⁴

Anthranilate derivatives

Anthranilates, or ortho-aminobenzoates, are an interesting class of UV filters. Meradimate ((1R,2S,5R)-2-isopropyl-5-methylcyclohexyl 2-aminobenzoate)(see Figure 3.14) is on the US FDA Category I listing.

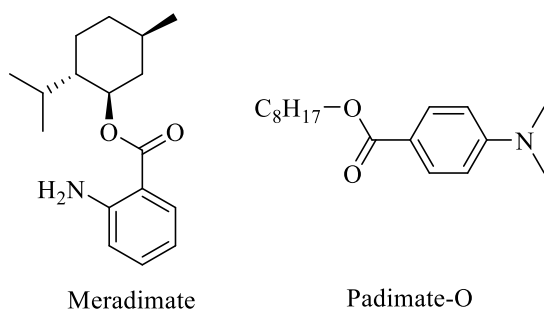


Figure 3.14 Meradimate and Padimate-O

This class of compounds offers an elegant example of the effect of chemical structure on UV absorbance characteristics. This effect, termed here the ortho effect, has been observed in numerous organic compounds. Meradimate, has a λ_{\max} of 336 nm, whereas padimate-O, a para-disubstituted aminobenzoate, has a λ_{\max} of only 307 nm. This dramatic 29 nm shift in the maximum absorption is clearly due to the ease in electron delocalization in the ortho-disubstituted compounds for which the geometry allows a “through space” assistance. This also results in lower molar extinction coefficients in the anthranilates than the para-aminobenzoates, in a manner analogous to that described for the salicylates. Again, the steric crowding in the ortho-disubstituted compound causes the molecule to deviate from coplanarity, thereby reducing the intensity of the absorbance. Anthranilates, as with salicylates, are stable and safe compounds to use owing to this ortho-disubstituted

relationship and, as in salicylates, they do not exhibit any significant solvent shift effects in cosmetic formulations.⁴

Dibenzoylmethane derivatives

Dibenzoylmethanes, or substituted diketones, are a relatively new class of UV filters. Only one molecule of this group, Avobenzone (4-tert-butyl-4'-methoxydibenzoylmethane) (see Figure 3.15), is still authorised for use as all previously available derivatives were withdrawn from the market because of a high incidence of contact and photocontact dermatitis.⁴³ This group of UV filters exhibits properties resulting from a keto–enol tautomerism. The keto form of these compounds only has a λ_{max} of about 260 nm, however, the predominant enol form has a λ_{max} exceeding 350 nm, making them suitable candidates for UVA protection.

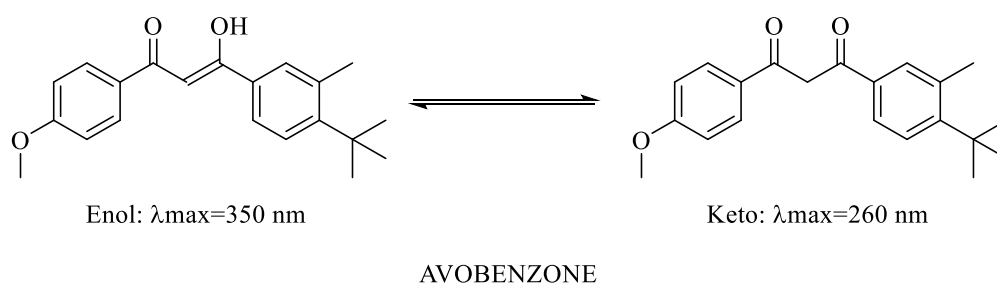


Figure 3.15 Enol and keto forms of Avobenzone

Ecamsule derivatives

Another UVA filter is ecamsule ([[(3Z)-3-[[4-[(Z)-[7,7-dimethyl-2-oxo-1-(sulfomethyl)-3-bicyclo[2.2.1]heptanylidene]methyl]phenyl]methylidene]-7,7-dimethyl-2-oxo-1-bicyclo[2.2.1]heptanyl]methanesulfonic acid) also known as Mexoryl SX (Figure 3.16). It is a photostable strong short UVA absorber, which absorbs UV radiation between 290 and 390 nm with a peak at 345 nm.⁴⁴ It is a camphor derivative and it seems to prevent photodermatoses, to block UV induced pigmentation and immunosuppression, and to preserve skin elasticity slowing down photoaging.⁴⁴ When exposed to UV radiation, ecamsule undergoes reversible photoisomerization, followed by photoexcitation. The absorbed energy is then released as thermal energy, without penetrating the skin.

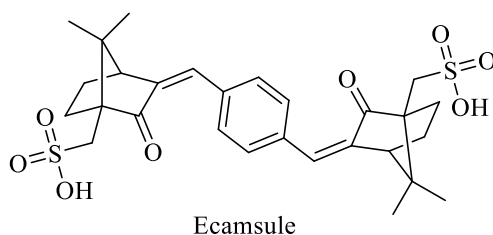


Figure 3.16 Ecamsule

3.1.2.3 Organic Broad UV filters

Only three organic UV filters are able to filter both UVA and UVB rays. These three compounds are Tinosorb M (2,2'-methanediylbis[6-(2*H*-benzotriazol-2-yl)-4-(2,4,4-trimethylpentan-2-yl)phenol]), Mexoryl XL (2-(2*H*-benzotriazol-2-yl)-4-methyl-6-[2-methyl-3-[1,3,3,3-tetramethyl-1-[(trimethylsilyl)oxy]-1-disiloxanyl]propyl]phenol) and Tinosorb S (2,2'-[6-(4-methoxyphenyl)-1,3,5-triazine-2,4-diyl]bis{5-[(2-ethylhexyl)oxy]phenol}) and their use is approved within the EU, Canada, Australia, Japan, and other countries, but not in the United States.

Tinosorb M

Tinosorb M (2,2'-methanediylbis[6-(2*H*-benzotriazol-2-yl)-4-(2,4,4-trimethylpentan-2-yl)phenol]) (see Figure 3.17) or Bisotrizole is a broad-spectrum UV radiation absorber, absorbing UVB as well as UVA rays with two peaks in its absorption spectrum at 303 nm and 360 nm. Bisotrizole is a hybrid UV absorber and it also works by reflecting and scattering UV. It is the only organic UV filter produced in microfine organic particles (< 200nm),⁴⁵ like microfine zinc oxide and titanium dioxide. Where other organic UV absorbers need to be dissolved in either the oil or water phase, bisotrizole dissolves poorly in both. The large size of the molecule minimizes skin penetration and its molecular structure facilitates energy dissipation by intramolecular heat transfer and vibrational relaxation.

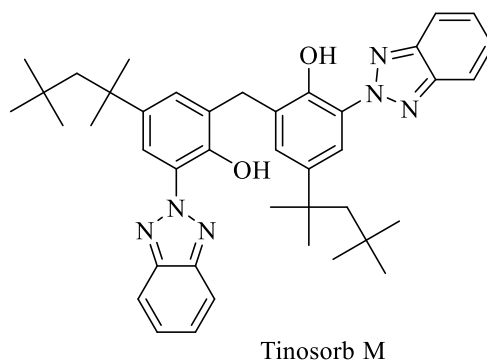


Figure 3.17 Tinosorb M

Mexoryl XL

Mexoryl XL (2-(2*H*-Benzotriazol-2-yl)-4-methyl-6-[2-methyl-3-[1,3,3,3-tetramethyl-1-[(trimethylsilyl)oxy]-1-disiloxanyl]propyl]phenol) or Drometrizole trisiloxane (see Figure 3.18) is a lipophilic benzotriazole derivative. It is a broad-spectrum UV absorber with two absorption peaks, one at 303 nm (UVB) and one at 344 nm (UVA). The molecule can be divided in two parts, the hydroxyphenylbenzotriazole group is responsible for wide range UV absorption, whereas the siloxane chain renders the molecule more lipophilic.

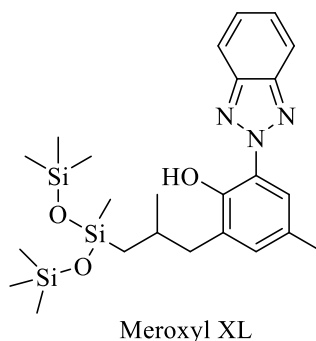


Figure 3.18 Mexoryl XL

Tinosorb S

In the year 2000 the first UV filter based on hydroxyphenyltriazine (HPT) technology, a triazine named Tinosorb S (2,2'-[6-(4-Methoxyphenyl)-1,3,5-triazine-2,4-diyl]bis{5-[(2-ethylhexyl)oxy]phenol}) or Bemotrizinol was added to the positive list of European cosmetic UV filters. Tinosorb S is an oil-soluble organic compound with strong broad-spectrum absorption. Due to its outstanding filter efficacy, combined with its inherent photostability and compatibility with all types of cosmetic filters as well as other cosmetic

ingredients, Tinosorb S represents a new generation of cosmetic UV filters. Its structure is depicted below in Figure 3.19.

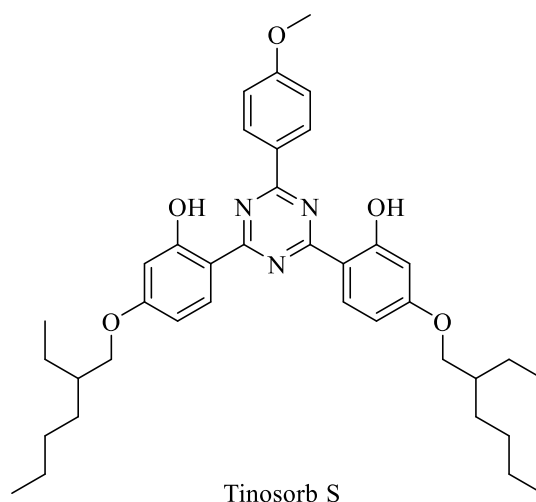


Figure 3.19 Tinosorb S

The strong absorption shown in the UVB range of tri-phenyl-triazines is due to its $\pi\pi^*$ character. The broad-spectrum structure was obtained with two ortho-hydroxyl groups on different phenyl moieties giving a compound that shows absorption maxima at 310 and 343 nm and $\epsilon_{\max} = 46,800$ and 51,900, respectively measured in ethanol. Tinosorb S contains two intramolecular hydrogen bridges that enable an excited-state intramolecular proton transfer (phototautomerism) after photoexcitation. This is followed by internal conversion and rapid energy dissipation, resulting in inherent photostability. Thus, the presence of ortho-hydroxy groups not only influences the shape of the absorption spectrum, but also the photostability.³

3.2. Properties of UV filters

The most important properties of UV absorbers for use in sunscreen are:

- UV-spectroscopic performance
- solubility in media used in sunscreen formulations
- photostability

UV-Spectroscopic Performance

There are two features which are important for the UV-spectroscopic performance of a UV filter:

- The wavelength(s) at which the extinction is at maximum (λ_{\max}), thus defining whether the substance is a UVA, a UVB, or a UVBroad-spectrum absorber.
- The extinction efficiency, which is best expressed as the $E_{1,1}$ value, referring to the theoretical extinction of a 1% solution of the substance, measured at an optical path length of 1 cm.

The $E_{1,1}$ value can be calculated using the Beer-Lambert law with the molar extinction coefficient ϵ and the molar mass M via the equation:

$$E_{1,1} = \epsilon [L / (\text{mol cm})] \cdot 10 [\text{g/L}] / M [\text{g/mol}] \cdot 1 [\text{cm}]$$

Thus, the $E_{1,1}$ value has the meaning of extinction per mass of the UV absorber. A further important quantity is the mean value of the specific extinction over the spectral range from 290 to 400 nm, $(E_{1,1})_{\text{mean}}$, characterizing the area under the UV extinction curve.

Solubility

Most UV absorbers used in sunscreens are reasonably hydrophobic, which means that their solubility in oils is higher than that in water. In most cases it is desirable to be able to achieve a concentration of an individual filter in the order of 5%. Most formulations on the market are oil/water emulsions with an oil content of around 30%. Thus, the solubility of hydrophobic UV absorbers in oils should be at least 15% in order to achieve a final concentration of 5% in the emulsion. With water-soluble filters the solubility should be in a comparable range.

The solubility is measured by stirring an excess of the active ingredient in the respective oil for 7 days at 25°C. After this time the undissolved material is separated by centrifugation and filtration and the concentration of the UV absorber in the clear saturated solution is determined via UV spectroscopy.

Photostability

There are two advantages of photostable filter systems:

- There is no loss of extinction upon irradiation and filter efficiency is constant with time. Thus, the amount of filter required to maintain a certain effect is less compared to an unstable system.
- There is no need to worry about the toxicology of possible photoproducts.

Photostability is an important requirement for filtering molecules and the degree of photodegradation is determined by comparison of the areas under the curves in the HPLC traces between irradiated samples and the corresponding amount of a non-irradiated sample. The UV filter's fate is best understood as a competition between the many pathways the molecule can take between its elevation to an excited state and its return to the ground state. All of the pathways result in the dissipation of excited state energy. Some of the pathways are destructive to the molecule (e.g., fragmentation, some types of isomerization, bimolecular reaction) whereas others are non-destructive (e.g., fluorescence, phosphorescence, some types of isomerization, energy transfer to another molecule). Each pathway is associated with its own rate constant. If non-destructive pathways predominate, then, relatively speaking, the molecule will be photostable. Conversely, if destructive pathways predominant, then the molecule will be unstable.

Sunscreen parameters

In-vitro Sunburn Protection Factor (SPF): In 1974, Greiter introduced the term Sun Protection Factor (SPF) to replace the term "Schulze factor". From then until now SPF has been a popular and widely adopted term in the evaluation of sunscreens. The Sun Protection Factor can be defined, as proposed by the FDA in 1978, as the numerical ratio between the minimal erythemal dose (MED) of sunscreen-protected skin, applied in the

amount of 2 mg/cm² and the minimal erythemal dose of unprotected skin, a mathematical relation that can be represented by the equation:

$$\text{SPF} = \text{MED (protected skin)} / \text{MED (unprotected skin)}$$

UVB rays are approximately 1000 times less erythemal than UVA rays. SPF values give information on the protection afforded towards UVB and UVA II (315-340 nm) but not towards UVA I (340-400 nm) and therefore SPF is of poor utility in understanding the UVA protection provided by a sunscreen. Because UVA rays also play a significant role in cellular damage, it is important to establish, not only the SPF value of a sunscreen formulation but, also the UVA protection it provides to ensure a broad defence toward all UV radiation.

Commonly used *in vivo* methods for determining UVA protection are **IPD** (immediate pigment darkening) and **PPD** (persistent pigment darkening).

The **IPD** response, which occurs during UVA exposure, appears as a transient grey-brown pigmentation and fades within minutes after exposure is completed. The threshold dose for the IPD response is measured with and without sunscreen protection to assess the UVA protection index. Since pigmentation develops relatively early after UVA exposure the test response is essentially immediate but pigmentation disappears rapidly after irradiation is interrupted leading to evaluation errors, along with significant individual variability in response.

The **PPD** test is more widely used than IPD to verify UVA protection, and it is included in the European Commission recommendations for assessment of UVA protection. PPD is a skin response linearly dependent on the amount of UVA that enters the epidermis, and the response is equally sensitive throughout the UVA range. The UVA protection factor of a product is calculated on the Minimal Persistent Pigment Darkening Dose of protected skin (MPDp) divided by that of unprotected skin (MPDu); MPDu and MPDp are defined as the quantity of radiant energy required to produce the first unambiguous reaction.

$$\text{UVA protection factor} = \frac{\text{MPDp}}{\text{MPDu}}$$

The test product is applied in the amount of 2 mg/cm², as for the SPF test, and the UVA dose required to induce minimal pigmentation (MPD) is greater than 10 J/cm²

(approximately 40 minutes of midday summer sunlight), thus also the stability of sunscreens is challenged during this test.

A number of *in vitro* methods are described in the literature to characterise the UVA, or more generically the UV, filtering capabilities of sunscreens. These include:

In vitro UVA protection factor (UVAPF): UVAPF is the absolute UVA protection afforded by a sunscreen product, calculated from the measured *in-vitro* transmittance after irradiation and weighted with the PPD action spectrum and with the “standard” output spectrum of a UVA-filtered solar simulator.

In-vitro UVA protection factor (UVAPF0) before UV exposure: The *in vitro* UVA protection factor measured before sample UV exposure. It is derived from the transmittance curve of the unexposed sample, weighted with the PPD action spectrum and with the “standard” output spectrum of a UVA-filtered solar simulator, after adjustment to the labelled SPF.

Critical Wavelength Value (λ_c): The critical wavelength λ_c value for the test product is defined as that wavelength where the area under the absorbance spectrum for the irradiated product from 290 nm to λ_c is 90% of the integral of the absorbance spectrum from 290 nm to 400 nm. The products reaching a critical wavelength of 370 nm or greater are considered broad-spectrum sunscreens⁴⁵.

UVA-UVB Ratio: Absorption of a 1.3 mg/cm² film is measured between 290 nm and 400 nm. The ratio of areas under the curve between 290-315 nm (UVB region) is compared with the area under the curve between 315-400 nm. Pre-irradiation of the sample is required.

The Protection Grade of UVA (PA): This system, based on the PPD reaction, is widely adopted in Asian countries. According to the Japan Cosmetic Industry Association, PA+ corresponds to a UVA protection factor between two and four, PA++ between four and eight, and PA+++ more than eight. This system was revised in 2013 to include PA++++ which corresponds to a PPD rating of sixteen or above.

Water-resistant sunscreen: Maintains the labelled SPF value after two sequential immersions in water for 20 min (40 min total).

Very water-resistant sunscreen: Maintains the labelled SPF value after four sequential immersions in water for 20 min (80 min total).

3.3 The regulatory frameworks

Sunscreens are generally evaluated using one of the following methods, and subsequently labelled according to specific country guidelines.

US-FDA method: The FDA proposal measures *in vitro* UV transmittance through a sunscreen film using the critical wavelength method. Sunscreen products offering primarily UVB protection would have a critical wavelength less than 320 nm, whereas those providing both UVB and UVA protection would have critical wavelengths between 320 and 400 nm. The FDA requires that sunscreen products have a critical wavelength of at least 370 nm (the mean value must be equal to or greater than 370 nm) to be labelled as providing “broad spectrum” UVA and UVB protection.

Australia: Australian standard (AS) method uses a spectrophotometer for measurements of the solar radiation transmitted by a sunscreen product to yield a percentage of UVA radiation absorbed by the product. According to this test, a product is designated as a long wave protector only if it transmits less than 10% of the incoming UV radiation between 320 and 360 nm.

European countries: COLIPA is an association within the cosmetic industry that voluntarily initiates the harmonization of labelling and product testing activities for sunscreen products. COLIPA guidelines are dedicated mainly to liquid and emulsion-type sun protection products. The test for UVA protection factors (UVAPF) evaluation should be based on the assessment of UV transmittance through a thin film (0.75 mg/cm²) of the sunscreen sample spread on a roughened substrate, before and after exposure to a controlled dose of UV radiation from a strictly defined UV source. This method allows *in vitro* measurement of UVAPF values, which are shown to correlate quite well with *in vivo* results, determined with the PPD method.

Japan: Japan Cosmetic Industry Association (JCIA) provides self-regulated standards. JCIA is a signatory to the COLIPA International SPF test method and JCIA has adopted ISO standards as they are published. For SPF, ISO 24444 is accepted. In Japan, for UVA, *in vivo* testing is required and labelling is according to ratings of Protection Grade of UVA (PA) i.e. PA+, PA++, PA +++ and PA++++.

China: Sunscreens are regulated under the Hygienic Standard for Cosmetics 2007. Currently sunscreens can only be labelled up to SPF 30+. The product must be labelled in Chinese and have a Chinese name. Water resistance norms should be followed if labelled.

3.4 Safety of the UV absorbers

A margin of safety (MOS) is calculated as the ratio between the no-observable adverse effect level (NOAEL) and the systemic exposure determined via the percutaneous absorption data. The European authorities require a MOS of 100-fold. Modern filters reach MOS values in excess of 1000-fold. A major concern with the conventional UV absorbers has always been skin penetration. Even if a substance is supposed to be “inert” it should not enter the body. In order to penetrate the skin, a substance has to be lipophilic. In other words, there should be practically no penetration of water-soluble substances. Highly lipophilic substances tend to stay in the upper layer of stratum corneum and are thus also useful for water-resistant formulations. The skin penetration of UV filters can be influenced by the formulation, some ingredients may act as enhancers and some may inhibit penetration. Another very important factor is the molecular weight (MW) of the UV absorber. The “500-Da rule for the skin penetration of chemical compounds and drugs” has recently been proposed for the development of drugs to describe the MW limit beyond which larger molecules cannot pass the corneal layer. Arguments for the 500-Da rules are: (1) virtually all common contact allergens are under 500 Da. Larger molecules are not known as contact sensitizers, they cannot penetrate and thus cannot act as allergens in man; (2) the most commonly used pharmacological agents applied in topical dermatotherapy are all under 500 Da; and (3) all known topical drugs used in transdermal drug-delivery systems are under 500 Da. As it seems logical to restrict the development of new innovative compounds to MW<500 Da when topical dermatological therapy or percutaneous systemic therapy or vaccination is the objective, we may conclude that it makes sense to restrict the search for new sunscreen actives to MW>500 Da. In any case, all new sunscreen actives have to undergo the scrutiny of safety testing because these compounds not only need to protect the consumer from the genotoxic effects of UVR, but themselves need to be devoid of genotoxic effects. While approved OTC sunscreens do not need to be tested, new sunscreen candidates usually undergo a battery of tests, each with its own advantages, disadvantages and limitations. *In vitro* models used to assess the potential for genetic damage include the reverse mutation (Ames) test in bacteria, and the mouse lymphoma test in mammalian cells. The ability of a chemical or formulation to induce broader scale genetic damage in chromosomes is assessed in the mouse micronucleus assay, which measures the more macroscopic histological changes in chromosomes after *in*

vivo treatment of mice. A positive response suggesting mutagenic potential is cause for concern and usually triggers either more extensive testing or rejection of the new sunscreen candidate. In addition to these classical genotoxicity tests, other more investigative models have also been developed to screen for genotoxic potential, as well as photogenotoxic potential. These models include direct incubation with DNA, bacteria, and yeast, either with or without radiation. While not definitive measures of safety, these models streamline the screening process and are usually followed up with testing in the more validated, *in vivo*-relevant safety models. Indeed the lack of correlation of some *in vitro* results with effects in humans points to the need to interpret results from *in vitro* models with caution. This is due to the fact that *in vitro* models cannot emulate the *in vivo* dynamics of drug exposure, absorption, metabolism, and elimination from the treatment site, all of which have the potential to affect toxicity. Investigative models have also been developed for prediction of a compound's potential for producing skin irritation, as assessed by direct cell damage *in vitro*. Accordingly, *in vitro* cytotoxicity assessment is a relatively quick means of obtaining data suggestive of irritation potential. The model includes treatment of mammalian cells (fibroblasts or keratinocytes) *in vitro* with the chemical, and measuring cellular uptake of a dye, which is indicative of cell damage.⁴⁶

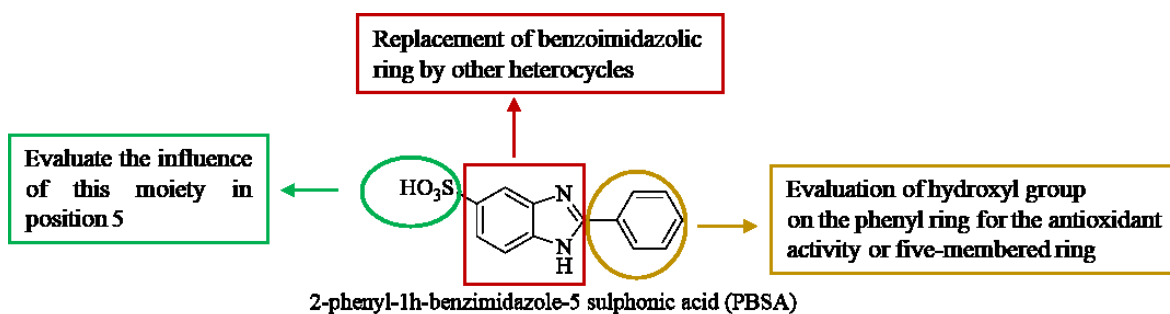
Photocytotoxicity employs a similar model, with the inclusion of exposure to UVR to simulate the solar spectrum. Indeed, use of this model has found acceptance in the European Union, due to its strong correlation with *in vivo* photoirritation. In order to identify the potential for ocular toxicity early in the program, the cytosensor method, the tissue equivalent assay (TEA), or the *ex vivo* rabbit ocular toxicity models may be used⁴.

4. Aim

The ideal sunscreen should absorb the harmful UV radiation in the region 280-380nm, to furnish a broad spectrum protection, and it should possess a large molar extinction coefficient (ϵ) at its λ_{max} . Values for ϵ exceeding 25.000 would be extremely desirable as this would afford the maximum possible protection with the least amount of sunscreen in the cosmetic formulations. Again the UV filters should have good solubility in emollients. Solid sunscreens such as the benzophenones, avobenzone, camphor derivatives, and PABA require special care to solubilize them in their formulations because they tend to crystallize out on the skin. Inorganic and organic particulates with silicone backbones have to be suspended properly in the formulation and the phase in which they are incorporated is chosen carefully to allow for maximum stability. Ideally the λ_{max} and the molar extinction coefficient ϵ should not be affected by solvents. Excessively polar sunscreen chemicals are stabilized by polar solvents, thereby lowering the energy requirements of the ground state of the sunscreen. This in turn will cause a hypsochromic shift (to shorter wavelengths) in polar solvents. On the other hand, sunscreens that are not too polar in their ground state but more polar in their photochemical excited states, will experience a bathochromic shift (to longer wavelengths) in polar solvents. The ideal sunscreen would be one in which the polarity of the ground state and that of the photochemically excited state are similar in nature. Hence, a hypsochromic shift (owing to the solvent stabilization of the ground state) will be counterbalanced by the bathochromic shift (owing to the solvent stabilization of the photochemically excited state).

Furthermore, the ideal sunscreen should have excellent photostability and be photochemically inert. If isomerization such as *cis-trans* or *keto-enol* is possible in the molecule, then the degradation quantum yields should be low, indicating that the isomerization is reversible. It should be compatible with cosmetic vehicles and ingredients, and be easy to use and handle. It should not discolour the skin, stain clothing, cause stinging sensations, deposit crystals, cause drying of the skin, or produce off-odours when applied to the skin or to the hair. The UV filter should be available isomerically pure, should be chemically stable for prolonged storage, should be chemically inert to other cosmetic ingredients, should protect against UVB radiation and long-wavelength UVA radiation and should act as a reactive oxygen species (ROS) scavenger. The ideal sunscreen should be inexpensive to use. So, with this purpose in mind the aim of my project is to design and synthesize compounds with dual capabilities that filter broadly

against UV A/B radiation and display antioxidant activity. The first approach explored was to use the commercial sunscreen PBSA (2-phenyl-1H-benzimidazol-5-sulfonic acid) as starting point (see Figure 4.1).



PBSA provides good protection against UVB rays but lacks filtering capacity for UVA radiation and it is devoid of antioxidant activity. With the aim of introducing antioxidant activity whilst maintaining its UV filtering capacity, PBSA was modified through addition of phenolic hydroxyl groups on the phenyl ring and also by substituting the functional group in position 5 of the benzimidazole ring to evaluate the influence of this moiety on UV-filtering and antioxidant capabilities. Accordingly, different classes of derivatives were synthesized belonging either to the series with isosteric modifications of PBSA (see Figure 4.1) or the purine class (see Figure 4.2 below).

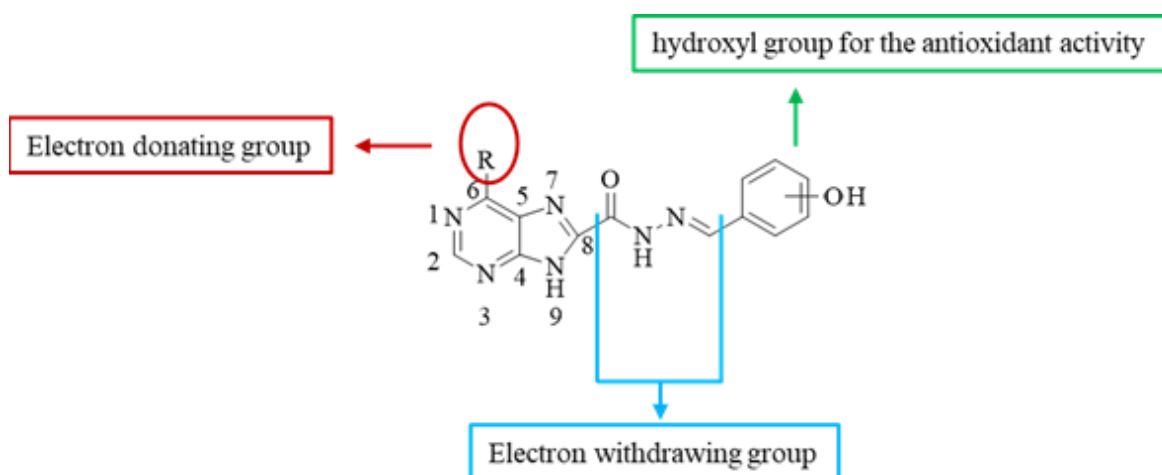


Figure 4.2 SAR study for the purine class

The purine class was selected in light of the data reported by Castellano,⁵⁴ in particular he demonstrated that the UV absorbance spectrum can be tailored via judicious choice of substituents at C(6) and C(8). Indeed, introduction of an acceptor substituents at C(8),

together with the typical donor substituent at C(6), creates a “Push-Pull” system that leads to a notable shift in the UV absorbance spectrum with an increase of the absorption maxima and a redshift of the low-energy absorption band to generate a strong absorbance band in the UVA region.

For this work a hydrazone group was chosen as the acceptor substituent at C(8) as this functionality permits further elaboration of the structure to include the anti-oxidant moiety, as successfully demonstrated by Prof. Manfredini in other series of heteroaromatic-hydrazones.⁶²

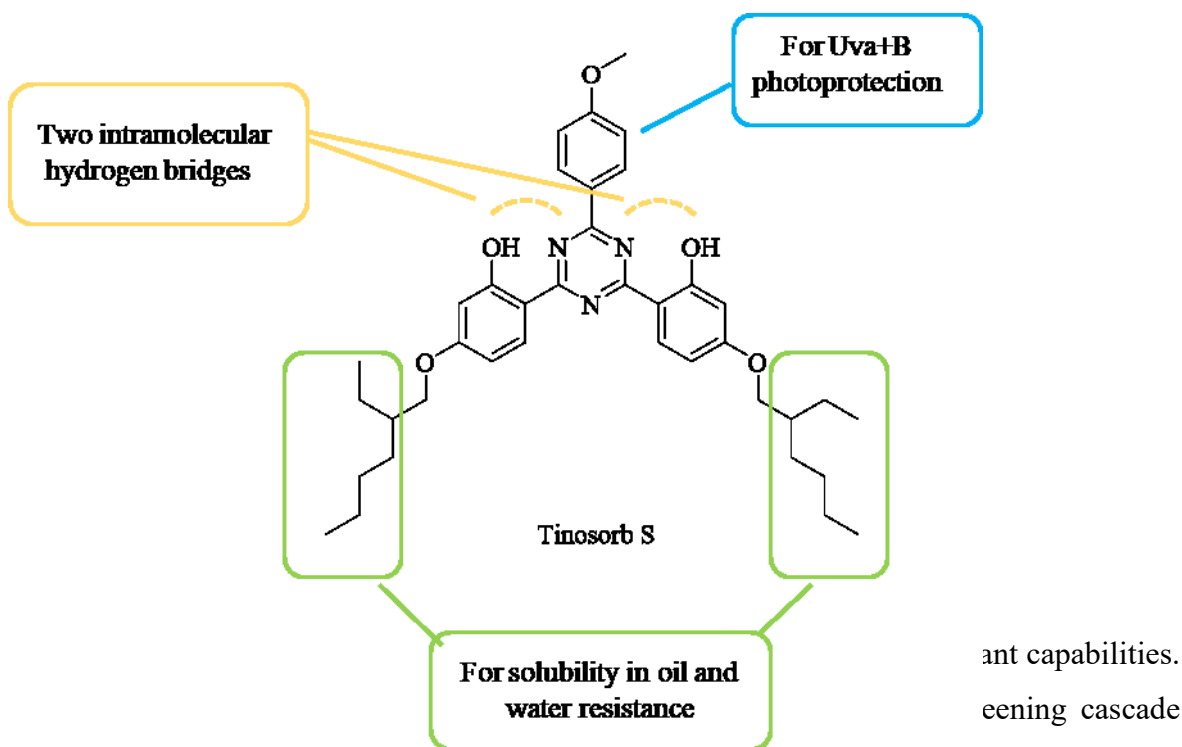
In order to maximise the anti-oxidant properties of target molecules the anti-oxidant moieties to be linked to the purine-hydrazone scaffold were carefully chosen based on literature reports that indicated these groups were able to bestow strong anti-oxidant activity.

Some derivatives of the purine class were prepared with a D-ribose substituent at N(9), attached through a β -glycosidic bond, as some adenosine derivatives have been reported to show an ability to reduce ROS production.⁶⁶

Hence, the addition of the carbohydrate group was explored to evaluate if this led to enhanced ant-oxidant properties.

This work was developed between the University of Ferrara and Aptuit, an Evotec company. At first I collaborated through the synthesis of a series of compounds derived from the isosteric modification of PBSA but then I focalized my work on the preparation of a library of purine derivatives. The synthesized compounds were evaluated for their UV-filter, antioxidant, antifungal and antiproliferative activities and for hERG channel activity. In the last part of my PhD I worked on a second approach using Tinosorb S (bis-ethylhexyloxyphenol methoxyphenyl triazine), a photo-stable broad-spectrum UV-filter, as a starting point. In the year 2000, this UV-filter based on hydroxyphenyltriazine (HPT) technology with strong broad-spectrum activity was added to the positive list of European cosmetic UV filters. Due to its outstanding filter efficacy, combined with its inherent photostability and compatibility with all types of cosmetic filters, as well as other cosmetic ingredients, Tinosorb S represents a new generation of cosmetic UV filters. Again, my interest was in developing novel derivatives from Tinosorb S to identify a dual acting compound with both broad UV A/B filter and antioxidant activities. To achieve this goal I proposed different chemical modifications of Tinosorb S, based on the scientific literature.¹ Consequently, a strategy was designed to maintain the pharmacophore of the molecule

responsible for its broad activity against UV A/B and to elaborate the lipophilic sidechains in order to introduce the antioxidant activity (see Figure 4.3).



(incorporation in the cosmetic formulation, toxicity and phototoxicity studies, and photostability).

4.1 PBSA derivatives

4.1.1. Chemistry: Design and Synthesis

Isosteric modifications of PBSA is a strategy that has been employed within the research group of Prof. Manfredini to design and prepare derivatives of PBSA in order to realize compounds with good antioxidant activity and broad UV A-B filter capabilities. To this purpose, PBSA was modified on the benzimidazole core by replacement of this moiety with other fused bicyclic heterocycles. In particular I completed the exploration that was ongoing in parallel at the University of Ferrara by synthesizing derivatives where the core was replaced with benzoxazole or 6-hydroxypurine.

Benzoxazole is an aromatic system where benzene is fused to an oxazole ring and benzoxazole containing structures are well known for its antifungal, antioxidant, antiallergic, antitumoral and antiparasitic activity. Benzoxazole derivatives are also of

interest as optical brighteners in laundry detergents, as for example 4,4'-(E)-bis(benzoxazolyl)stilbene and 2,5-bis(benzoxazol-2-yl)thiophene. These optical brighteners, optical brightening agents (OBAs), fluorescent brightening agents (FBAs), or fluorescent whitening agents (FWAs), are chemical compounds that absorb light in the ultraviolet and violet region (usually 340-370 nm) of the electromagnetic spectrum and re-emit light in the blue region (typically 420-470 nm) by fluorescence.

Purine is a heterocyclic, aromatic, organic compound consisting of a pyrimidine ring fused to an imidazole ring. The word purine was coined by the German chemist Emil Fischer in 1884.⁴⁷ He synthesized purine for the first time in 1898. The starting material for the reaction sequence was uric acid, which had been isolated from kidney stones by Carl Wilhelm Scheele in 1776.⁴⁸ Uric acid was reacted with PCl_5 to give 2,6,8-trichloropurine, which was converted into 2,6-diiodopurine with HI and PH_4I , and reduction using zinc dust gave purine (see Figure 4.4).

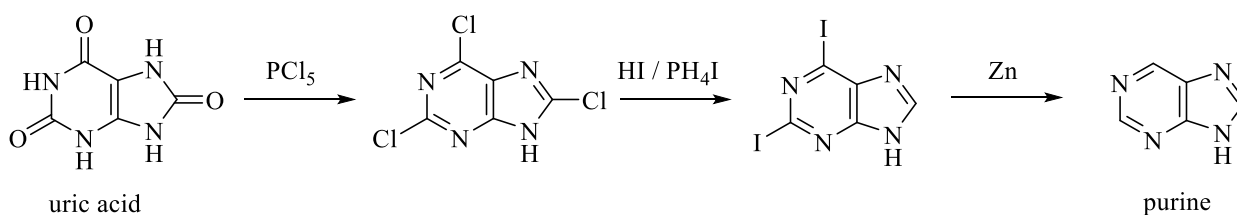


Figure 4.4 Purine synthesis

Purine is both a very weak acid (pK_a 2.39) and an even weaker base (pK_a 8.93).⁴⁹ If dissolved in pure water, the pH will be halfway between these two pK_a values. The Traube purine synthesis (1900) is a classic reaction, named after Wilhelm Traube, between an amino-substituted pyrimidine and formic acid.⁵⁰(see Figure 4.5).

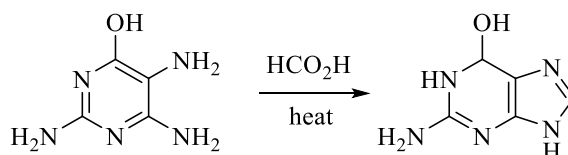


Figure 4.5 Traube Purine synthesis

The electrons of the purine ring are extensively delocalized. The principal contributing structures are shown below (see Figure 4.6). As these structures suggest, positions 2, 6, and 8 are susceptible to attack by nucleophiles, and positions 3 and 7 are electron rich, and are susceptible to attack by electrophiles.⁵¹

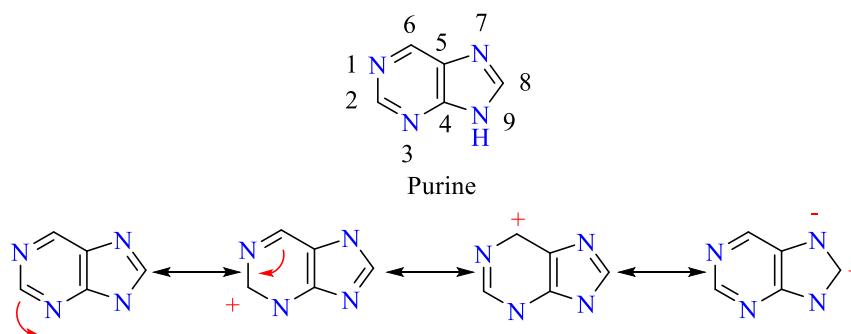


Figure 4.6 Purine reactivity

The two most common purines are adenine and guanine (see Figure 4.7), whose ultraviolet absorption spectra are shown in Figure 4.8. The purines xanthine, hypoxanthine, and uric acid (see Figure 4.9) are also important metabolites, although they are far less abundant than adenine and guanine.

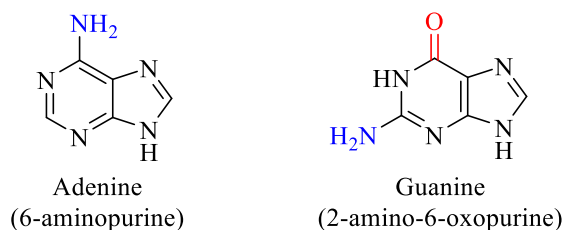


Figure 4.7 Structures of Adenine and Guanine

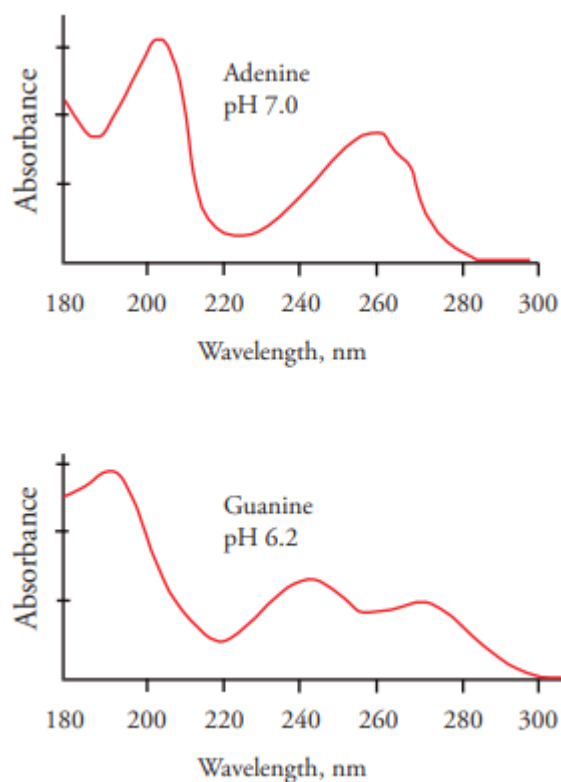


Figure 4.8 UV absorption spectra of Adenine and Guanine

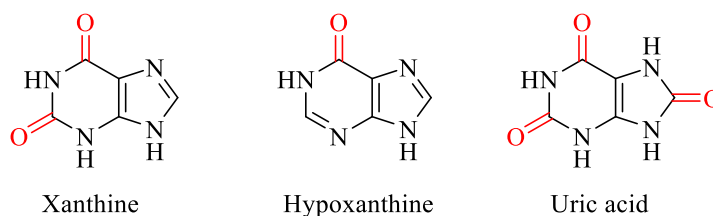


Figure 4.9 Structures of Xanthine, hypoxanthine and Uric acid

Purine analogues have shown antimicrobial, antifungal, antitumor, antiproliferative and antiviral activity.⁵²

Considering the points described above, PBSA was modified on the benzimidazole core, or LHS (left-hand side), on the linker (from 0 to 4 atoms) and on the phenyl ring, or RHS (right-hand side) as depicted in Figure 4.10 below:

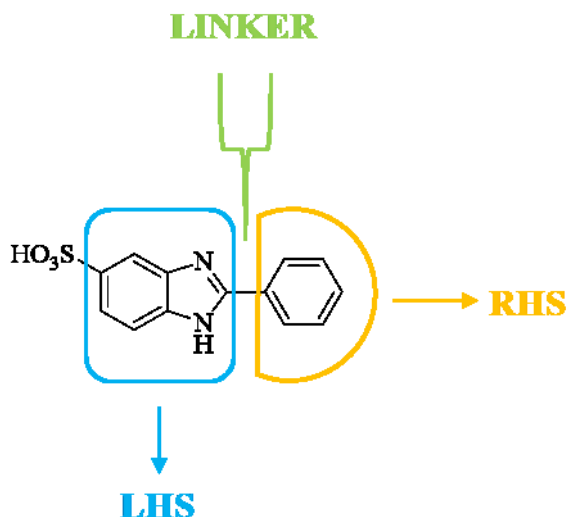


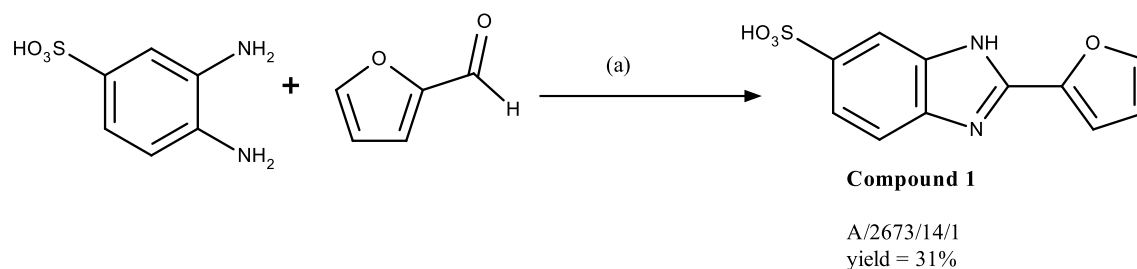
Figure 4.10 PBSA modifications

Accordingly, to facilitate the discussion the synthesized compounds have been classified into two groups, the first group without a linker and the second group with a hydrazone motif as linker between the RHS and the LHS.

In the literature, several procedures are described for the synthesis of benzimidazole rings including the condensation reaction of an *o*-diaminobenzene with a carboxylic acid, or the corresponding aldehyde in the presence of an oxidizing agent in stoichiometric amount. After evaluation of the described routes, we focused our attention on a method that allows the desired compounds to be obtained with good yield, at low cost and in a short time.

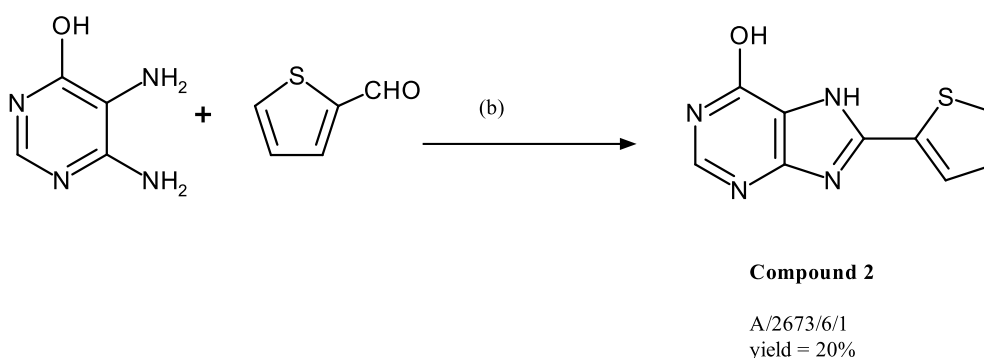
4.1.2 Group 1: Structures without a linker

The method that furnished **compound 1** (A/2673/14/1) consists in reacting the diamine and an aldehyde in ethanol in the presence of stoichiometric amount of sodium bisulfite to afford the target compound with a yield of 31%. The progress of the reaction was monitored by UPLC (ultra-high performance liquid chromatography) analysis. The product was purified by reverse-phase (C18) column chromatography and all final compounds were fully characterized by $^1\text{H-NMR}$ and $^{13}\text{C-NMR}$ (see Scheme 1).



Scheme 1: Synthesis of 2-(furan-2-yl)-1H-1,3-benzodiazole-6-sulfonic acid. Reagents and conditions: (a) EtOH, NaHSO₃, reflux, overnight

Purine compounds were synthesized by condensation reaction of 6-hydroxy-4,5-diaminopyrimidine with the corresponding aldehyde in an appropriate solvent under the conditions indicated in detail below. For the synthesis of **compound 2** (A/2673/6/1) it was necessary to explore various different conditions before achieving successful results using 1 eq of conc. H₂SO₄ as shown below:



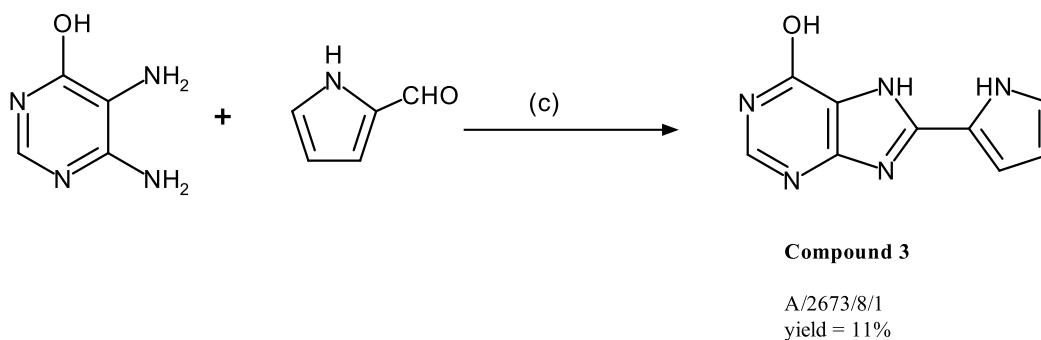
Scheme 2: Synthesis of 8-(thiophen-2-yl)-7H-purin-6-ol. Reagents and conditions: (b) DMSO, conc. H₂SO₄, 80°C, overnight.

The reaction was monitored by UPLC-MS.

The crude was purified by reverse chromatography (C18 cartridge) due to its high polarity and low solubility. The final compound was characterized by NMR and UPLC-MS.

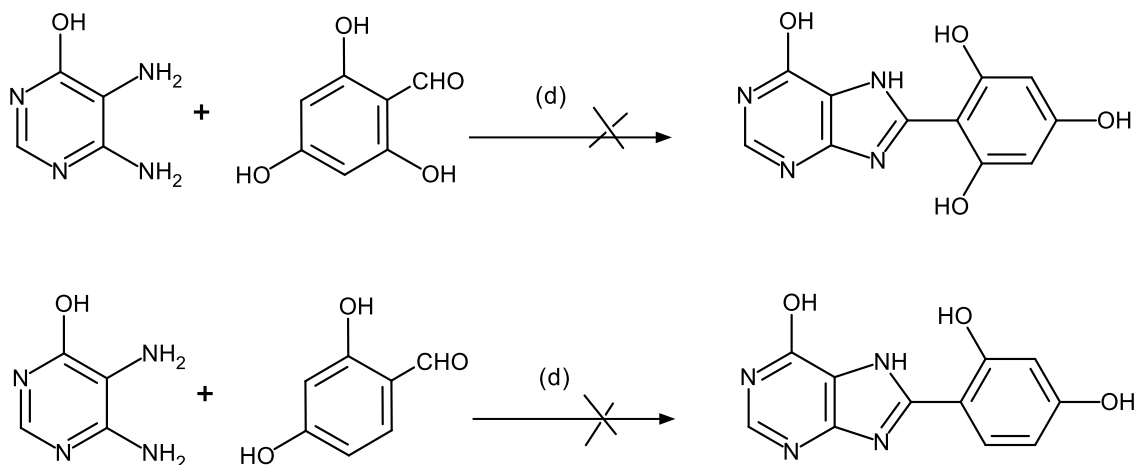
Another approach was used for the preparation of **compound 3** (A/2673/8/1).

In this case the condensation reaction between 2-pyrrolaldehyde and 6-hydroxy-4,5-diaminopyrimidine was carried out in the presence of iron(III) chloride hexahydrate. DMF was used as solvent to resolve the critical issue related to low solubility:



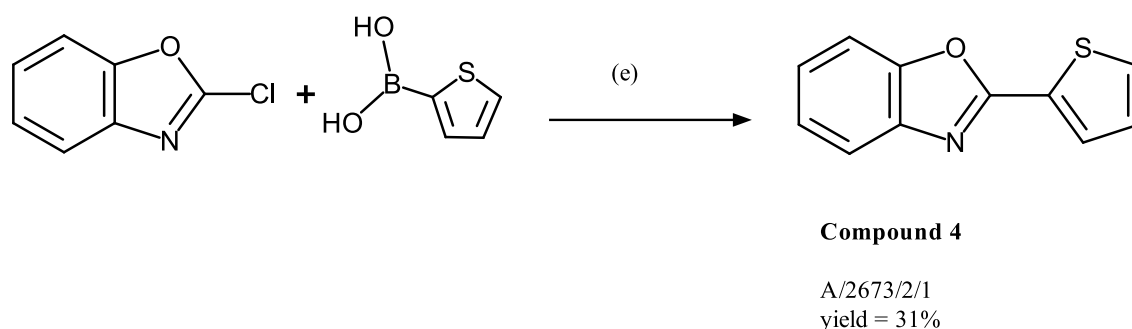
Scheme 3: Synthesis of 8-(1H-pyrrol-2-yl)-7H-purin-6-ol. Reagents and conditions: (c) DMF FeCl₃•6H₂O, 80°C, overnight

All attempts to synthesize 2-(6-hydroxy-7H-purin-8-yl)benzene-1,3,5-triol and 4-(6-hydroxy-7H-purin-8-yl)benzene-1,3-diol were unsuccessful. This could be due to the steric hindrance caused by the 2-hydroxy/2,6-dihydroxy groups on the benzaldehyde:



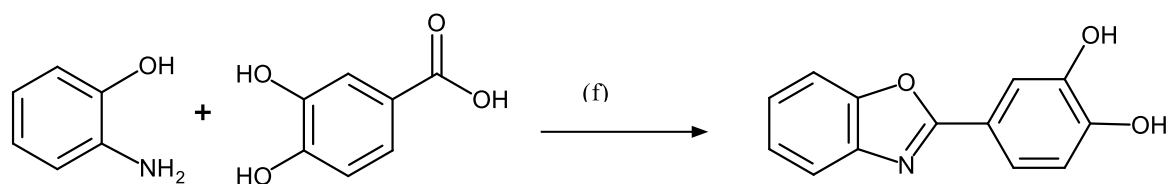
Scheme 4: Attempted synthesis of 2-(6-hydroxy-7H-purin-8-yl)benzene-1,3,5-triol and 4-(6-hydroxy-7H-purin-8-yl)benzene-1,3-diol. Reagents and conditions: (d) EtOH, Na₂S₂O₄, reflux, overnight

Two different methodologies were used for the synthesis of the benzoxazole derivatives. For compound **4** (A/2673/2/1) a Suzuki-Miyaura coupling was applied using 2-chlorobenzoxazole and 2-thienylboronic acid as starting materials. The reaction was performed under a nitrogen atmosphere in a screw-cap vial. All reagents including the catalyst PdCl₂(Amphos)₂, the boronic acid and the inorganic base potassium acetate were purchased from commercial sources and used as received. A mixture of anhydrous dioxane and distilled water that had been purged with a stream of nitrogen was used as solvent. The reaction showed a good profile and the excess of boronic acid was washed out using an alkaline work-up. The final compound A/2673/2/1 was isolated with a purity of 98% and a yield of 31% after column chromatography on silica gel.



Scheme 5: Synthesis of 2-(thiophen-2-yl)-1,3-benzoxazole. Reagents and conditions: (e) dioxane/water, PdCl₂(Amphos)₂, potassium acetate, 100°C, 12 hours

In contrast, compound **5** (A/2673/4/1), which also belongs to the benzoxazole series, was obtained from the reaction between 3,4-dihydroxybenzoic acid and 2-aminophenol in the presence of p-toluenesulfonic acid. The reaction was performed in refluxing xylene. The crude obtained from this condensation was purified by silica gel chromatography. The final compound named A/2673/4/1 was isolated with a yield of 30% and a purity of 98%.



Compound 5

A/2673/4/1
yield= 30%

Scheme 6: Synthesis of 4-(1,3-benzoxazol-2-yl)benzene-1,2-diol. Reagents and conditions:

(f) TsOH.H₂O, xylene, reflux, 12 hours

<p>A/2673/2/1</p>	<p>A/2673/4/1</p>
<p>A/2673/6/1</p>	<p>A/2673/8/1</p>
<p>A/2673/14</p>	

Table 1. Synthesized compounds belonging to Group 1

4.1.3. Group 2: Structures with a hydrazone linker

A number of indole-hydrazone compounds have been reported by Manfredini *et al* for their potential radical-scavenging activity⁵⁴ while 8-cyanopurines have been reported to have a good UV filtering capability⁵⁴, along with other 8-substituted purines as shown in Figure 4.11.

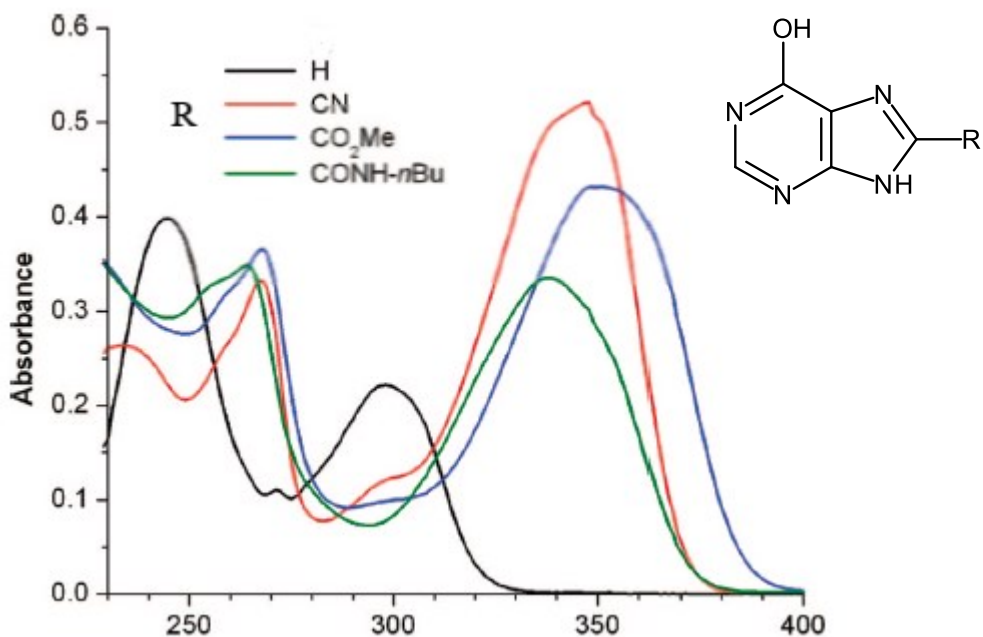


Figure 4.11 Absorption data for purine series

As the cyano group is not amenable to further functionalisation, the 8-amidopurine was taken in consideration for merging with indole-hydrazone to give a new class of compounds which have the potential to show both antioxidant and UV-filtering properties as shown in Figure 4.12.

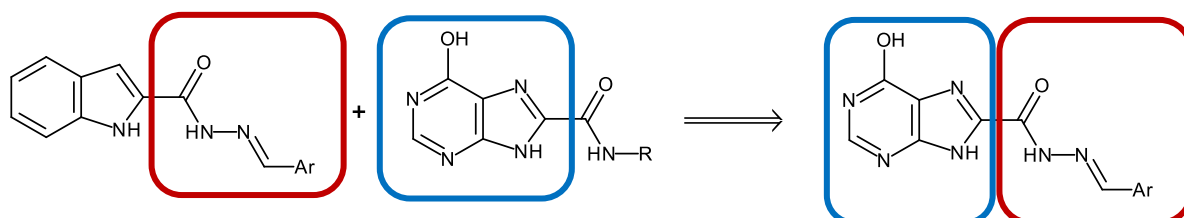


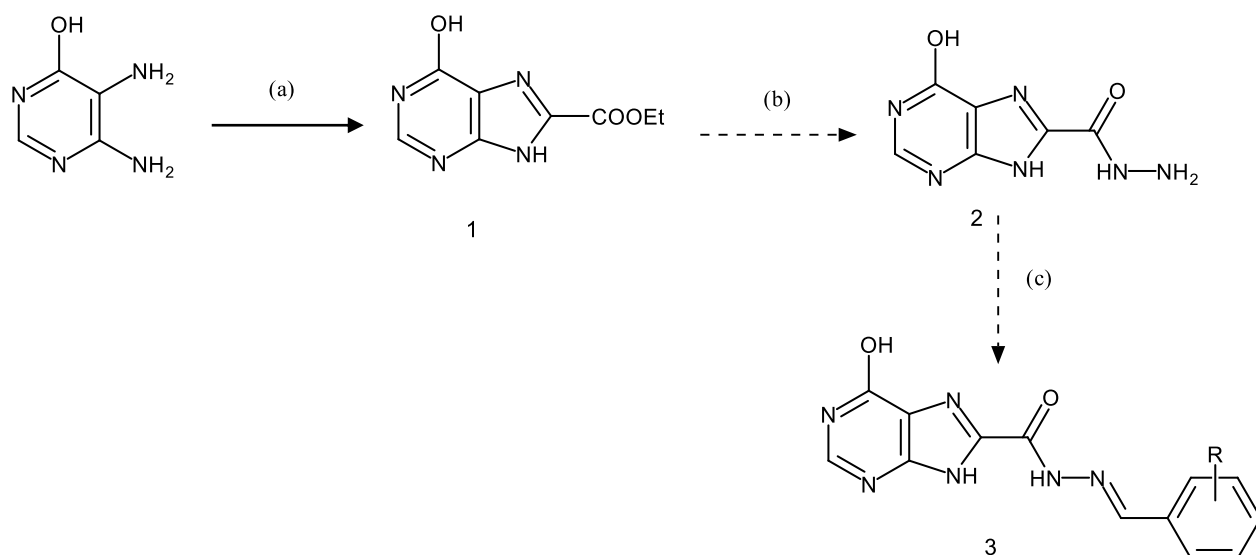
Figure 4.12 Genesis of the Purine hydrazone series

As reported by Castellano,⁵⁴ (see Figure 4.11) the functionalization of position 8 of purines is possible when donor groups OH, NH₂, are present in position 6. Unfortunately, the most commonly reported reactions at this position are cyanation/carbonylation, or in general palladium catalysed reactions, therefore a halogen, such as bromine, has first to be inserted in position 8 of the purine.

The drawback with these two types of reactions is that both use very toxic reagents (zinc cyanide and carbon monoxide, respectively) and the operators who perform these reactions must possess a proper licence to handle and use these materials. In addition, the carbonylation reaction often has to be run under high pressure, therefore limiting this protocol to establishments with appropriate facilities.

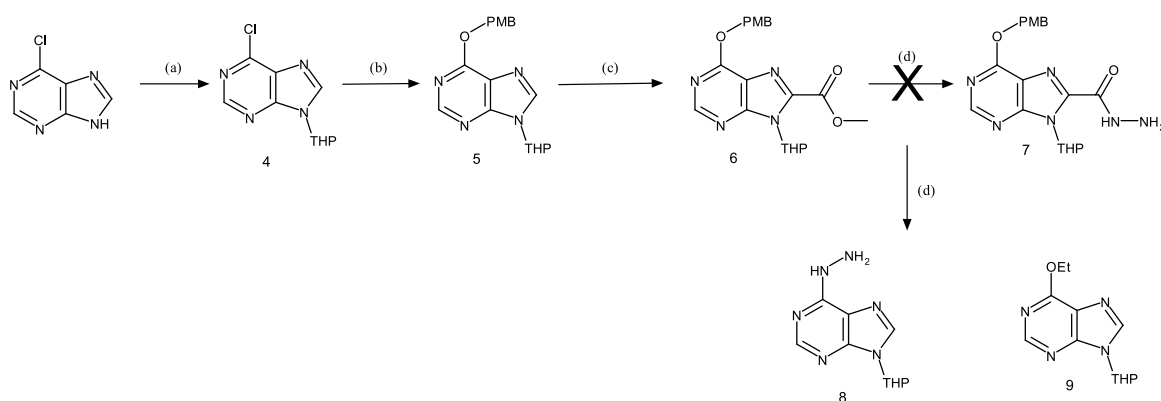
To avoid these inconveniencies, a strategy was chosen wherein the purine was directly constructed with the 8 position already substituted with an ethyl ester. This choice required a significant effort to synthesize this kind of molecule, with 4 different synthetic strategies being investigated before identifying a successful synthetic route.

The first synthetic approach investigated was the preparation of the purine core functionalized with an ethyl ester group (see Scheme 7). The reaction between an ortho-diaminopyrimidine and ethyl triethoxyacetate did not give any desired product, probably due to the poor solubility of the starting material, and therefore this approach was abandoned.



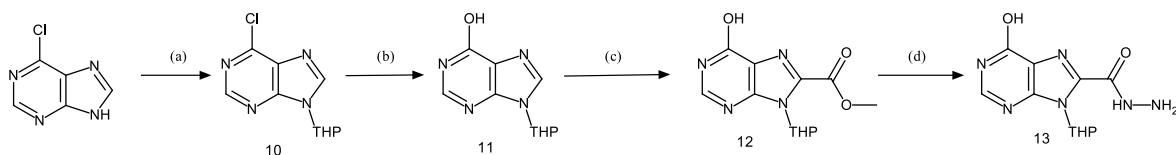
Scheme 7. Reagents and conditions: (a) (EtO)₃ CCOEt, 120°C, no reaction;

In the second approach explored, 6-chloropurine was protected with tetrahydropyran to obtain compound 4. The chlorine was displaced by p-methoxybenzyl alcohol (PMB-OH) in an S_NAr reaction to afford derivative 5. Insertion of the carboxylic ester group was achieved by deprotonating position 8 of the purine with LDA, then quenching the carbanion with ethyl chloroformate to give compound 6 in moderate yield. Hydrazinolysis of the ester 6, surprisingly, did not furnish the desired hydrazide 7. Instead the formation of compounds 8 and 9 was observed, where hydrazine and solvent, respectively, have replaced the p-methoxybenzyloxy group and decarboxylation has also occurred.



Scheme 8 Reagents and conditions: (a) 2,3-DHP, TsOH, AcOEt 90°C, (b) PMB-OH, K_2CO_3 , DMF, 60°C, (c) LDA, -78°C, then EtOCOCl, (d) Hydrazine, EtOH, 78°C

In order to avoid nucleophilic substitution at the 6 position of the purine, the hydroxyl group was left unprotected and the reactions were carried out in a similar manner to the second approach to provide compound 13 in moderate to good yield. Unfortunately, the extremely poor solubility of hydrazide 13 prevented the use of this compound for the synthesis of the final molecules, and for this reason this approach was abandoned.



Scheme 9. Reagents and conditions: (a) 2,3-DHP, TsOH, EtOAc, 90°C, (b) NaOH, H_2O , (c) LDA, -78°C then EtOCOCl, (d) Hydrazine, EtOH, 78°C

In the final approach, inosine was used for the synthesis of the key building block as shown in Scheme 10. This procedure proved to be successful and had the added benefit of providing two related derivatives, with and without ribose.

Protection of the ribose ring with the Corey protocol gave the poly-silylated inosine in good yield. When 15 is treated with LDA (5 equivalents) below -70°C , a clear solution of the lithiated species resulted. It is important that the temperature was kept below -70°C in order to minimize the deprotonation of other sites. To confirm lithiation had taken place under these conditions, after 1 hour a quench with CD_3OD gave, after a quick purification, the deuterated analogue of compound 2. The ^1H -NMR spectrum of this deuterated derivative in CDCl_3 showed that the metallation had taken place at the 8 position in a regioselective manner ($\sim 70\%$ incorporation of deuterium achieved) (see Figure 4.13).

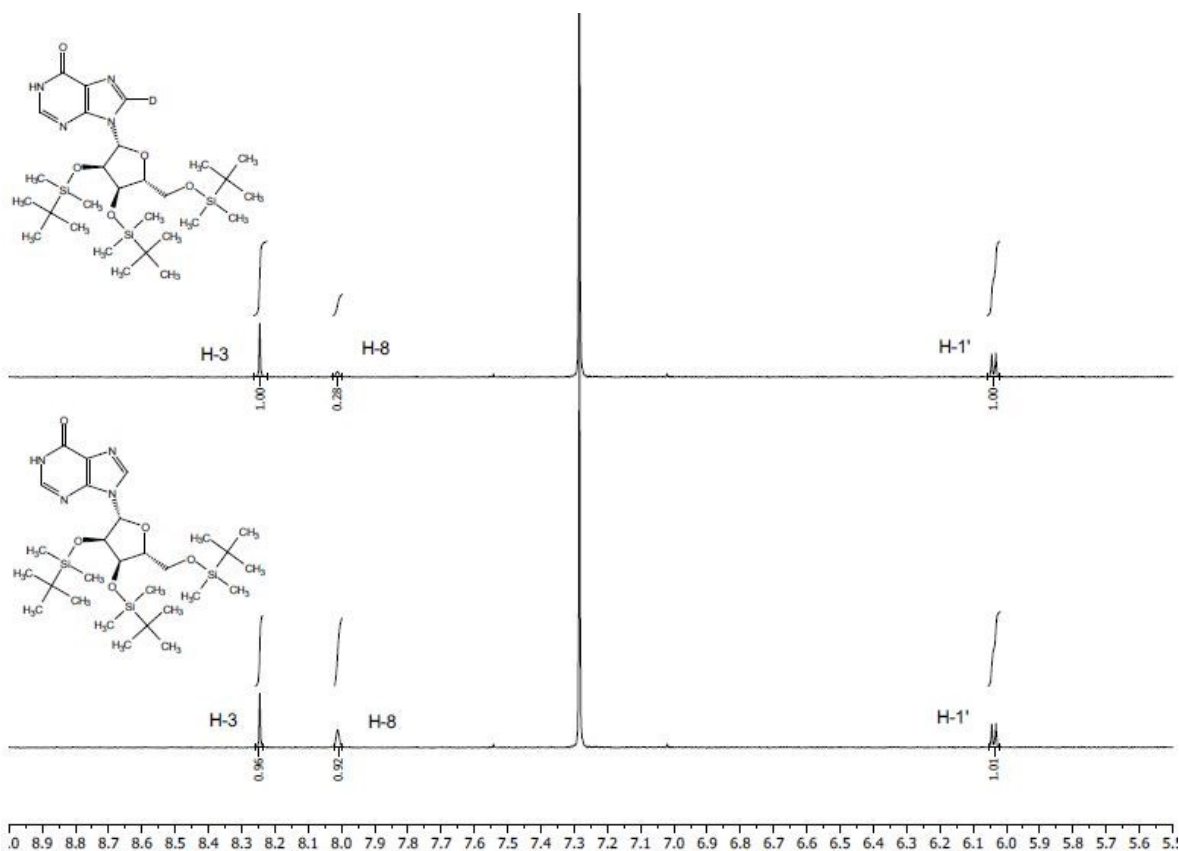
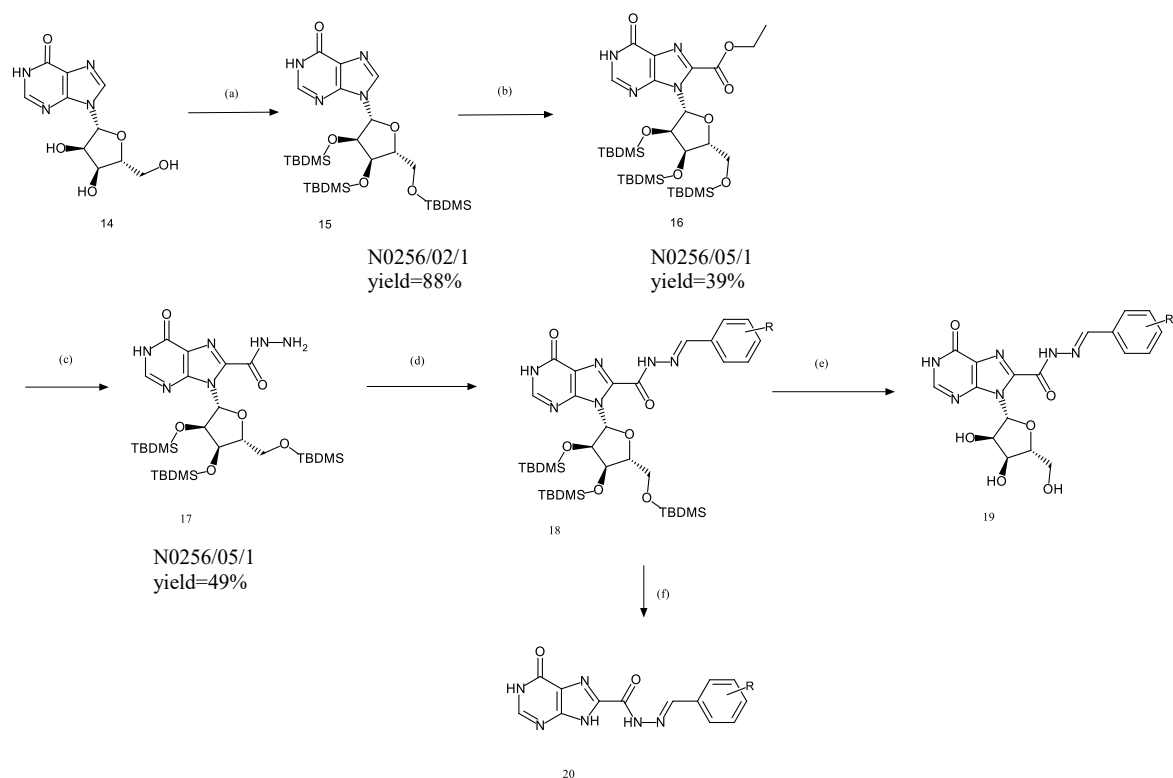


Figure 4.13 NMR analyses

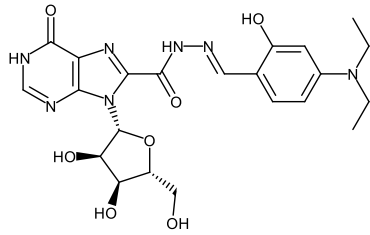
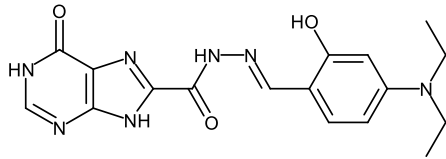
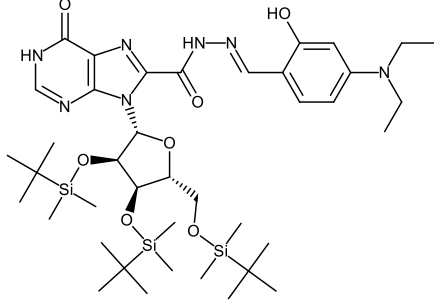
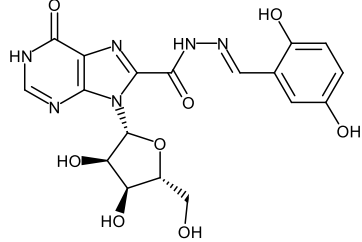
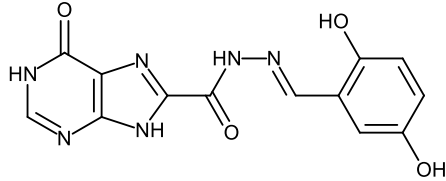
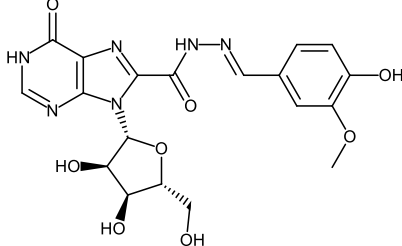
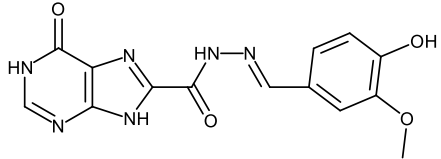
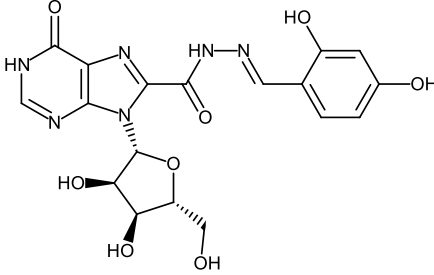
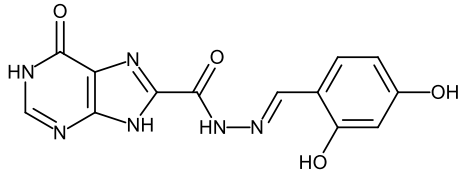
Encouraged by this result the quench was then carried out with ethyl chloroformate (3 equivalents), taking care to dry solvents and reagents with molecular sieves for this step, to obtain the desired ester in good yield. It is recommended to quench the reaction with acetic acid and purify directly in order to avoid an aqueous work up with ammonium chloride,

because these molecules are likely to stay in the aqueous layer. Reaction with hydrazine is then readily performed at ambient temperature to obtain the key hydrazone building block 17. Formation of the hydrazone was achieved by condensing with the appropriate aldehyde to provide an intermediate that could be deprotected with a fluoride salt to selectively remove the silyl protecting groups, or with hydrochloric acid to remove the entire sugar. The silyl deprotection could be effected using the classical TBAF reagent, but in this case subsequent purification was difficult to achieve, therefore triethylammonium fluoride was used which did not present this problem.



Scheme 10. Reagents and conditions: (a) TBDMS-Cl, imidazole, DMF, (b) LDA, -78°C then EtOCOC1, (c) Hydrazine, EtOH, (d) Ar-CHO, EtOH, (e) Et_3NHf , THF, (f) HCl, H_2O

This synthetic approach has been applied, with the appropriate aryl-aldehydes, to provide 11 final compounds (yields 17%-100%). The structures of the compounds, which were all isolated as the E geometric isomers, can be seen in the summary table below (Table 2):

 <p>A/4114/24/1</p>	 <p>A/4114/26/1</p>
 <p>A/4114/20/1</p>	
 <p>A/4114/34/1</p>	 <p>A/4114/32/1</p>
 <p>N0256-27-1</p>	 <p>N0256-28-1</p>
 <p>N0256-17-1</p>	 <p>N0256-25-1</p>

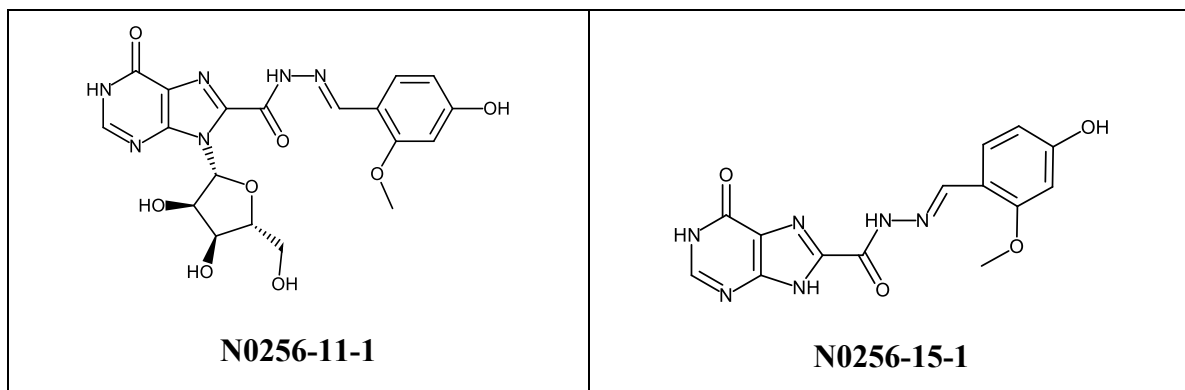


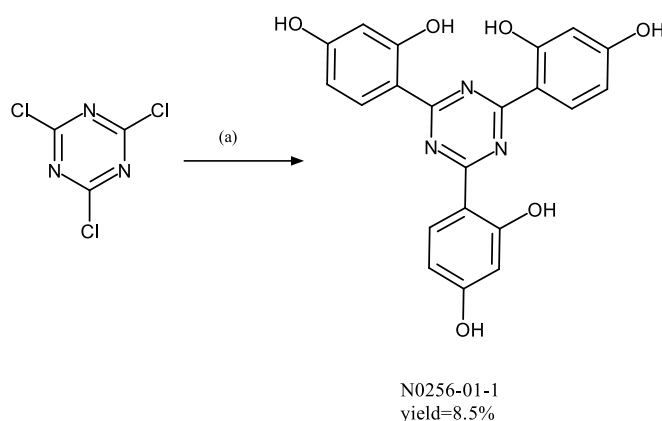
Table 2. Synthesized compounds belonging to Group 2

4.1.4. Group 3: Tinosorb S derivatives

Many UV filters on the market present a triazine moiety as a core substructure. The introduction of antioxidant groups such as polyphenols to this core is expected to endow the molecule with radical scavenging properties. Following this hypothesis two polyphenolic derivatives were synthesized via a Friedel-Crafts reaction between cyanuric trichloride and resorcinol or phloroglucinol in the presence of AlCl_3 ⁵⁵ (Scheme 11 and Scheme 12).

The tri-substituted triazine products were isolated in low to moderate yield (from 8.7% to 54%).

Scheme 11. Reagents and conditions: (a) benzene-1,3-diol, AlCl_3 , 10 min, 0°C ; $0^\circ\text{C} \rightarrow 60^\circ\text{C}$; 6 h, 60°C



Scheme 12. Reagents and conditions: (a) phloroglucinol, AlCl_3 , 10 min, 0°C ; $0^\circ\text{C} \rightarrow 60^\circ\text{C}$; 6 h, 60°C

These two products showed a generally good profile in terms of antioxidant/filter capabilities but they also exhibited a significant issue related to low solubility and were deeply coloured rendering them incompatible for topical formulation.

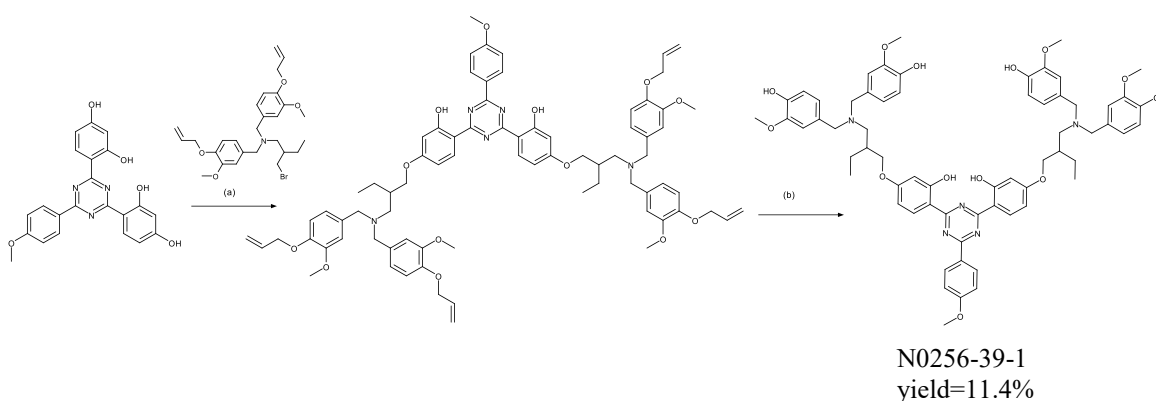
Subsequently, an alternative approach was followed wherein the lipophilic chains of Tinosorb S were functionalised with a group that shows antioxidant properties. For this mix and match strategy vanillinamine was selected as the antioxidant group based on

information reported in the literature and previous studies conducted within the Manfredini research group.

In particular, the literature reports that tertiary amines exhibit greater activity compared to primary amines and imines, which therefore makes a tertiary amine the best choice for this application. In addition, quaternary salts were devoid of any activity, suggesting the importance of the nitrogen lone pair and basicity for the radical scavenging activity.⁴

The phenolic functionality also exhibits an important role on the antioxidant properties, with an increasing number of OH or MeO groups in the molecule leading to improved antioxidant activity. On the contrary, reducing the number of phenolic moieties results in a decrease of activity. So the lipophilic sidechain functionalised with vanillinamine is expected to offer a good balance due to the presence of both a OH and a OMe group, as well as a tertiary amine.⁵⁶

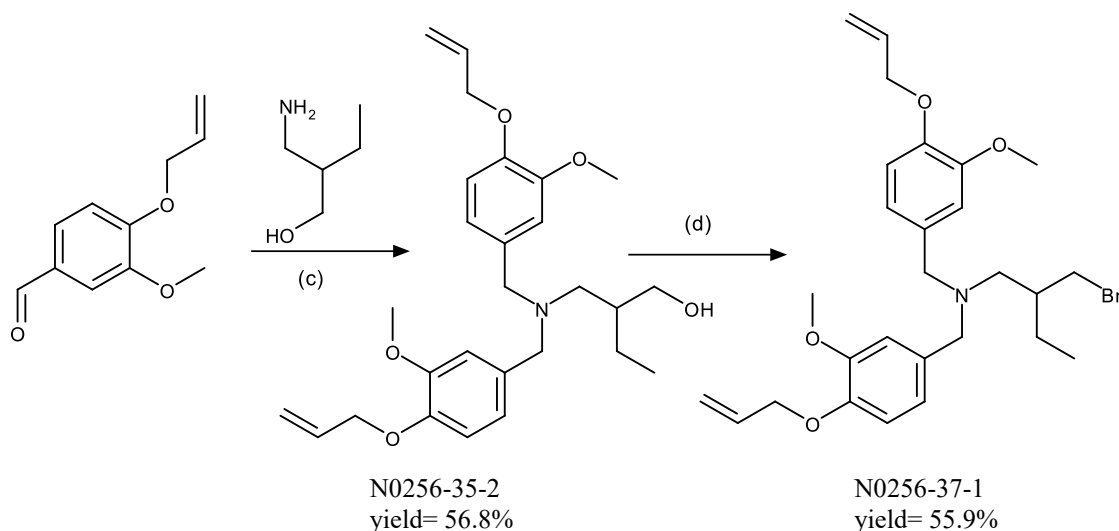
Synthesis of N0256-39-1 was achieved via a convergent synthesis with an alkyl bromide and a phenol as shown in Scheme 13.



Scheme 13. Reagents and conditions: Synthesis of N0256-39-1 (a) K_2CO_3 , DMF, 1 h, 100°C; (b) 10% Pd/C, 10% KOH in MeOH, r.t., 8h

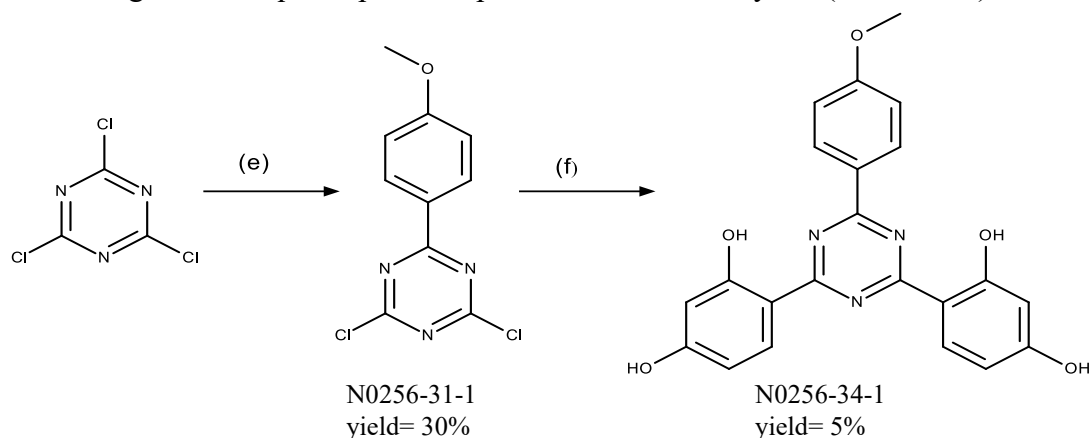
The synthesis of the required alkyl bromide was accomplished by reacting commercially available o-allyl vanillin with the corresponding amine under reductive amination conditions. At first, the conditions reported by Lin⁵⁷ ($NaCNBH_3$, $ZnCl_2$) were tried given the close similarity of the substrates, however, no reaction occurred. Instead this transformation was achieved by reaction of vanillin with the amine in refluxing dioxane in the presence of acetic acid to furnish the imine which was promptly reduced with $Na(AcO)_3BH$ to give the di-vanillin derivative in moderate yield. The alcohol functionality

was subsequently converted into the bromide by using an Appel reaction with CBr_4 and Ph_3P as shown in Scheme 14.



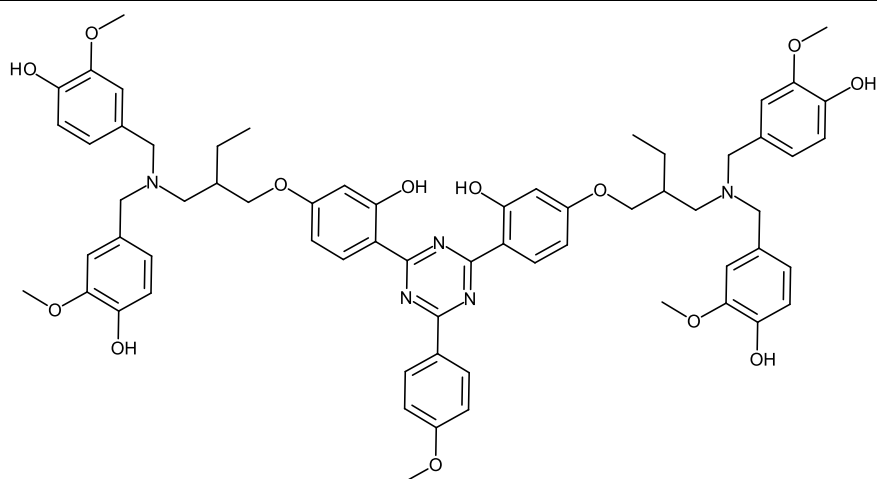
Scheme 14. Synthesis of alkyl bromide. Reagents and conditions: (c) AcOH, dioxane, 1 hr, 100°C; (d) CBr_4 , Ph_3P , DCM, 0°C \rightarrow r.t, 2h

Synthesis of the phenolic portion is reported starting from 2,4,6-trichloro-1,3,5-triazine by a selective Suzuki cross coupling to give the mono substituted triazine,⁵⁸ but all attempts to repeat this procedure gave only traces of the desired product so this approach was abandoned. An alternative to the Suzuki coupling, 2,4,6-trichloro-1,3,5-triazine was reacted with anisole in the presence of AlCl_3 under Friedel-Crafts conditions⁵⁹ to give the mono-arylated triazine in satisfactory yield. Successive further Friedel-Crafts reaction with resorcinol gave the required phenolic portion, albeit in low yield (Scheme 15).

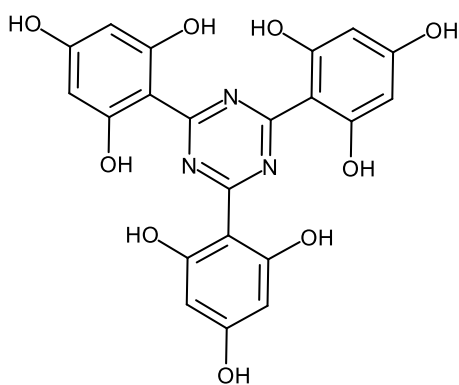


Scheme 15. Synthesis of phenolic portion. Reagents and conditions: (e) AlCl_3 , anisole, resorcinol, DCM, r.t., 2h; (f) resorcinol, AlCl_3 , 40°C, 8h.

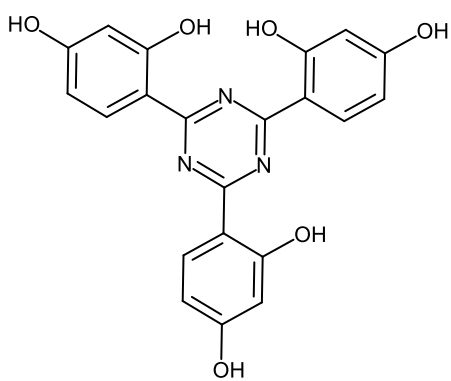
The reaction between the alkyl bromide and the phenolic derivative was achieved in good yield, and the crude isolated product was used directly for the final step. The deprotection of the allyl protecting groups can be effected with different methodologies. For this substrate the use of tetrakis(triphenylphosphine)palladium(0) and K_2CO_3 in methanol at ambient temperature⁵⁹ was found to be compatible and mild enough to obtain the final compound (Scheme 13).



N0256-39-1



N0256-30-1



N0256-01-1

Table 3. Synthesized compounds belonging to Group 3

5. Biological discussion

5.1 Antioxidant capability

All synthesized compounds were evaluated in two different *in vitro* antioxidant assays to verify the antioxidant capacity of the molecule against both oxidant species and free radicals. The reference compound PBSA was also tested to verify its lack of antioxidant activity. The molecules were evaluated in the following assays: DPPH (2,2-diphenyl-1-picryl-hydrazyl radical) and FRAP (Ferric Reducing Antioxidant Power) which are described below.

5.1.1 DPPH Test

DPPH (2,2-diphenyl-1-picryl-hydrazyl) radical is a stable nitrogen-centred free radical characterized by an absorption maximum at 517 nm that decreases in the presence of H-donor molecules. The deep purple colour of the radical changes in the presence of an antioxidant agent. The decreasing absorbance, due to the reduction of the DPPH radical, is used to evaluate free radical scavenging capacity of the compounds. The antioxidant capability of a test article is calculated by measuring the inhibition ratio of the initial concentration of DPPH radical at 517 nm and the remaining concentration after the addition of the test article to this solution. The antioxidant activity of the test articles is expressed as the percentage of inhibition at the concentration tested.

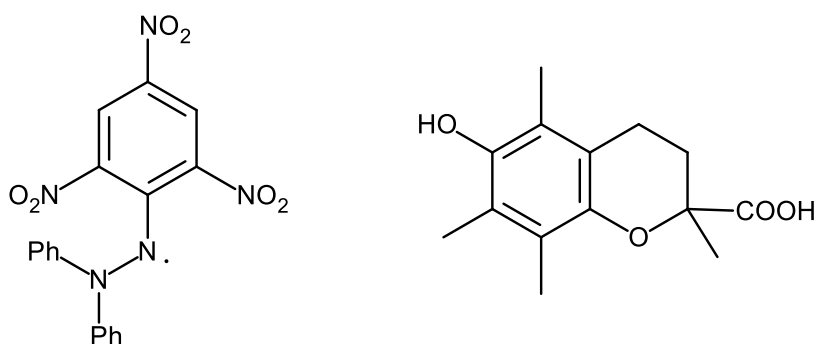
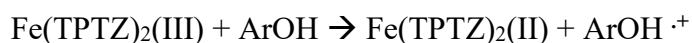


Figure 5.1 The structures of the DPPH radical and Trolox

5.1.2 FRAP Test

This method was initially developed by Benzie and Strain to measure plasma antioxidant power,⁶⁰ but subsequently the use of this method has spread to include the evaluation of the antioxidant power of molecules and extracts. The FRAP (Ferric Reducing Antioxidant Power) assay is based on the reduction of ferric ion (Fe^{3+}) to ferrous ion (Fe^{2+}) in the presence of TPTZ (2,4,6-tris(2-pyridyl)-s-triazine). It is performed at pH 3.6. In the presence of an antioxidant the ferric-tripyridyltriazine complex is reduced to the corresponding ferrous complex. The chemical reaction of the FRAP method for a phenol based antioxidant is the following:



The $\text{Fe}(\text{TPTZ})_2(\text{III})$ complex shows a yellowish colour, but, in the presence of an antioxidant the Fe^{3+} is reduced to the Fe^{2+} form and an intense blue colour with an absorption maximum at 593 nm is observed. The antioxidant activity is determined by measuring the change in absorbance at 593 nm using Trolox as the calibration standard, then results are expressed as micromoles of Trolox equivalents per gram of sample ($\mu\text{mol TE/g}$).⁶¹

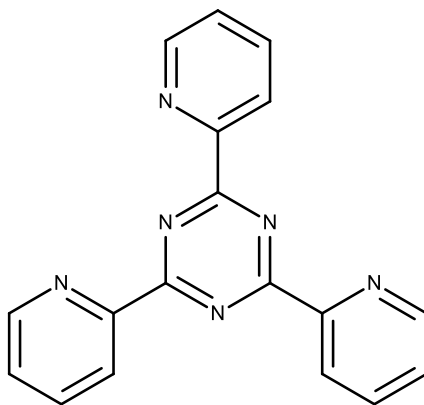


Figure 5.2 The structure of TPTZ

5.2 Results

The results of the antioxidant assays for all synthesized compounds are presented in Table 4. The reference compound PBSA was also tested for comparison. PBSA was inactive in the DPPH assay and it only showed a minimal, almost insignificant, activity in the FRAP assays, therefore the lack of appreciable antioxidant activity of this product was confirmed. The antioxidant power of the newly synthesized compounds changes according to the substitutions on the phenyl ring on the RHS of the compound as reported in Table 4:

Class	Product	FRAP ($\mu\text{mol TE/g}$)	DPPH (% inhibition @ 1 mg/mL)
Class I: without linker	A/2673/2/1	88,70	15
	A/2673/4/1	8494,93	90
	A/2673/6/1	51,09	19
	A/2673/8/1	35,15	8
	A/2673/14/1	BLQ	11
	PBSA	0,79	BLQ
Class II: hydrazone linker	A/4114/20/1	202,95	20
	A/4114/24/1	2490,67	42
	A/4114/26/1	3094,3	87
	A/4114/34/1	340,26	67
	A/4114/32/1	362,28	59
	N0256-11-1	1665,67	46
	N0256-15-1	1676	74
	N0256-27-1	1853,98	85
	N0256-28-1	1128,25	78
	N0256-17-1	212,88	22
N0256-25-1	403,22	70	
Class III: Tinosorb derivatives	N0256-39-1	379,76	71(72)^a
	N0256-30-1	1375,61	84(47)^a
	N0256-01-1	67,20	24(-)
	Tinosorb S	166,94	33

Table 4. Results from FRAP and DPPH Antioxidant assays

^a in brackets the values of the test @ 0.1 mg/mL.

All the synthesised compounds were evaluated for their *in vitro* antioxidant activity in DPPH and FRAP assays. We first evaluated the percentage of inhibition of the DPPH radical by synthesized compounds at the concentration of 1 mg/mL. The threshold of inhibition for the DPPH assay was set to 50% to progress the compounds for the next step of the screening cascade.

Compounds of **Class I** were generally poorly active in this assay apart from compound **A/2673/4/1** which showed a DPPH inhibition of 90% and a FRAP value of 8494 $\mu\text{mol TE/g}$. This suggests that the hydroxyl groups, which are absent in the other derivatives of this class, are very important for the antioxidant activity.

The substituents on the phenyl ring in the **Class II** structures were chosen from previous series, such as benzofuranhydrazones, benzoimidazolehydrazones and indolehydrazones,⁶² where these substitution patterns gave promising results. In general, the compounds without the sugar moiety were found to be active, confirming that also in this purinehydrazone series the presence of electron rich aryl groups like diethylaminophenol (**A/4114/26/1**), polyphenols (**A/4114/32/1**, **A/4114/25/1**), vanillin (**A/4114/28/1**) or its isomer (**A/4114/15/1**) leads to structures possessing scavenging properties.

The literature reports the benefits of D-ribose as an agent for reducing radical formation⁶³. The derivatives containing the sugar group also showed good antioxidant activity, with compounds **A/4114/34/1** and **N0256-27-1** exceeding the 50% inhibition threshold in the DPPH assay. Among the other derivatives **A/4114/24/1** and **N0256-11-1** inhibited just below the threshold and only **N0256-17-1** showed a lower inhibition of just 22%.

Within **Class III**, compound **N0256-01-1**, despite the presence of dihydroxyphenyl, showed a poor antioxidant activity. This result suggests that, in this case, the radical scavenging ability is not dependent only on the number of hydroxyl groups present but also on the rest of the core (compare with **N0256-25-1**). Adding a further hydroxyl group (**N0256-30-1**) restored the activity to good levels. This improvement can be explained by the fact that **N0256-01-1** forms an intramolecular hydrogen bond between the ortho hydroxy and the nitrogen of the triazine, thereby preventing the OH group to be effectively delocalised in the ring. Consequently, the activity of **N0256-01-1** is comparable to the monophenol series, prepared in previous studies, which proved to be poorly active. Derivative **N0256-39-1** was of particular interest, because it showed an inhibition of 71% at 1 mg/mL in the DPPH assay. Repeating the test at a lower concentration (0.1 mg/mL) gave the same high level of inhibition suggesting that inhibition is still in plateau. Thus, it

can be concluded that this compound exhibits the most potent antioxidant activity in the DPPH assay among the group of compounds prepared, and it will be tested at even lower concentrations to determine its IC₅₀ value.

Photoprotective activity

For the evaluation of the effectiveness of a sunscreen only the *in vivo* method is officially accepted by the FDA and COLIPA. Nevertheless, *in vitro* photoprotection studies have been developed because of the high costs, the time intensive nature and the issues related to volunteer recruitment associated with *in vivo* SPF determination.

Therefore, before progressing with a cosmetic formulation the UV spectra of the synthesized compounds were acquired, because SPF is correlated with the UV absorption spectrum. With a UV spectrum it is possible to determine the wavelength of maximum absorption (λ_{max}) and, by using the Beer-Lambert equation, to determine the molar extinction coefficient (ϵ).

$$A = \epsilon \cdot c \cdot d$$

where

A = sample absorbance

ϵ = molar extinction coefficient

c = concentration (mol/L)

d = optical path length (cm)

UV Spectra of the compounds in solution were collected from 290 - 400 nm, the software used automatically determines theoretical SPF, UVAPF, critical wavelength value (λ_c) and UVA/UVB ratio as preliminary data [SPF Calculator Software (version 2.1), Shimadzu, Milan, Italy], which are shown in Table 5.

Class	Product	SPF	UVAPF0	UVA/UVB	λ_c (nm)	ϵ
Class I: without linker	A/2673/2/1	14,00	-	0,10	335	21721
	A/2673/4/1	3,58	-	0,66	377	17882
	A/2673/6/1	10,10	-	0,29	343	20311
	A/2673/8/1	19,23	-	0,00	329	20987
	A/2673/14/1	8,09	-	0,15	329	33165
	PBSA	3,10	1,03	0,29	322	25000
Class II: hydrazone linker	A/4114/20/1	1,43	2,66	1,11	394	32674
	A/4114/24/1	1,65	3,53	1,09	394	27159
	A/4114/26/1	1,98	5,05	1,19	393	22976
	A/4114/34/1	4,50	5,58	1,38	379	20455
	A/4114/32/1	4,82	6,02	1,34	379	14652
	N0256-11-1	3,50	5,35	1,93	370	25690
	N0256-15-1	7,05	7,46	1,85	369	24210
	N0256-27-1	32,79	10,78	1,54	362	75827
	N0256-28-1	2,30	2,00	1,31	359	10537
	N0256-17-1	4,84	7,75	2,03	371	30397
	N0256-25-1	8,04	8,83	1,95	370	24905
Class III: Tinosorb derivatives	N0256-39-1	52,62	14,57	0,69	370	42471
	N0256-30-1	9,85	6,51	2,53	362	52011
	N0256-01-1	19,57	18,92	1,74	369	52171
	Tinosorb S	13,04	6,35	1,09	365	45862

Table 5. Results from photoprotective assays

PBSA is a UVB filter, whereas the aim of this work is to find compounds with the capability of filtering both UVA and UVB. In general, most of the synthesised compounds showed a significant photoprotection activity with respect to PBSA, and the UVB protection is reported as an SPF value.

Compounds of **Class I** are better than the reference compound PBSA, generally exhibiting a good photoprotection profile. Replacement of the benzimidazole core of PBSA with 6-hydroxypurine and substitution of the phenyl ring with pyrrole provides a compound,

A/2673/8/1, with an enhanced SPF value of 19,23. Another interesting combination of isosteric modifications is the replacement of the core of PBSA with benzoxazole and the phenyl ring with thiophene. In fact, A/2673/2/1 has an SPF value of 14. In **Class II** the compounds that bear a OH and/or a OMe moiety are generally slightly more protective than PBSA. The diethylamino group, which is present in A/4114/20/1, A/4114/24/1 and A/4114/26/1, seems to be detrimental for SPF which drops to values < 2 . Surprisingly, **N0256-27-1** was found to have an exceptional SPF value of 32. Compounds of **Class III** are all comparable or better than Tinosorb S with a range of SPF values between 9 and 52. The value of 52 belongs to **N0256-39-1** which is the best SPF value ever achieved within the Manfredini group.

UVAPF0 values indicate the protection offered by a sunscreen product against chronic damage (i.e. tumor formation) induced by UVA. A value of $\geq 1/3$ of the SPF is considered sufficient for protection against UVA by European regulation. The only two compounds which do not meet this requirement are **N0256-39-1**, **N0256-27-1**.

Critical wavelength (λ_c) is the parameter that provides information on the breadth of spectrum of a UV-filter. It is classified in five numerical categories: 0 ($\lambda_c < 325$ nm), 1 ($325 \leq \lambda_c \leq 335$), 2 ($335 \leq \lambda_c \leq 350$), 3 ($350 \leq \lambda_c < 370$) and 4 ($\lambda_c \geq 370$). Our interest is to find compounds with $\lambda_c \geq 370$ nm, and twelve derivatives synthesised in this work belong to category 4. In class I only 1 derivative (A/2673/4/1) is a broad spectrum filter. In class II, apart from 2 derivatives, all the compounds can be considered UVA and UVB filters. In this class the role of the D-ribose seems not to affect the capability of filtering UV rays. Also in class III, N0256-39-1 and N0256-01-1 have acceptable λ_c values of 370 nm and 369 nm, respectively.

It is desirable that the extinction coefficient of the new molecules is > 25000 . Nine compounds meet this requirement, but excellent values ($\epsilon > 40000$) belong to compounds **N0256-27-1** ($\epsilon = 75827$), **N0256-39-1** ($\epsilon = 42471$), **N0256-30-1** ($\epsilon = 52011$) and **N0256-01-1** ($\epsilon = 52171$).

Finally, we determined the UVA/UVB absorbance ratio in order to understand the balance of absorbance through the entire UV spectrum. According to EU recommendations the UVA / UVB ratio should be $> 1/3$. In our case, apart from the members of Class I, all synthesized compounds have good UVA/UVB ratios.

Antiproliferative activity

The compounds A/2673/2/1, A/2673/4/1, A/2673/6/1, A/2673/8/1 and A/2673/14/1 were tested on human melanoma Colo38 cell lines to determine their antiproliferative activity (Table 6). A/2673/4/1 and A/2673/2/1 exhibited the most potent activities of the series, showing an antiproliferative effect on the Colo38 cells at micromolar concentrations (IC_{50} = 60.5 and 91.8 μ M, respectively).

All other compounds showed antiproliferative activities above 200 μ M and were considered poorly active.

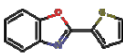
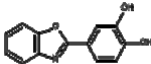
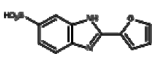
Compound	COLO38 (μ M) IC_{50}
A/2673/2/1	91.8 \pm 4.6
A/2673/4/1	60.5 \pm 3.5
A/2673/6/1	215.4 \pm 20.6
A/2673/8/1	394.5 \pm 29.7
A/2673/14/1	>500

Table 6. Results from antiproliferative assays

Antibacterial activity

The compounds A/2673/2/1, A/2673/4/1, A/2673/14/1 were also tested in vitro for antibacterial activity against a panel of Gram-positive and Gram-negative bacteria, including some strains belonging to the “ESKAPE” panel.

The acronym “ESKAPE” encompasses six pathogens associated with growing multidrug resistance and virulence: *Enterococcus faecium*, *Staphylococcus aureus*, *Klebsiella pneumoniae*, *Acinetobacter baumannii*, *Pseudomonas aeruginosa* and *Enterobacter spp*⁶⁴. ESKAPE pathogens are responsible for the majority of nosocomial infections and are capable of “escaping” the biocidal action of antimicrobial agents.

Strain	Denomination*	Characteristics	APV212299A A/2673/2/1	APV212300A A/2673/4/1	APV212301A A/2673/14/1	Meropenem
						
<i>E. coli</i>	ATCC 25922	Wild Type	>128	>128	>128	≤0.25
	ACC00029	<i>ΔtolC</i>	>128	64	>128	≤0.25
<i>K. pneumoniae</i>	ATCC-BAA-1705	KPC-2	>128	>128	>128	16
	ACC00612	KPC-2	>128	>128	>128	32
	ACC00026	Wild Type	>128	>128	>128	≤0.25
	ACC00027	<i>ΔtolC</i>	>128	64	>128	≤0.25
<i>A. baumannii</i>	ACC00473	Wild Type	>128	128	128	≤0.25
	ACC00474	<i>ΔadeIJK</i>	>128	32	128	≤0.25
	ACC00475	<i>ΔadeABC</i>	>128	128	128	≤0.25
<i>P. aeruginosa</i>	ACC00489	Wild Type	>128	>128	>128	0.5
	ACC00032	<i>ΔmexAB-oprM</i> <i>ΔmexCD-oprJ</i> <i>ΔmexEF-oprN</i>	>128	64	>128	≤0.25
	ACC00490	<i>Δ(mexAB-oprM)</i> <i>Δ(mexCD-oprJ)</i> <i>Δ(mexEF-oprN)</i> <i>Δ(mexJK)</i> <i>Δ(mexXY)</i> <i>ΔopmH</i>	>128	64	>128	≤0.25
<i>S. aureus</i>	ATCC 29213	MSSA	>128	64	>128	≤0.25

<i>S. pneumoniae</i>	ATCC 49619	Pen S	>128	>128	>128	≤0.25
<i>E. faecalis</i>	ATCC 29212	Van-S	>128	128	>128	8
<i>H. influenzae</i>	ACC00021		>128	32	>128	≤0.25
<i>S. cerevisiae</i>	ATCC 7752		>128	>128	>128	>32

* ATCC are reference strains - ACC are clinical Isolates

	CLSI MIC standard value (µg/mL)
	Meropenem
<i>E. coli</i> ATCC25922	0.008-0.06
<i>S. aureus</i> ATCC29213	0.03-0.12
<i>S. pneumoniae</i> ATCC49619	0.03-0.25
<i>E. faecalis</i> ATCC29212	2-8

Table 7. Results from antibacterial assays

From these results it can be seen that bacterial efflux pumps are playing a role in the observed antibacterial activity. Indeed, comparing the MIC values between wild type Gram negative bacteria and isogenic strains in which efflux pumps have been silenced it is observed that A/2673/4/1 showed very low or no antibacterial activity in wild type strains whereas a minimum activity (MIC 32-64 mg/mL) was evident in a number of deletion strains (*E. coli* $\Delta tolC$, *K. pneumoniae* $\Delta tolC$, *A. baumannii* $\Delta adeIJK$, *P. aeruginosa* $\Delta mexAB-oprM$ $\Delta mexCD-oprJ$ $\Delta mexEF-oprN$, *P. aeruginosa* PAOI $\Delta(mexAB-oprM)$ $\Delta(mexCD-oprJ)$ $\Delta(mexEF-oprN)$ $\Delta(mexJK)$ $\Delta(mexXY)$ $\Delta oprM$).

6. Conclusions

The UVA and UVB rays are responsible for both direct damage and the indirect damage caused by radical species. This highlights the importance of providing a complete photoprotection against UV radiation including the scavenging of reactive species.

For this reason, in recent years there has been a trend in sunscreen research to identify molecules with both sunscreen and antioxidant capabilities. To this purpose, this work has focussed on introducing antioxidant capabilities to structures with known UV filtering activity. Among the synthesised molecules, compounds **N0256-39-1** and **N0256-01-1** have emerged as balanced agents with both broad sunscreen and antioxidant properties. In addition, **N0256-27-1** shows an encouraging profile, with high SPF and good antioxidant activity, although its critical lambda falls slightly below the 370 nm requirement. The next step would be to progress these molecules, including them in cosmetic formulations, in order to confirm their UV properties. In the case of a positive outcome, phototoxicity, photostability, cytotoxicity and stability assays will be performed to further assess the value of these compounds.

Tinosorb S and its derivative **N0256-39-1** have validated the principle of mix and match between antioxidants and sunscreens, and have opened new opportunities for further development of structures belonging to **Class III**. The profile of **N0256-39-1** is very promising because it improved the already excellent properties of Tinosorb S. In fact, **N0256-39-1** has an SPF of 52, 4-fold higher than that of Tinosorb S. In addition, it has gained the critical antioxidant properties that the reference compound lacked.

The chemical approach developed to synthesize the key intermediate is suitable for future exploration and expansion of the SAR.

All the compounds which showed >50% inhibition in the DPPH assay will be sent for IC₅₀ determination.

In conclusion, the objectives of my PhD, to find new molecules with both photoprotective and radical scavenging properties, were achieved and I hope these molecules can have a long life in the cosmetic world.

7. Experimental Section

7.1 General Methods

All solvents used were commercially available and were used without further purification. Reactions were typically run using anhydrous solvents under an inert atmosphere of nitrogen.

Analytical Methods

^1H and ^{13}C nuclear magnetic resonance (NMR) spectroscopy were carried out using one of the following instruments: a Bruker Avance 400 instrument equipped with probe DUAL 400MHz S1, a Bruker Avance 400 instrument equipped with probe 6 S1 400 MHz 5mm ^1H - ^{13}C ID, a Bruker Avance III 400 instrument with nanobay equipped with probe Broadband BBFO 5 mm direct, a 400 MHz Agilent Direct Drive instrument with ID AUTO-X PFG probe, all operating at 400 MHz, or an Agilent VNMRS500 Direct Drive instrument equipped with a 5 mm Triple Resonance $^1\text{H}\{^{13}\text{C}/^{15}\text{N}\}$ cryoprobe operating at 500 MHz for ^1H and 125 MHz for ^{13}C . The spectra were acquired in the stated solvent at around room temperature unless otherwise stated. In all cases, NMR data were consistent with the proposed structures. Characteristic chemical shifts (δ) are given in parts-per-million using conventional abbreviations for designation of major peaks: e.g. s, singlet; d, doublet; t, triplet; q, quartet; dd, doublet of doublets; dt, doublet of triplets; br, broad.

Where thin layer chromatography (TLC) has been used it refers to silica gel TLC using silica gel F254 (Merck) plates, R_f is the distance travelled by the compound divided by the distance travelled by the solvent on a TLC plate. Column chromatography was performed using an automatic flash chromatography (Biotage SP1 or Isolera) system over Biotage silica gel cartridges (KP-Sil or KP-NH) or in the case of reverse phase chromatography over Biotage C18 cartridges (KP-C18).

Total ion current (TIC) and DAD UV chromatographic traces together with MS and UV spectra associated with the peaks were taken on a UPLC/MS AcquityTM system equipped with PDA detector and coupled to a Waters single quadrupole mass spectrometer operating in alternated positive and negative electrospray ionization mode. [LC/MS-ES (+/-): analyses performed using an Acquity UPLCTM CSH, C18 column (50 × 2.1mm, 1.7 μm particle size), column temperature 40 °C, mobile phase: A-water + 0.1% HCOOH/ B- CH₃CN + 0.1% HCOOH, flow rate: 1.0 mL/min, runtime = 2.0 min,

gradient: t=0 min 3%B, t= 1.5 min 99.9% B, t = 1.9 min 99.9% B, t= 2.0 min 3% B, stop time 2.0 min. Positive ES 100-1000, Negative ES 100-1000, UV detection DAD 210-350 nm].

The identities of the compounds were determined by UPLC-MS, using electrospray ionization and the values are expressed as m/z (mass over charge), and NMR techniques. UV spectrophotometric analyses were carried out on a UV-VIS spectrophotometer (Shimadzu UV-2600) or on a Life Science UV/VIS spectrophotometer (Beckman Coulter™, DU®530, Single Cell Module).

Compound preparation

Where the preparation of starting materials is not described, these are commercially available, known in the literature, or readily obtainable by those skilled in the art using standard procedures. Where it is stated that compounds were prepared analogously to earlier examples or intermediates, it will be appreciated by the skilled person that the reaction time, number of equivalents of reagents and temperature can be modified for each specific reaction and that it may be necessary or desirable to employ different work-up or purification techniques. Where reactions are carried out using microwave irradiation, the microwave used is a Biotage Initiator. The actual power supplied varies during the course of the reaction in order to maintain a constant temperature.

Liquid Chromatography-Mass Spectrometry Method A

Instrument Name: MDAP_Fractionlynx; Method Description: Semi preparative MDAP Method; LC/MS System: Fractionlynx (Waters) with ZQ MS detector; LC/MS

Conditions:

Column: XSelect CSH Prep. C18 5 µm OBD 30 x 100 mm @ r.t.; Loop volume: 1 ml

Solvents: A = 10 mM aqueous ammonium bicarbonate solution adjusted to pH 10 with ammonia; B = Acetonitrile

Gradient:

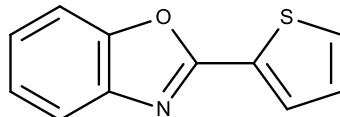
Time (min)	Flow Rate	% A	% B	Curve
------------	-----------	-----	-----	-------

	(ml/min)			
initial	40.0	90.0	10.0	-
10.0	40.0	40.0	60.0	6
10.5	40.0	0.0	100.0	6
14.5	40.0	0.0	100.0	6
15.0	40.0	90.0	10.0	6

The curve parameter followed Waters definition (6 = linear, 11 = step); Acquisition stop time: 15 min; UV Conditions: UV detection range: 210 nm to 350 nm; Acquisition rate: 1.0 spectra/s; MS Conditions: Ionisation mode: Positive Electrospray (ES+); Scan Range: ES+ 100 to 900 AMU; Scan Duration: 0.50 seconds.

7.2 Synthetic Procedures

7.2.1. Synthesis of 2-(thiophen-2-yl)-1,3-benzoxazole (A/2673/2/1):



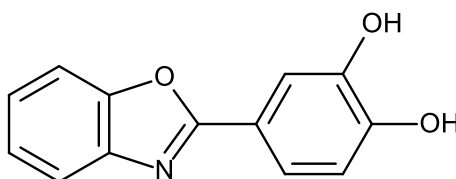
A mixture of 2-chlorobenzoxazole (300mg 1.95mmol), 2-thienylboronic acid (375mg 2.94mmol), potassium acetate (288mg 2.948mmol), and PdCl₂(Amphos)₂ (27mg) in dioxane/water (6.5ml/1.24mL) was stirred at 100° C in a screw-capped glass vial for 12 h. The reaction was cooled to ambient temperature and extracted with organic solvent (ether). The organic extract was subjected to an aqueous workup (1 N NaOH solution was used to facilitate removal of excess boronic acid), dried over anhydrous Na₂SO₄, and concentrated under vacuum. The crude material was purified by column chromatography on silica gel (from 100% Cy to 50/50 Cy/AcOEt) to afford the target compound 2-(thiophen-2-yl)-1,3-benzoxazole as white powder (122mg, 0.61mmol, 31% yield).

LC-MS: $m/z = 202.07$ [M+H]⁺, 1.11 min.

¹H NMR (400 MHz, DMSO-*d*₆) δ 8.02 – 7.92 (m, 2H), 7.79 – 7.72 (m, 2H), 7.43 – 7.38 (m, 2H), 7.32 (dd, $J = 4.9, 3.7$ Hz, 1H).

¹³C NMR (101 MHz, DMSO-*d*₆) δ ppm 158.32, 149.86, 141.37, 131.94, 130.51, 128.88, 128.48, 125.42, 124.98, 119.49, 110.74.

7.2.2. Synthesis of 4-(1,3-benzoxazol-2-yl)benzene-1,2-diol (A/2673/4/1):



3,4-Dihydroxybenzoic acid (369mg, 2.40mmol), 2-aminophenol (216mg, 1.98mmol), and p-TsOH.H₂O (1.90g, 10.0mmol) were stirred in refluxing xylenes (4mL). After 18 h

the reaction was cooled, extracted into AcOEt (5mL), and washed with saturated NaHCO₃ (2x5mL) and brine (5mL). The organics were then dried over Na₂SO₄, filtered, and concentrated to afford a crude.

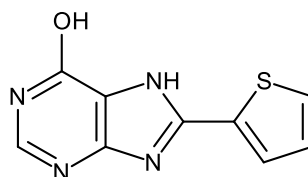
This crude was purified by silica gel chromatography (from 100% Cy to 50/50 Cy/AcOEt in 12 CV) to afford 4-(1,3-benzoxazol-2-yl)benzene-1,2-diol as a white solid (136mg, 0.6mmol, 30% yield).

LC-MS: $m/z = 228.15$ [M+H]⁺, 0.86 min.

¹H NMR (400 MHz, DMSO-*d*₆) δ 9.57 (b, 2H), 7.75 – 7.66 (m, 2H), 7.58 (d, $J = 2.1$ Hz, 1H), 7.53 (dd, $J = 8.2, 2.1$ Hz, 1H), 7.39 – 7.28 (m, 2H), 6.92 (d, $J = 8.3$ Hz, 1H).

¹³C NMR (101 MHz, DMSO-*d*₆) δ ppm 162.84, 150.01, 149.51, 145.77, 141.79, 124.61, 124.51, 119.62, 119.18, 117.31, 116.11, 114.26, 110.51.

7.2.3. Synthesis of 8-(thiophen-2-yl)-7H-purin-6-ol (A/2673/6/1):



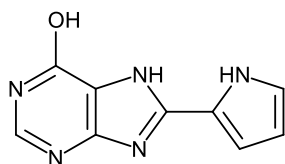
4,5-Diamino-6-hydroxypyrimidine (150mg, 1.19mmol) was dissolved in DMSO (6mL). A solution of 2-thiophenecarboxaldehyde (180mg, 0.66mmol) in 0.5 mL of DMSO was added dropwise over 3 min. followed by 1 equivalent of concentrated H₂SO₄ and the reaction mixture was heated to 80°C overnight. Ice was added to the mixture reaction and the precipitated solid was collected by filtration. The solid was washed with water/diethyl ether (1/1) and then the collected solid was purified by C-18 chromatography (from 100% water+0.1% formic acid to 100% ACN+0.1% formic acid in 12 CV) to afford the target compound 8-(thiophen-2-yl)-7H-purin-6-ol as a white solid (52mg, 0.24mmol, 20% yield).

LC-MS: $m/z = 219.1$ [M+H]⁺, 0.48 min.

¹H NMR (400 MHz, DMSO-*d*₆) δ 13.61 (s, 1H), 12.24 (s, 1H), 7.99 (s, 1H), 7.86 (s, 1H), 7.72 (dd, $J = 5.0, 1.2$ Hz, 1H), 7.20 (dd, $J = 5.0, 3.7$ Hz, 1H).

¹³C NMR (126 MHz, DMSO-*d*₆) δ ppm 155.96, 153.47, 152.20, 145.40, 133.01, 129.43, 128.73, 127.30, 116.28.

7.2.4. Synthesis of 8-(thiophen-2-yl)-7H-purin-6-ol (A/2673/8/1):



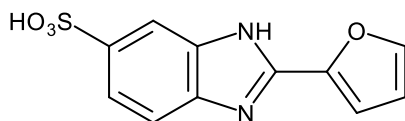
A mixture of 4,5-diamino-6-hydroxypyrimidine (300mg, 2.37mmol) in DMF (5mL) was treated with iron(III) chloride hexahydrate (160mg, 0.6mmol), followed by 2-pyrrolaldehyde (271mg, 2.85mmol). The reaction mixture was heated to 80°C for 16 h in a sealed vessel, then cooled to room temperature. The reaction mixture was concentrated and the residue was purified by preparative HPLC (Liquid Chromatography-Mass Spectrometry Method A) to give the target compound 8-(1H-pyrrol-2-yl)-7H-purin-6-ol (52mg, 0.26mmol, 11% yield).

LC-MS: $m/z = 202.09$ $[M+H]^+$, 0.43 min.

^1H NMR (400 MHz, $\text{DMSO-}d_6$) δ 13.25 (s, 1H), 12.16 (s, 1H), 11.75 (s, 1H), 7.94 (s, 1H), 6.91 (s, 2H), 6.16 (q, $J = 2.6$ Hz, 1H).

^{13}C NMR (101 MHz, $\text{DMSO-}d_6$) δ ppm 157.57, 153.73, 150.05, 144.38, 121.94, 121.60, 116.27, 116.69, 109.21.

7.2.5. Synthesis of 2-(furan-2-yl)-1H-1,3-benzodiazole-6-sulfonic acid (A/2673/14/1):



In 22mL of ethanol, 3,4-diaminobenzenesulfonic acid (300mg, 1.6mmol), furfural (153mg 1.6mmol), and sodium bisulfite (332mg, 3.2mmol) were mixed. The reaction was placed at 80 °C for 24 hours. After having evaporated the solvent, the crude product was treated with 5 mL of 5N aqueous HCl solution. The precipitate was then collected by filtration and the product was recrystallized from methanol to give a crude that was purified by preparative HPLC (Liquid Chromatography-Mass Spectrometry Method A) to

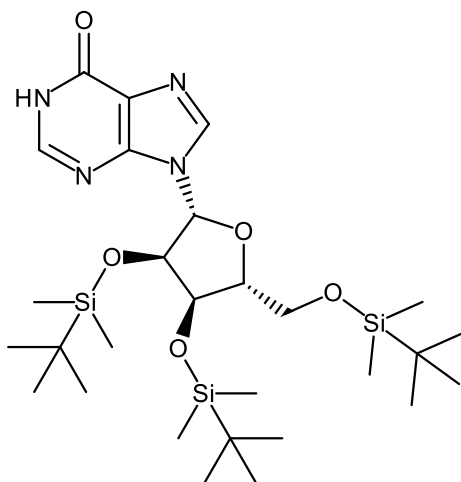
obtain the target compound 2-(furan-2-yl)-1H-1,3-benzodiazole-6-sulfonic acid (132mg, 0.5mmol, 31% yield).

LC-MS: $m/z = 219.1$ $[M+H]^+$, 0.48 min.

^1H NMR (400 MHz, $\text{DMSO-}d_6$) δ 8.25 (d, $J = 1.7$ Hz, 1H), 7.90 (d, $J = 1.3$ Hz, 1H), 7.78 – 7.68 (m, 2H), 7.60 (d, $J = 3.6$ Hz, 1H), 6.93 (dd, $J = 3.6, 1.8$ Hz, 1H), exchangeable protons not visible.

^{13}C NMR (101 MHz, $\text{DMSO-}d_6$) δ ppm 147.90, 146.05, 141.44, 140.08, 132.89, 132.02, 123.40, 116.19, 113.47, 110.94.

7.2.6. Synthesis of 9-[(2R,3R,4R,5R)-3,4-bis[(tert-butyl dimethylsilyl)oxy]-5-[(tert-butyl dimethylsilyl)oxy]methyl]oxolan-2-yl]-6,9-dihydro-1H-purin-6-one (N0256/02/1):



tert-Butyldimethylsilyl chloride (8.99g, 59.65mmol) was added to a stirred solution of (2R,3S,4R,5R)-2-(hydroxymethyl)-5-(6-hydroxypurin-9-yl)oxolane-3,4-diol (4.0g, 14.91mmol) and imidazole (8.12g, 119.3mmol) in DMF (75 mL). The reaction mixture was heated at 50°C overnight. Volatiles were removed and the residue was partitioned between ethyl acetate and saturated NaHCO_3 solution. The organic phase was separated and the aqueous layer was extracted three times with ethyl acetate. The organic phases were combined, dried over sodium sulfate, filtered and concentrated. The residue was purified by silica gel chromatography (from 100% Cy to 90/10 Cy/AcOEt in 12CV) to

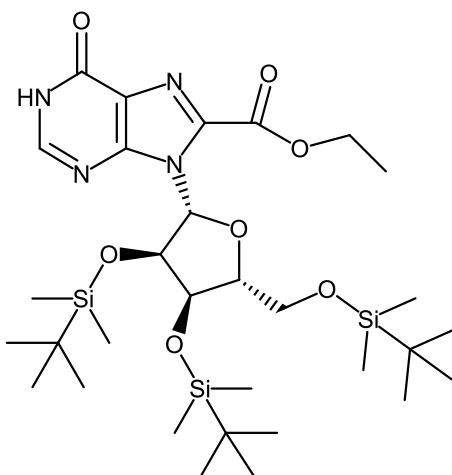
obtain the target compound 9-[(2R,3R,4R,5R)-3,4-bis[(tert-butyl(dimethyl)silyl)oxy]-5-[[tert-butyl(dimethyl)silyl]oxymethyl]oxolan-2-yl]-6,9-dihydro-1H-purin-6-one as a white solid (8.04g, 13.16mmol, 88% yield) as white solid.

LC-MS: $m/z = 611.6$ $[M+H]^+$, 1.82 min.

$^1\text{H NMR}$ (400 MHz, Chloroform- d) δ 11.61 (s, 1H), 8.22 (s, 1H), 7.99 (s, 1H), 6.01 (d, $J = 5.0$ Hz, 1H), 4.50 (t, $J = 4.7$ Hz, 1H), 4.30 (t, $J = 4.0$ Hz, 1H), 4.16 – 4.08 (m, 1H), 3.99 (dd, $J = 11.4, 3.7$ Hz, 1H), 3.80 (dd, $J = 11.4, 2.6$ Hz, 1H), 0.92 (s, 9H), 0.90 (s, 9H), 0.81 (s, 9H), 0.13 (s, 3H), 0.11 (s, 3H), 0.09 (s, 6H), -0.02 (s, 3H), -0.19 (s, 3H).

7.2.7. Ethyl

9-[(2R,3R,4R,5R)-3,4-bis[(tert-butyl(dimethyl)silyl)oxy]-5-[[tert-butyl(dimethyl)silyl]oxymethyl]oxolan-2-yl]-6-oxo-6,9-dihydro-1H-purine-8-carboxylate (N0256/05/1):



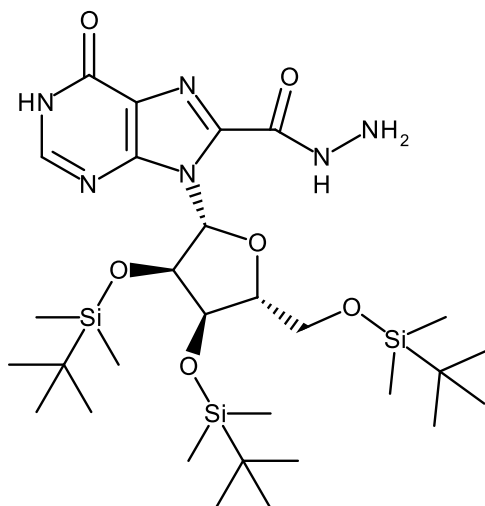
2.0 M in THF/heptane/ethylbenzene LDA solution (32.9mL, 65.79mmol) was placed in a three-necked flask equipped with a gas-inlet adaptor, a thermometer, and a rubber septum. To this solution was added a mixture of 9-[(2R,3R,4R,5R)-3,4-bis[[tert-butyl(dimethyl)silyl]oxy]-5-[[tert-butyl(dimethyl)silyl]oxymethyl]oxolan-2-yl]purin-6-ol (8.04g, 13.16mmol) in THF (130mL), under positive pressure of nitrogen, at such a rate that the temperature did not exceed -70°C . The mixture was stirred for 1.5 h below -70°C , then ethyl chloroformate (3.77mL, 39.48mmol) was added and the reaction mixture was stirred for a further 3 h. The reaction was then quenched by addition of acetic acid (3.77mL, 65.79mmol). Evaporation of the solvent followed by silica gel chromatography

(from 100% DCM to 95/5 DCM/EtOH in 12CV) furnished the target compound ethyl 9-[(2R,3R,4R,5R)-3,4-bis[(tert-butyl(dimethyl)silyl)oxy]-5-[[tert-butyl(dimethyl)silyl]oxymethyl]oxolan-2-yl]-6-oxo-6,9-dihydro-1H-purine-8-carboxylate (3.54g, 5.182mmol, 39% yield).

LC-MS: $m/z = 681.5 [M+H]^+$, 1.87 min.

1H NMR (400 MHz, Chloroform- d) δ 8.24 (s, 1H), 7.08 (d, $J = 8.1$ Hz, 1H), 5.80 (d, $J = 7.8$ Hz, 1H), 4.88 (td, $J = 8.0, 4.7$ Hz, 2H), 4.48 (qd, $J = 7.0, 2.8$ Hz, 1H), 4.32 (d, $J = 4.9$ Hz, 1H), 4.17 (s, 1H), 3.99 – 3.83 (m, 1H), 3.71 (t, $J = 12.0$ Hz, 1H), 0.96 – 0.96 (m, 12H), 0.77 (s, 9H), 0.75 (s, 9H), 0.12 (s, 3H), 0.11 (s, 3H), -0.10 (s, 3H), -0.11 (s, 3H), -0.52 (s, 3H), -0.60 (s, 3H).

7.2.8. Synthesis of 9-[(2R,3R,4R,5R)-3,4-bis[(tert-butyl(dimethyl)silyl)oxy]-5-[[tert-butyl(dimethyl)silyl]oxymethyl]oxolan-2-yl]-6-oxo-6,9-dihydro-1H-purine-8-carboxamide (N0256/06/1):



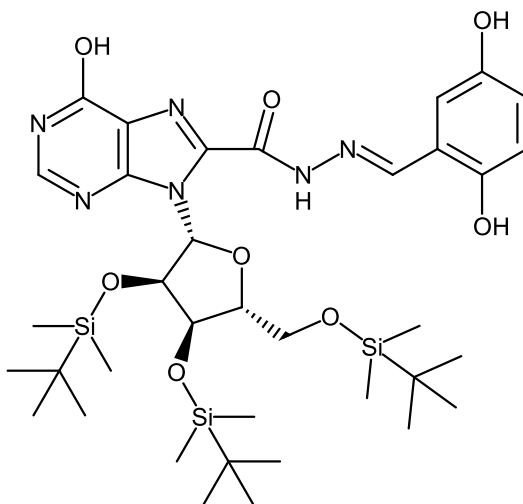
Ethyl 9-[(2R,3R,4R,5R)-3,4-bis[[tert-butyl(dimethyl)silyl]oxy]-5-[[tert-butyl(dimethyl)silyl]oxymethyl]oxolan-2-yl]-6-oxo-6,9-dihydro-1H-purine-8-carboxylate (3.54g, 5.18mmol) was dissolved in MeOH (10mL) and hydrazine hydrate 50-60 % (2.0mL, 120mmol) was added. The mixture was stirring over the weekend at room temperature. After evaporation of the solvent, the residue was chromatographed on silica gel (from

100% Cy to 50/50 Cy/AcOEt in 10 CV and then DCM/EtOH 90/10 for 6CV) to afford the target compound 9-[(2R,3R,4R,5R)-3,4-bis[(tert-butyldimethylsilyl)oxy]-5-[[tert-butyldimethylsilyl]oxy]methyl]oxolan-2-yl]-6-oxo-6,9-dihydro-1H-purine-8-carbohydrazide (1.7g, 2.54mmol, 49% yield) as a yellow solid.

LC-MS: $m/z = 669.4$ $[M+H]^+$, 1.72 min.

1H NMR (500 MHz, DMSO- d_6) δ -0.36 - 0.16 (m, 18 H), 0.67 - 0.97 (m, 27 H), 3.64 (dd, $J = 10.8, 4.5$ Hz, 1 H), 3.90 (ddd, $J = 7.4, 4.4, 3.0$ Hz, 1 H), 3.95 - 3.98 (m, 1 H), 4.49 (dd, $J = 4.7, 3.0$ Hz, 1 H), 5.40 (dd, $J = 5.8, 4.7$ Hz, 1 H), 6.87 (d, $J = 5.8$ Hz, 1 H), 8.11 (s, 1 H), hydrazine protons not visible.

7.2.9. Synthesis of 9-[(2R,3R,4R,5R)-3,4-bis[(tert-butyldimethylsilyl)oxy]-5-[[tert-butyldimethylsilyl]oxy]methyl]oxolan-2-yl]-N'-[(E)-(2,5-dihydroxyphenyl)methylidene]-6-hydroxy-9H-purine-8-carbohydrazide (A/4114/22/1):

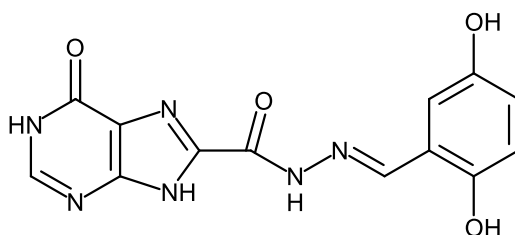


9-[(2R,3R,4R,5R)-3,4-Bis[[tert-butyl(dimethyl)silyl]oxy]-5-[[tertbutyl(dimethyl)silyl]oxymethyl]oxolan-2-yl]-6-hydroxypurine-8-carbohydrazide (1000mg, 1.53mmol) was dissolved in ethanol (7mL) and 2,5-dihydroxybenzaldehyde (561mg, 2.70mmol) was added. The mixture was heated and stirred at 80 °C for 6 hours then the solid was filtered off and dried to obtain crude target product that was used directly in the next step. 9-[(2R,3R,4R,5R)-3,4-bis[(tert-butyldimethylsilyl)oxy]-5-[[tert-butyldimethylsilyl]oxy]methyl]oxolan-2-yl]-N'-[(E)-(2,5-dihydroxyphenyl)methylidene]-6-

-hydroxy-9H-purine-8-carbohydrazide (921mg, 1.17mmol, 43% yield).

LC-MS: $m/z = 788.7$ $[M+H]^+$, 1.76 min.

7.2.10. Synthesis of N'-[(E)-(2,5-dihydroxyphenyl)methylidene]-6-oxo-6,9-dihydro-1H-purine-8-carbohydrazide (A/4114/32/1):



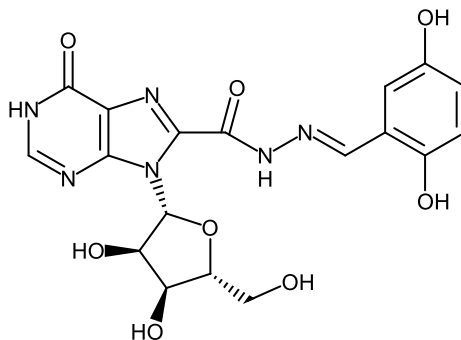
9-[(2R,3R,4R,5R)-3,4-bis[(tert-butyl dimethylsilyl)oxy]-5-[(tert-butyl dimethylsilyl)oxy]methyl}oxolan-2-yl]-N'-[(E)-(2,5-dihydroxyphenyl)methylidene]-6-hydroxy-9H-purine-8-carbohydrazide (460.0mg, 0.580mmol) was dissolved in THF (3mL) and 4M HCl in dioxane (0.58mL, 2.33mmol) was added. The reaction mixture was stirred overnight at r.t. A massive precipitation was observed, so diethyl ether was added and the solid was filtered off and then washed several times with diethyl ether. The obtained solid was collected and put under vacuum to afford the target compound N'-[(E)-(2,5-dihydroxyphenyl)methylidene]-6-oxo-6,9-dihydro-1H-purine-8-carbohydrazide (85mg, 0.27mmol, 46% yield).

LC-MS: $m/z = 315.19$ $[M+H]^+$, 0.73 min.

^1H NMR (500 MHz, DMSO- d_6) δ 6.72 - 6.77 (m, 2 H), 6.94 (d, $J = 2.4$ Hz, 1 H), 8.07 (d, $J = 3.2$ Hz, 1 H), 8.73 (s, 1 H), 12.41 (br. s., 1 H), 12.68 (s, 1H), exchangeable protons not visible.

^{13}C NMR (101 MHz, DMSO- d_6) δ ppm 162.54, 155.70, 154.97, 150.24, 148.15, 145.21, 142.57, 141.81, 120.54, 119.52, 118.15, 117.88, 113.39.

7.2.11. Synthesis of 9-[(2R,3R,4S,5R)-3,4-dihydroxy-5-(hydroxymethyl)oxolan-2-yl]-N'-[(E)-(2,5-dihydroxyphenyl)methylidene]-6-oxo-6,9-dihydro-1H-purine-8-carbohydrazide (A/4114/34/1):



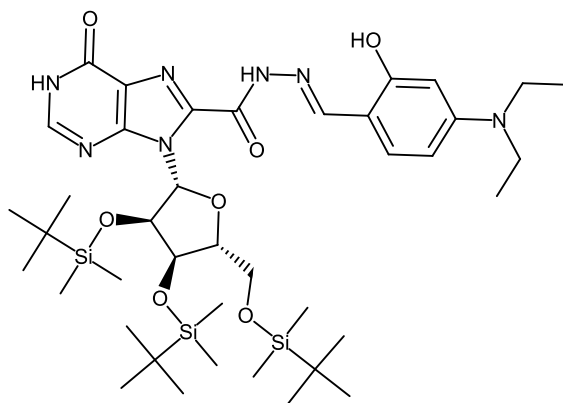
9-[(2R,3R,4R,5R)-3,4-Bis[(tert-butyl dimethylsilyl)oxy]-5-[(tert-butyl dimethylsilyl)oxy]methyl]oxolan-2-yl]-N'-[(E)-(2,5-dihydroxyphenyl)methylidene]-6-hydroxy-9H-purine-8-carbohydrazide (460mg, 0.58mmol) was dissolved in THF (3mL) and triethylammonium fluoride (0.333mL, 2.03mmol) was added. The mixture was stirred overnight at r.t and then the volatiles were removed under vacuum. The obtained solid was purified by C-18 chromatography to afford the target compound 9-[(2R,3R,4S,5R)-3,4-dihydroxy-5-(hydroxymethyl)oxolan-2-yl]-N'-[(E)-(2,5-dihydroxyphenyl)methylidene]-6-oxo-6,9-dihydro-1H-purine-8-carbohydrazide (84mg, 0.19mmol, 32% yield).

LC-MS: $m/z = 447.17$ $[M+H]^+$, 0.72 min.

^1H NMR (400 MHz, $\text{DMSO-}d_6$) δ 12.69 (s, 2H), 10.32 (s, 1H), 9.00 (s, 1H), 8.73 (s, 1H), 8.22 (s, 1H), 6.95 (d, $J = 2.1$ Hz, 1H), 6.81 (d, $J = 6.0$ Hz, 1H), 6.79 – 6.75 (m, 2H), 5.35 (d, $J = 6.3$ Hz, 1H), 5.14 (d, $J = 5.2$ Hz, 1H), 4.98 – 4.89 (m, 2H), 4.23 (q, $J = 4.9$ Hz, 1H), 3.93 (q, $J = 4.5$ Hz, 1H), 3.75 – 3.65 (m, 1H), 3.59 – 3.50 (m, 1H).

^{13}C NMR (101 MHz, $\text{DMSO-}d_6$) δ ppm 161.08, 156.56, 151.54, 150.24, 148.15, 147.06, 142.19, 139.29, 124.52, 120.4, 118.15, 117.88, 113.39, 87.65, 85.24, 72.36, 70.25, 60.87

7.2.12. Synthesis of 9-[(2R,3R,4R,5R)-3,4-bis[(tert-butyl dimethylsilyl)oxy]-5-([dimethyl(propan-2-yl)silyl]oxy)methyl]oxolan-2-yl]-N'-[(E)-[4-(diethylamino)-2-hydroxyphenyl]methylidene]-6-oxo-6,9-dihydro-1H-purine-8-carbohydrazide (A/4114/20/1):



9-[(2R,3R,4R,5R)-3,4-Bis[[tert-butyl(dimethyl)silyl]oxy]-5-[[tertbutyl(dimethyl)silyl]oxymethyl]oxolan-2-yl]-6-hydroxypurine-8-carbohydrazide (1000mg, 1.53mmol) was dissolved in ethanol (7mL) and 4-diethylamino-2-hydroxybenzaldehyde (349mg, 1.8mmol) was added. The mixture was heated and stirred at 80°C for 6 hours, then the solid was filtered off, and dried to obtain crude target compound that was used directly in the next step.

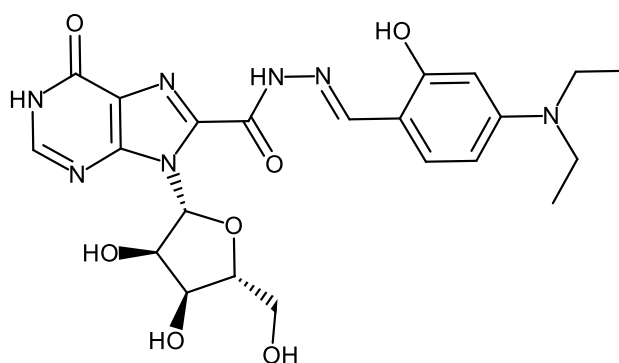
9-[(2R,3R,4R,5R)-3,4-bis[(tert-butyl dimethylsilyl)oxy]-5-[[tert-butyl dimethylsilyl]oxy]methyl}oxolan-2-yl]-N'-[(E)-(2,5-dihydroxyphenyl)methylidene]-6-hydroxy-9H-purine-8-carbohydrazide (340mg, 0.40mmol, 27% yield) as a yellow solid.

LC-MS: $m/z = 841.54$ [M+H]⁺, 3.04 min.

¹H NMR (400 MHz, DMSO-*d*₆) δ 12.45 (bs, 2H), 11.34 (s, 1H), 8.56 (s, 1H), 8.15 (s, 1H), 7.17 (d, *J* = 8.8 Hz, 1H), 6.86 (d, *J* = 5.9 Hz, 1H), 6.28 (dd, *J* = 8.9, 2.4 Hz, 1H), 6.13 (d, *J* = 2.5 Hz, 1H), 5.45 (t, *J* = 5.2 Hz, 1H), 4.57 – 4.46 (m, 1H), 4.01 (dd, *J* = 11.0, 7.2 Hz, 1H), 3.97 – 3.89 (m, 1H), 3.66 (dd, *J* = 10.7, 4.3 Hz, 1H), 3.37 (q, *J* = 7.2 Hz, 4H), 1.12 (t, *J* = 7.0 Hz, 6H), 0.94 (s, 9H), 0.82 (s, 9H), 0.76 (s, 9H), 0.15 (s, 3H), 0.14 (s, 3H), 0.00 (s, 3H), -0.04 (s, 3H), -0.08 (s, 3H), -0.32 (s, 3H).

¹³C NMR (101 MHz, DMSO-*d*₆) δ ppm 161.28, 159.62, 156.31, 151.09, 150.77, 146.78, 143.17, 137.67, 127.2, 125.18, 110.45, 104.94, 99.85, 88.20, 85.20, 76.20, 74.52, 62.4, 44.21x2, 25.78x3, 25.75x3, 25.66x3, 19.47, 17.88, 17.25, 12.91x2, -4.50x2, -4.75x2, -5.67x2.

7.2.13. Synthesis of N'-[(E)-[4-(diethylamino)-2-hydroxyphenyl]methylidene]-9-[(2R,3R,4S,5R)-3,4-dihydroxy-5-(hydroxymethyl)oxolan-2-yl]-6-oxo-6,9-dihydro-1H-purine-8-carbohydrazide (A/4114/24/1):



9-[(2R,3R,4R,5R)-3,4-bis[[tert-butyl(dimethyl)silyl]oxy]-5-[[tert-butyl(dimethyl)silyl]oxymethyl]oxolan-2-yl]-N-[(E)-[4-(diethylamino)-2-hydroxyphenyl]methylideneamino]-6-hydroxypurine-8-carboxamide (200mg, 0.23mmol) was dissolved in THF (3.2mL) and N,N-diethylethanamine; trihydrofluoride (0.135mL, 0.83mmol) was added. The mixture was stirring overnight at r.t and then the volatiles were removed under vacuum. The solid obtained was purified by C-18 chromatography to afford The solid obtained was purified by C-18 chromatography (from 100% water+0.1%formic acid to 50/50 water+0.1%formic acid/ acetonitrile +0.1%formic acid) to afford 9-[(2R,3R,4R,5R)-3,4-bis[[tert-butyl(dimethyl)silyl]oxy]-5-[[tert-butyl(dimethyl)silyl]oxymethyl]oxolan-2-yl]-N-[(E)-[4-(diethylamino)-2-hydroxyphenyl]methylideneamino]-6-hydroxypurine-8-carboxamide (83 mg, 0.17 mmol, 70% yield) as pale-yellow solid.

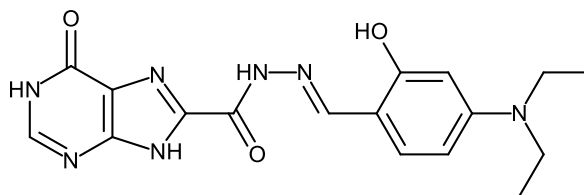
LC-MS: $m/z = 502.48 [M+H]^+$, 0.68 min.

$^1\text{H NMR}$ (400 MHz, $\text{DMSO-}d_6$) δ 12.54 (d, $J = 8.5$ Hz, 2H), 11.40 (bs, 1H), 8.57 (s, 1H), 8.20 (s, 1H), 7.16 (d, $J = 8.7$ Hz, 1H), 6.83 (d, $J = 6.1$ Hz, 1H), 6.28 (d, $J = 8.7$ Hz, 1H), 6.13 (s, 1H), 5.34 (d, $J = 6.1$ Hz, 1H), 5.14 (d, $J = 5.0$ Hz, 1H), 5.01 – 4.85 (m, 2H), 4.28 – 4.15 (m, 1H), 3.99 – 3.85 (m, 1H), 3.74 – 3.63 (m, 1H), 3.60 – 3.47 (m, 1H), 2.92 (d, $J = 10.9$ Hz, 4H), 1.11 (t, $J = 7.0$ Hz, 6H).

$^{13}\text{C NMR}$ (101 MHz, $\text{DMSO-}d_6$) δ ppm 161.08, 159.62, 156.56, 151.54, 151.09, 147.06, 143.17, 139.29, 127.2, 124.52, 110.45, 104.94, 99.85, 87.65, 85.24, 72.36, 70.25, 60.87, 44.21x2, 12.91x2.

7.2.14. Synthesis of N'-[(E)-[4-(diethylamino)-2-hydroxyphenyl]methylidene]-9-[(2R,3R,4S,5R)-3,4-

**dihydroxy-5-(hydroxymethyl)oxolan-2-yl]-6-oxo-6,9-dihydro-1H-purine-8-carbohydra-
zide (A/4114/26/1):**



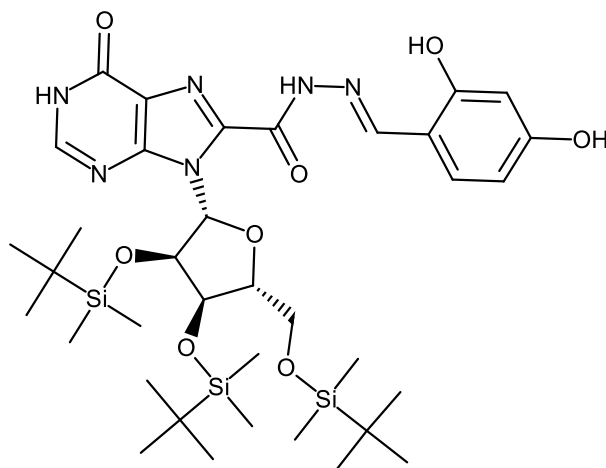
9-[(2R,3R,4R,5R)-3,4-bis[[tert-butyl(dimethyl)silyl]oxy]-5-[[tert-butyl(dimethyl)silyl]oxymethyl]oxolan-2-yl]-N-[(E)-[4-(diethylamino)-2-hydroxyphenyl]methylideneamino]-6-hydroxypurine-8-carboxamide (100mg, 0.120mmol) was dissolved in THF (1.4mL) and hydrogen chloride 4M in dioxane (0.12 mL, 0.470 mmol) was added. The mixture reaction was stirred overnight r.t. A massive precipitation was observed, so diethyl ether was added and the solid was filtered off and then it was washed several times with ether. The solid obtained was collected and put under vacuum to afford N-[(E)-[4-(diethylamino)-2-hydroxyphenyl]methylideneamino]-6-hydroxy-9H-purine-8-carboxamide (35 mg, 0.095 mmol, 80% yield) as a pale yellow solid.

LC-MS: $m/z = 370.38 [M+H]^+$, 0.71 min.

$^1\text{H NMR}$ (400 MHz, $\text{DMSO-}d_6$) δ 12.41 (s, 3H), 8.61 (s, 1H), 8.16 – 8.02 (m, 2H), 7.20 (s, 1H), 6.32 (s, 1H), 6.16 (s, 1H), 3.39 (q, $J = 6.6$ Hz, 4H), 1.11 (t, $J = 7.0$ Hz, 6H).

$^{13}\text{C NMR}$ (101 MHz, $\text{DMSO-}d_6$) δ ppm 162.54, 159.62, 155.7, 154.97, 151.09, 146.77, 145.21, 141.81, 127.2, 119.52, 110.28, 104.94, 99.85, 44.21x2, 12.91x2.

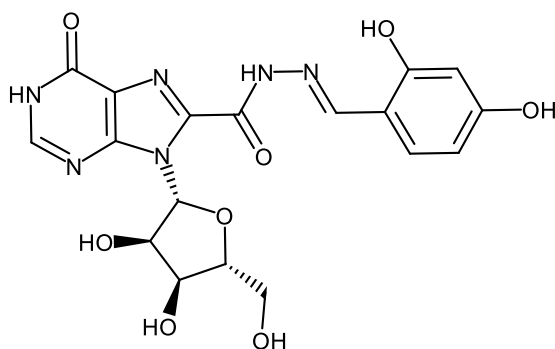
7.2.15. Synthesis of 9-[(2R,3R,4R,5R)-3,4-bis[(tert-butyl)dimethylsilyl]oxy]-5-[[tert-butyl)dimethylsilyl]oxy]methyl}oxolan-2-yl]-N'-[(E)-(2,4-dihydroxyphenyl)methylidene]-6-oxo-6,9-dihydro-1H-purine-8-carbohydrazide (N0256-07-1):



9-[(2R,3R,4R,5R)-3,4-bis[[Tert-butyl(dimethyl)silyl]oxy]-5-[[tert-butyl(dimethyl)silyl]oxymethyl]oxolan-2-yl]-6-hydroxypurine-8-carbohydrazide (300mg, 0.450mmol) was dissolved in ethanol (2mL) and 2,4-dihydroxybenzaldehyde (74.32mg, 0.540mmol) was added. The mixture was heated at 120°C for 24 hours, then a solid was filtered off to obtain the crude target compound 9-[(2R,3R,4R,5R)-3,4-bis[(tert-butyl dimethylsilyl)oxy]-5- {[tert-butyl dimethylsilyl)oxy]methyl} oxolan-2-yl]-N'-[(E)-(2,4-dihydroxyphenyl)methylidene]-6-oxo-6,9-dihydro-1H-purine-8-carbohydrazide (63mg, 0.080mmol, 17.8% yield) that was used directly in the next step.

LC-MS: $m/z = 788.47$ $[M+H]^+$, 1.80 min.

7.2.16. Synthesis of 9-[(2R,3R,4S,5R)-3,4-dihydroxy-5-(hydroxymethyl)oxolan-2-yl]-N'-[(E)-(2,4-dihydroxyphenyl)methylidene]-6-oxo-6,9-dihydro-1H-purine-8-carbohydrazide (N0256-17-1):



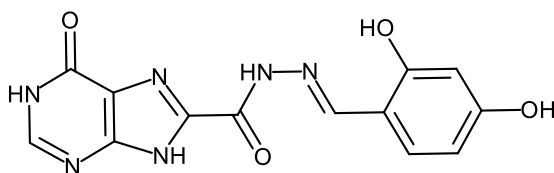
9-[(2R,3R,4R,5R)-3,4-bis[[Tert-butyl(dimethyl)silyl]oxy]-5-[[tert-butyl(dimethyl)silyl]oxymethyl]oxolan-2-yl]-N-[(E)-(2,4-dihydroxyphenyl)methylideneamino]-6-hydroxypurine-8-carboxamide (100mg, 0.130mmol) was dissolved in THF (1.086mL) and N,N-diethylethanamine trihydrofluoride (0.07mL, 0.440mmol) was added. The mixture was stirring overnight at r.t. and then the volatiles were removed under vacuum. The solid obtained was purified by C-18 chromatography (from 100% water+0.1%formic acid to 50/50 water+0.1%formic acid/acetonitrile+0.1%formic acid) to afford the target compound 9-[(2R,3R,4R,5R)-3,4-bis[[tert-butyl(dimethyl)silyl]oxy]-5-[[tert-butyl(dimethyl)silyl]oxymethyl]oxolan-2-yl]-N-[(E)-(2,4-dihydroxyphenyl)methylideneamino]-6-hydroxypurine-8-carboxamide (15mg, 0.130mmol, 26.5% yield) as white solid.

LC-MS: $m/z = 447.2 [M+H]^+$, 0.52 min.

^1H NMR (500 MHz, $\text{DMSO-}d_6$) δ ppm 3.52 (ddd, $J = 12.1, 7.1, 5.2$ Hz, 1 H), 3.69 (dt, $J = 11.9, 4.6$ Hz, 1 H), 3.91 (q, $J = 4.6$ Hz, 1 H), 4.16 - 4.26 (m, 1 H), 4.87 - 4.98 (m, 2 H), 5.14 (d, $J = 5.2$ Hz, 1 H), 5.35 (d, $J = 6.3$ Hz, 1 H), 6.32 (d, $J = 2.2$ Hz, 1 H), 6.37 (dd, $J = 8.5, 2.2$ Hz, 1 H), 6.81 (d, $J = 6.0$ Hz, 1 H), 7.28 (d, $J = 8.5$ Hz, 1 H), 8.20 (s, 1 H), 8.62 - 8.71 (m, 1 H), 10.03 (s, 1 H), 11.38 (s, 1 H), 12.43 - 12.94 (m, 2 H).

^{13}C NMR (125 MHz, $\text{DMSO-}d_6$) δ ppm 161.51, 160.16, 156.86, 154.80, 151.48, 150.09, 147.67, 140.85, 132.10, 124.38, 110.88, 108.31, 103.14, 89.77, 86.36, 72.47, 70.94, 62.51.

7.2.17. Synthesis of N'-[(E)-(2,4-dihydroxyphenyl)methylidene]-6-oxo-6,9-dihydro-1H-purine-8-carboxamide (N0256-25-1):



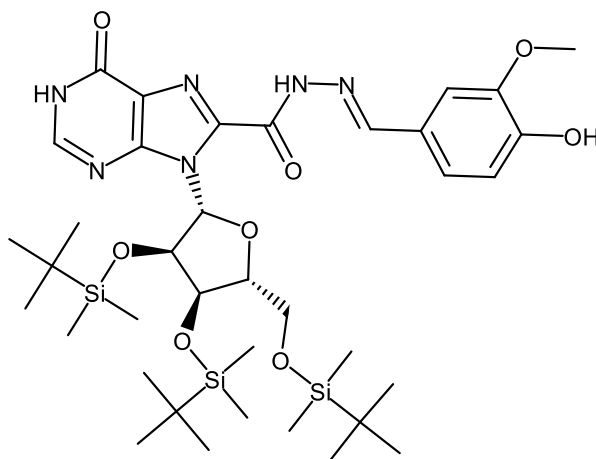
9-[(2R,3R,4R,5R)-3,4-bis[[Tert-butyl(dimethyl)silyl]oxy]-5-[[tert-butyl(dimethyl)silyl]oxymethyl]oxolan-2-yl]-N'-[(E)-(2,4-dihydroxyphenyl)methylideneamino]-6-hydroxypurine-8-carboxamide (120mg, 0.150 mmol) was dissolved in THF (1.7mL) and a 4M solution of hydrogen chloride in dioxane (0.15mL, 0.610mmol) was added. The mixture reaction was stirred overnight r.t. A massive precipitation was observed, so diethyl ether was added and the solid was filtered off and then it was washed a several times with diethyl ether. The solid obtained was collected and dried under vacuum to afford the target compound N'-[(E)-(2,4-dihydroxyphenyl)methylidene]-6-oxo-6,9-dihydro-1H-purine-8-carbohydrazide (9 mg, 0.029mmol, 19% yield) as a white solid.

LC-MS: $m/z = 315.18$ $[M+H]^+$, 0.53 min.

^1H NMR (400 MHz, $\text{DMSO}-d_6$) δ ppm 6.31 (d, $J = 2.2$ Hz, 1 H), 6.36 (dd, $J = 8.5, 2.3$ Hz, 1 H), 7.25 (d, $J = 8.6$ Hz, 1 H), 8.03 (s, 1 H), 8.66 (s, 1 H), 9.90 - 12.73 (m, 4 H), 13.18 - 14.69 (m, 1 H).

^{13}C NMR (125 MHz, $\text{DMSO}-d_6$) 162.54, 161.19, 160.47, 155.70, 154.97, 146.84, 145.21, 141.81, 130.77, 119.52, 110.85, 109.06, 102.36.

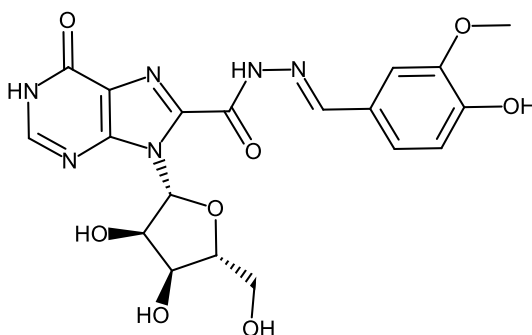
7.2.18. Synthesis of 9-[(2R,3R,4R,5R)-3,4-bis[(tert-butyldimethylsilyl)oxy]-5-[(tert-butyldimethylsilyl)oxymethyl]oxolan-2-yl]-N'-[(E)-(4-hydroxy-3-methoxyphenyl)methylidene]-6-oxo-6,9-dihydro-1H-purine-8-carbohydrazide (N0256-14-1):



9-[(2R,3R,4R,5R)-3,4-bis[[Tert-butyl(dimethyl)silyl]oxy]-5-[[tert-butyl(dimethyl)silyl]oxymethyl]oxolan-2-yl]-6-hydroxypurine-8-carbohydrazide (250.0mg, 0.370mmol) was dissolved in ethanol (1.7mL) and 4-hydroxy-3-methoxybenzaldehyde (68.22mg, 0.450mmol) was added. The mixture was heated at 80°C for 24 hours, then the solid was filtered off and dried to obtain crude target product that was used directly in the next step. 9-[(2R,3R,4R,5R)-3,4-bis[[tert-butyl(dimethyl)silyl]oxy]-5-[[tert-butyl(dimethyl)silyl]oxymethyl]oxolan-2-yl]-N'-[(E)-4-hydroxy-3-methoxyphenyl]methylidene]-6-oxo-6,9-dihydro-1H-purine-8-carbohydrazide (256mg, 0.319mmol, 85.3% yield).

LC-MS: $m/z = 803.73[M+H]^+$, 3.04min.

7.2.19. Synthesis of 9-[(2R,3R,4S,5R)-3,4-dihydroxy-5-(hydroxymethyl)oxolan-2-yl]-N'-[(E)-(4-hydroxy-3-methoxyphenyl)methylidene]-6-oxo-6,9-dihydro-1H-purine-8-carbohydrazide (N0256-27-1):



9-[(2R,3R,4R,5R)-3,4-bis[[Tert-butyl(dimethyl)silyl]oxy]-5-[[tert-butyl(dimethyl)silyl]oxymethyl]oxolan-2-yl]-6-hydroxy-N-[(E)-(4-hydroxy-3-

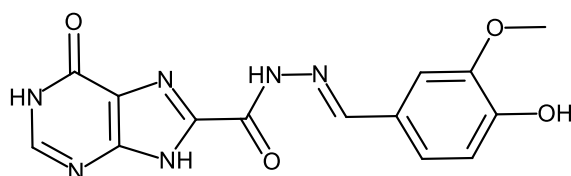
methoxyphenyl)methylideneamino]purine-8-carboxamide (100mg, 0.120mmol) was dissolved in THF (0.943mL) and triethylammonium fluoride (0.44mL, 0.440mmol) was added. The mixture was stirring overnight at r.t. and then the volatiles were removed under vacuum. The obtained solid was purified by C-18 chromatography to afford the target compound 9-[(2R,3R,4R,5R)-3,4-bis[[tert-butyl(dimethyl)silyl]oxy]-5-[[tert-butyl(dimethyl)silyl]oxymethyl]oxolan-2-yl]-6-hydroxy-N-[(E)-(4-hydroxy-3-methoxyphenyl)methylideneamino]purine-8-carboxamide (100.0mg, 0.120mmol, 47% yield).

LC-MS: $m/z = 461.35 [M+H]^+$, 0.71 min.

^1H NMR (500 MHz, $\text{DMSO-}d_6$) δ 3.53 (ddd, $J=12.1, 7.0, 5.4$ Hz, 1 H), 3.69 (ddd, $J=11.8, 4.6, 4.5$ Hz, 1 H), 3.84 (s, 3 H), 3.92 (q, $J=4.4$ Hz, 1 H), 4.16 - 4.26 (m, 1 H), 4.86 - 4.99 (m, 2 H), 5.13 (d, $J=5.1$ Hz, 1 H), 5.35 (d, $J=6.3$ Hz, 1 H), 6.77 (d, $J=6.0$ Hz, 1 H), 6.85 (d, $J=8.1$ Hz, 1 H), 7.08 (dd, $J=8.2, 1.6$ Hz, 1 H), 7.31 (d, $J=1.5$ Hz, 1 H), 8.20 (s, 1 H), 8.46 (s, 1 H), 9.61 (s, 1 H), 12.32 (s, 1 H), 12.66 (br s, 1 H).

^{13}C NMR (125 MHz, $\text{DMSO-}d_6$) δ ppm 156.4, 154.6, 150.1, 149.5, 149.3, 148.0, 147.1, 141.0, 125.5, 123.8, 122.4, 115.5, 109.1, 89.3, 85.9, 72.0, 70.5, 62.1, 55.5.

7.2.20. Synthesis of N'-[(E)-(4-hydroxy-3-methoxyphenyl)methylidene]-6-oxo-6,9-dihydro-1H-purine-8-carboxamide (N0256-28-1):



9-[(2R,3R,4R,5R)-3,4-bis[[Tert-butyl(dimethyl)silyl]oxy]-5-[[tert-butyl(dimethyl)silyl]oxymethyl]oxolan-2-yl]-6-hydroxy-N-[(E)-(4-hydroxy-3-methoxyphenyl)methylideneamino]purine-8-carboxamide (120.0mg, 0.150mmol) was dissolved in THF (1.7mL) and a 4M solution of HCl in dioxane (0.15mL, 0.600mmol) was added. The mixture reaction was stirred overnight r.t. A massive precipitation was

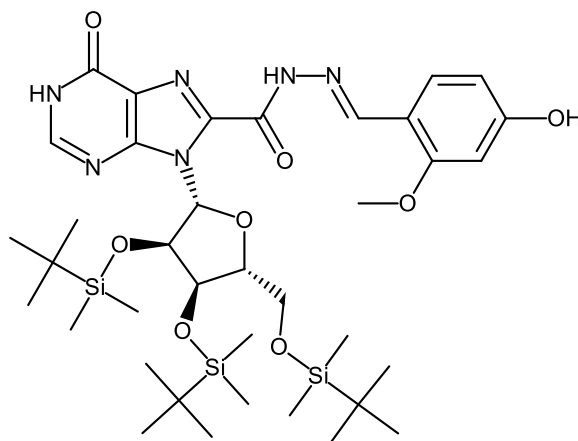
observed, so diethyl ether was added and the solid was filtered off and then washed several times with diethyl ether. The obtained solid was collected and purified by preparative HPLC (Liquid Chromatography-Mass Spectrometry Method A) to afford the target compound 6-hydroxy-N-[(E)-(4-hydroxy-3-methoxyphenyl)methylideneamino]-9H-purine-8-carboxamide (12mg, 0.037mmol, 24.47% yield).

LC-MS: $m/z = 329.25$ $[M+H]^+$, 0.51 min.

^1H NMR (600 MHz, $\text{DMSO-}d_6$) δ 3.84 (s, 3 H), 6.84 (d, $J = 8.1$ Hz, 1 H), 7.05 (dd, $J = 8.1, 1.5$ Hz, 1 H), 7.29 (d, $J = 1.3$ Hz, 1 H), 7.89 (s, 1 H), 8.33 (br s, 1 H), 8.46 (s, 1 H), 9.64 (br s, 1 H), 11.89 (br s, 1 H), 9-NH not visible.

^{13}C NMR (151 MHz, $\text{DMSO-}d_6$) δ ppm 55.54, 104.5, 108.98, 115.42, 122.05, 123.8, 126.26, 141.0, 147.99, 148.37, 148.94, 157.59x2, 164.

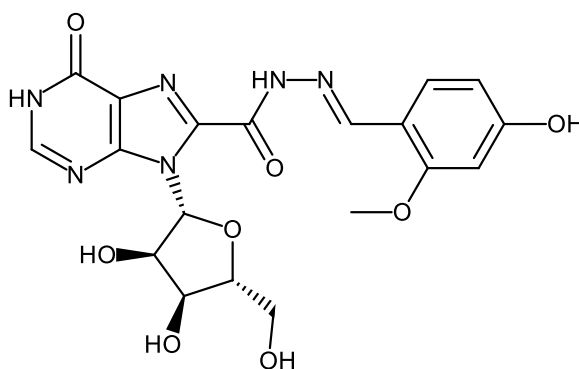
7.2.21. Synthesis of 9-[(2R,3R,4R,5R)-3,4-bis[(tert-butyl dimethylsilyl)oxy]-5-[[tert-butyl dimethylsilyl]oxymethyl]oxolan-2-yl]-N'-[(E)-(4-hydroxy-2-methoxyphenyl)methylidene]-6-oxo-6,9-dihydro-1H-purine-8-carbohydrazide (N0256-08-1):



9-[(2R,3R,4R,5R)-3,4-bis[[Tert-butyl(dimethyl)silyl]oxy]-5-[[tert-butyl(dimethyl)silyl]oxymethyl]oxolan-2-yl]-6-hydroxypurine-8-carbohydrazide (300.0mg, 0.450 mmol) was dissolved in ethanol (2mL) and 4-hydroxy-2-methoxybenzaldehyde (81.87 mg, 0.540mmol) was added. The mixture was heated at 80°C for 24 hours, then the solid was filtered off and dried to obtain crude target product that

was used directly in the next step. 9-[(2R,3R,4R,5R)-3,4-bis[(tert-butyl(dimethyl)silyl)oxy]-5-[(tert-butyl(dimethyl)silyl)oxymethyl]oxolan-2-yl]-N'-[(E)-(4-hydroxy-2-methoxyphenyl)methylidene]-6-oxo-6,9-dihydro-1H-purine-8-carbohydrazide (116mg, 0.144mmol, 32.21% yield). LC-MS: m/z = 801.50 [M+H]⁺, 1.77 min.

7.2.22. Synthesis of 9-[(2R,3R,4S,5R)-3,4-dihydroxy-5-(hydroxymethyl)oxolan-2-yl]-N'-[(E)-(4-hydroxy-2-methoxyphenyl)methylidene]-6-oxo-6,9-dihydro-1H-purine-8-carbohydrazide (N0256-11-1):



9-[(2R,3R,4R,5R)-3,4-bis[[Tert-butyl(dimethyl)silyl]oxy]-5-[[tert-butyl(dimethyl)silyl]oxymethyl]oxolan-2-yl]-6-hydroxy-N'-[(E)-(4-hydroxy-2-methoxyphenyl)methylideneamino]purine-8-carboxamide (53.0mg, 0.070mmol) was dissolved in THF (0.500mL) and triethylammonium fluoride (0.231mL, 0.231mmol) was added. The mixture was stirring overnight at r.t. and then the volatiles were removed under vacuum. The obtained solid was purified by C-18 chromatography to afford the target compound

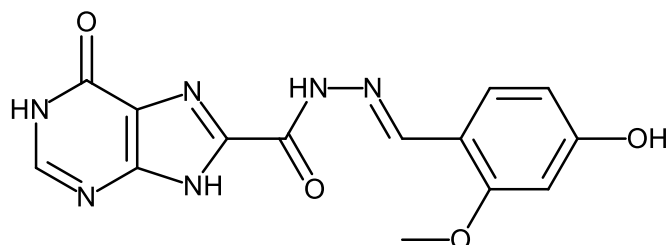
9-[(2R,3R,4S,5R)-3,4-dihydroxy-5-(hydroxymethyl)oxolan-2-yl]-N'-[(E)-(4-hydroxy-2-methoxyphenyl)methylidene]-6-oxo-6,9-dihydro-1H-purine-8-carbohydrazide (32mg, 0.070 mmol, 100% yield).

LC-MS: $m/z = 461.19 [M+H]^+$, 0.52 min.

^1H NMR (500 MHz, $\text{DMSO-}d_6$) δ 3.49 - 3.56 (m, 1 H), 3.68 (dt, $J = 11.8, 4.3$ Hz, 1 H), 3.79 (s, 3 H), 3.91 (q, $J = 4.6$ Hz, 1 H), 4.17 - 4.25 (m, 1 H), 4.91 (q, $J = 5.5$ Hz, 1 H), 4.93 - 5.01 (m, 1 H), 5.14 (br d, $J = 4.7$ Hz, 1 H), 5.36 (br d, $J = 6.0$ Hz, 1 H), 6.42 - 6.52 (m, 2 H), 6.73 (d, $J = 6.0$ Hz, 1 H), 7.70 (d, $J = 9.1$ Hz, 1 H), 8.19 (s, 1 H), 8.80 (s, 1 H), 9.73 - 13.26 (m, 2 H), 12.31 (s, 1 H).

^{13}C NMR (126 MHz, $\text{DMSO-}d_6$) δ ppm 55.56, 62.07, 70.48, 72.03, 85.86, 89.29, 98.97, 108.36, 113.36, 123.76, 126.94, 141.11, 145.74, 147.12, 149.52, 154.58, 156.54, 159.64, 161.39.

7.2.23. Synthesis of N'-[(E)-(4-hydroxy-2-methoxyphenyl)methylidene]-6-oxo-6,9-dihydro-1H-purine-8-carboxamide (N0256-15-1):



9-[(2R,3R,4R,5R)-3,4-bis[[Tert-butyl(dimethyl)silyl]oxy]-5-[[tert-butyl(dimethyl)silyl]oxymethyl]oxolan-2-yl]-6-hydroxy-N-[(E)-(4-hydroxy-2-methoxyphenyl)methylideneamino]purine-8-carboxamide (150.0mg, 0.180mmol) was dissolved in THF (2mL) and a 4M solution of HCl in dioxane (0.18mL, 0.710mmol) was added. The mixture reaction was stirred overnight r.t. A massive precipitation was observed, so diethyl ether was added and the solid was filtered off and the was washed several times with diethyl ether. The obtained solid was collected and dried under vacuum to afford the target compound

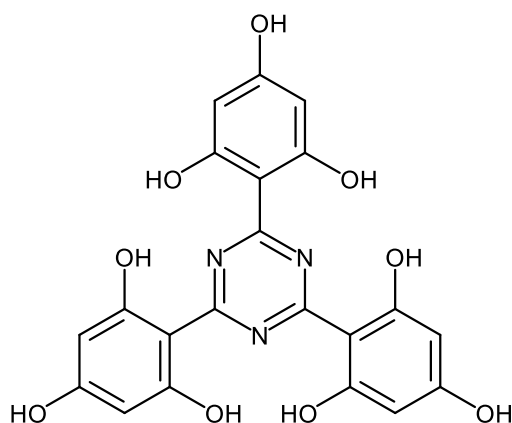
N'-[(E)-(4-hydroxy-2-methoxyphenyl)methylidene]-6-oxo-6,9-dihydro-1H-purine-8-carbohydrazide (53mg, 0.161mmol, 91% yield).

LC-MS: $m/z = 329.09$ $[M+H]^+$, 0.51 min.

^1H NMR (400 MHz, $\text{DMSO-}d_6$) δ 3.80 (s, 3 H), 6.32 - 6.59 (m, 2 H), 7.70 (d, $J = 9.0$ Hz, 1 H), 8.05 (d, $J = 3.7$ Hz, 1 H), 8.83 (s, 1 H), 9.62 - 13.01 (m, 2 H), 12.14 - 12.43 (m, 2 H).

^{13}C NMR (126 MHz, $\text{DMSO-}d_6$) δ ppm 55.56, 98.97, 108.29, 113.54, 123.00, 126.99, 142.39, 145.58, 146.48, 151.39, 154.22, 156.22, 159.58, 161.25.

7.2.24. Synthesis of 2-[4,6-bis(2,4,6-trihydroxyphenyl)-1,3,5-triazin-2-yl]benzene-1,3,5-triol (N0256-30-1):



To a 1:4 solution of dichloromethane and diethyl ether (5mL) was added 2,4,6-trichloro-1,3,5-triazine (100.0mg, 0.540mmol) and benzene-1,3,5-triol (68.39mg, 0.540mmol). After the compounds were dissolved at room temperature, the solution was cooled to 0°C. Anhydrous aluminium chloride (73.94mg, 0.540mmol) was then added to the stirring solution in three portions over a course of 10 minutes. The reaction was then quickly heated to reflux and the reaction was left to stir overnight (~20 h). The solvent of the reaction was then removed in vacuo and the solid resuspended in 10mL of 10% aqueous HCl solution. The colloidal solution was transferred to a 15mL centrifuge tube and was spun at 3400 rpm for 5 min. The supernatant was removed and the pellet was resuspended and spun at 3400 rpm for 5 min. twice with distilled water (10mL). The pellet was finally resuspended in 10mL diethyl ether to ensure any remaining

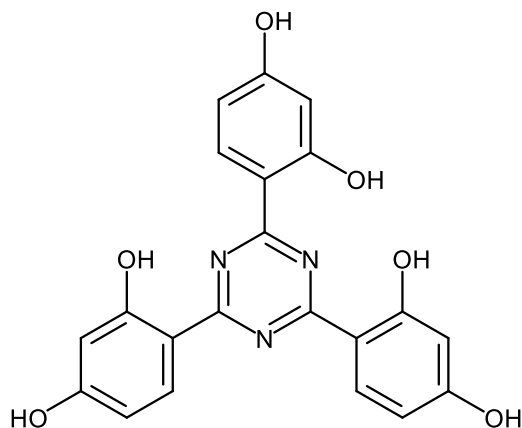
phloroglucinol from the reaction would be removed. After spinning the sample again at 3400 rpm for 5 min., the pellet was dissolved with ethanol and concentrated in vacuo to afford the target compound 2-[4,6-bis(2,4,6-trihydroxyphenyl)-1,3,5-triazin-2-yl]benzene-1,3,5-triol (88mg, 0.194mmol, 35.8% yield) as an orange-red solid.

LC-MS: $m/z = 454.17 [M+H]^+$, 0.67 min.

^1H NMR (500 MHz, $\text{DMSO-}d_6$) δ 5.88 (s, 6 H), 9.15 - 11.03 (m, 3 H), 12.25 (br s, 6 H).

^{13}C NMR (126 MHz, $\text{DMSO-}d_6$) δ ppm 95.14x3, 98.57x3, 163.19x6, 163.24x6, 166.41x3.

7.2.25. Synthesis of 4-[4,6-bis(2,4-dihydroxyphenyl)-1,3,5-triazin-2-yl]benzene-1,3-diol (N0256-01-1):



To 4mL of dry dichloroethane was added 2,4,6-trichloro-1,3,5-triazine (100.0mg, 0.540 mmol) and benzene-1,3-diol (180.0mg, 1.63mmol). The solution was heated to 70°C for 10 minutes to allow the solids to dissolve. The reaction was then cooled to 0°C and anhydrous aluminium chloride (216.0mg, 1.58mmol) was added to the stirring solution in three portions over a course of 10 min. The solution was then heated to 60°C for 6 h. After the solution was cooled to room temperature, the solvent was removed in vacuo. The solid was then resuspended in 10mL distilled water, transferred to a 15mL centrifuge tube and was spun at 3400 rpm for 5 min. The supernatant was removed and the pellet was resuspended with distilled water and spun at 3400 rpm for 5 min. The pellet was finally resuspended in 10mL diethyl ether to ensure no resorcinol remained. The pellet was then dissolved in ethanol and concentrated in vacuo to afford the target

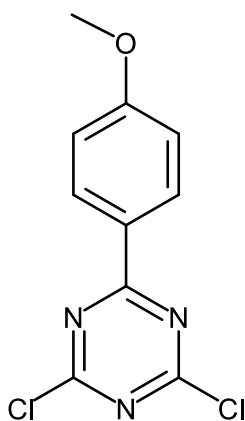
compound 4-[4,6-bis(2,4-dihydroxyphenyl)-1,3,5-triazin-2-yl]benzene-1,3-diol (19mg, 0.047mmol, 8.644% yield).

LC-MS: $m/z = 406.16 [M+H]^+$, 1.09 min.

^1H NMR (400 MHz, $\text{DMSO-}d_6$) δ 12.84 (s, 3H), 10.45 (s, 3H), 8.15 (d, $J = 8.9$ Hz, 3H), 6.51 (dd, $J = 8.9, 2.4$ Hz, 3H), 6.40 (d, $J = 2.3$ Hz, 3H).

^{13}C NMR (101 MHz, $\text{DMSO-}d_6$) δ ppm 168.01x3, 160.33x3, 158.49x3, 131.57x3, 109.92x3, 108.47x3, 105.61x3.

7.2.27. Synthesis of 2,4-dichloro-6-(4-methoxyphenyl)-1,3,5-triazine (N0256-31-1):



2,4,6-Trichloro-1,3,5-triazine (554.0mg, 3mmol), methoxybenzene (324.87mg, 3mmol) and resorcinol (36.39mg, 0.33mmol) were slowly added under atmospheric pressure to a methylene chloride solution (5mL) containing aluminium chloride (409mg, 3mmol). After the addition was complete the mixture was stirred for 18 h at room temperature. The solvent was then removed by evaporation and water was added to the residue to hydrolyse the aluminium chloride. The solid was filtered off and washed with water until neutral. Recrystallisation of the filter cake from tetrahydrofuran gave the pure product 2,4-dichloro-6-(4-methoxyphenyl)-1,3,5-triazine (228 mg, 0.890mmol, 29.64% yield).

LC-MS: $m/z = 238.09 [M+H-Cl]^+$, 0.77 min.

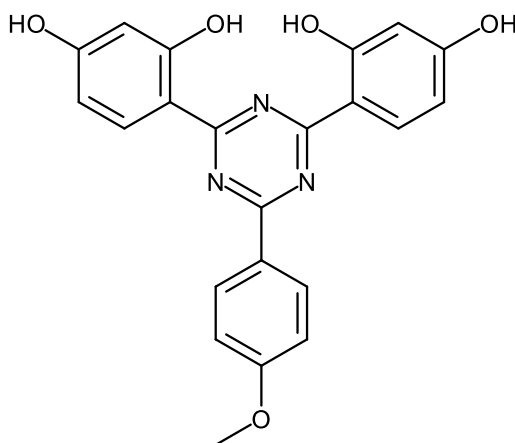
^1H NMR (400 MHz, Chloroform- d) δ 8.48 (d, $J = 9.1$ Hz, 2H), 7.01 (d, $J = 9.0$ Hz, 2H), 3.92 (s, 3H).

7.2.28.

Synthesis

of

4-[4-(2,4-dihydroxyphenyl)-6-(4-methoxyphenyl)-1,3,5-triazin-2-yl]benzene-1,3-diol
(N0256-34-1):



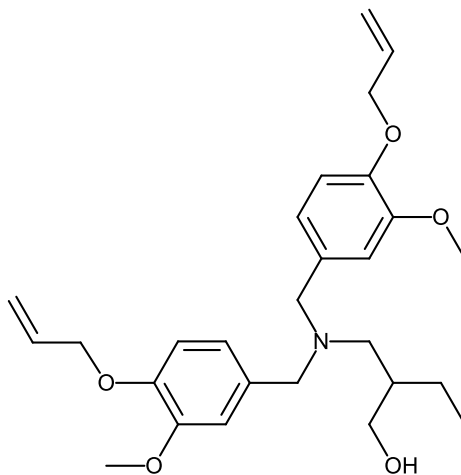
A mixture of 2,4-dichloro-6-(4-methoxyphenyl)-1,3,5-triazine (228.0mg, 0.890mmol) and resorcinol (215.67mg, 1.96mmol) in chlorobenzene (5mL) was heated at 40°C with stirring. At 40°C anhydrous aluminium chloride (267.09mg, 1.96mmol) was slowly introduced. The reaction mixture was stirred at 45°-50°C for about 3.5 h until the evolution of HCl finished. The chlorobenzene was removed from the reaction mixture. The residue was purified by silica gel chromatography (from 100% Cy+0.1% formic acid to 50/50 Cy+0.1% formic acid/AcOEt+0.1% formic acid) to afford the target compound 4-[4-(2,4-dihydroxyphenyl)-6-(4-methoxyphenyl)-1,3,5-triazin-2-yl]benzene-1,3-diol (17mg, 0.042mmol, 4.733% yield).

LC-MS: $m/z = 404.21$ [M+H]⁺, 1.28 min.

¹H NMR (400 MHz, Chloroform-d) δ 8.26 (d, J= 8.0 Hz, 2H), 7.16 (d, J= 8.0, 2H), 6.51 (d, J=4.0 Hz, 2H), 6.49 (s, 2H), 6.35 (d, J= 4.0 Hz, 2H), 3.88 (s, 3H), 3.92 (s, 3H).

¹³C NMR (101 MHz, DMSO-d₆) 161.08, 156.56, 151.54, 150.24, 148.15, 147.06, 142.19, 139.29, 124.52, 120.4, 118.15, 117.88, 113.39, 87.65, 85.24, 72.36, 70.25, 60.87

7.2.29. Synthesis of 2-[[bis({[3-methoxy-4-(prop-2-en-1-yloxy)phenyl]methyl})amino]methyl]butan-1-ol (N0256-35-2):



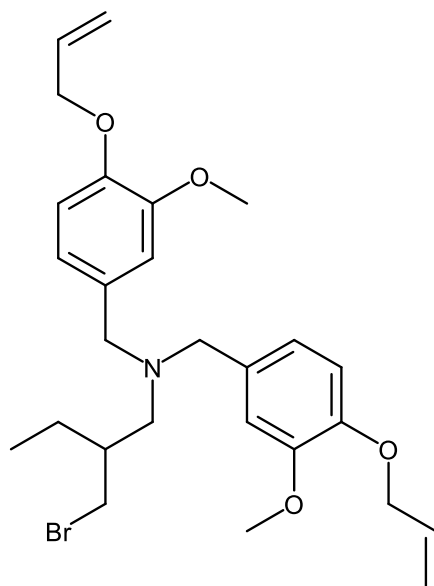
3-Methoxy-4-prop-2-enoxybenzaldehyde (570.07mg, 2.97mmol) and 2-(aminomethyl)butan-1-ol (101.99mg, 0.990mmol) in the presence of acetic acid (0.36mL, 6.33mmol) and sodium triacetoxyborohydride (1508.62mg, 7.12mmol) in 1,4-dioxane (3mL) were stirred overnight at room temperature. Then the solvent was removed under vacuum and the crude was purified by C-18 chromatography to afford the target compound 2-[[bis({[3-methoxy-4-(prop-2-en-1-yloxy)phenyl]methyl})amino]methyl]butan-1-ol (256mg, 0.562mmol, 56.84% yield).

LC-MS: $m/z = 456.41$ $[M+H]^+$, 0.76 min.

$^1\text{H NMR}$ (400 MHz, Chloroform- d) δ 6.90 – 6.73 (m, 6H), 6.08 (ddt, $J = 17.3, 10.7, 5.4$ Hz, 2H), 5.96 (s, 1H), 5.40 (dq, $J = 17.3, 1.6$ Hz, 2H), 5.28 (dq, $J = 10.5, 1.4$ Hz, 2H), 4.60 (dt, $J = 5.5, 1.5$ Hz, 4H), 3.97 (d, $J = 13.1$ Hz, 2H), 3.87 (s, 6H), 3.70 (dt, $J = 10.3, 3.0$ Hz, 1H), 3.25 (t, $J = 10.1$ Hz, 1H), 3.04 (d, $J = 13.1$ Hz, 2H), 2.52 (dd, $J = 12.6, 11.3$ Hz, 1H), 2.46 – 2.35 (m, 1H), 2.03 – 1.91 (m, 1H), 1.03 (q, $J = 7.1$ Hz, 2H), 0.88 (t, $J = 7.4$ Hz, 3H).

7.2.30. Synthesis of [2-(bromomethyl)butyl]bis({[3-methoxy-4-(prop-2-en-1-

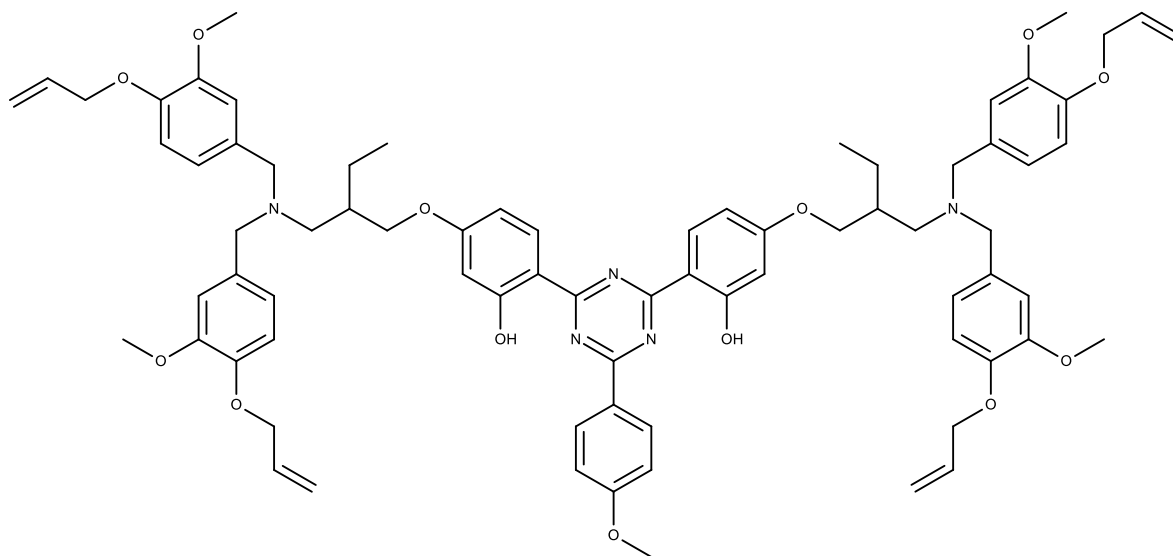
ylxy)phenyl]methyl})amine (N0256-37-1):



To a solution of 2-[[bis({[3-methoxy-4-(prop-2-en-1-yloxy)phenyl]methyl})amino]methyl]butan-1-ol (128.0mg, 0.280mmol) and tetrabromomethane (0.04mL, 0.370mmol) in DCM (3mL) was slowly added triphenylphosphine (110.54mg, 0.420mmol) at 0°C, then the temperature was raised at room temperature. After 2 hours the solvent was evaporated to afford crude target product that was used directly in the next step. [2-(bromomethyl)butyl]bis({[3-methoxy-4-(prop-2-en-1-yloxy)phenyl]methyl})amine (80mg, 0.154mmol, 54.92% yield).

LC-MS: $m/z = 518.34$ and 520.36 $[M+H]^+$, 0.92 min.

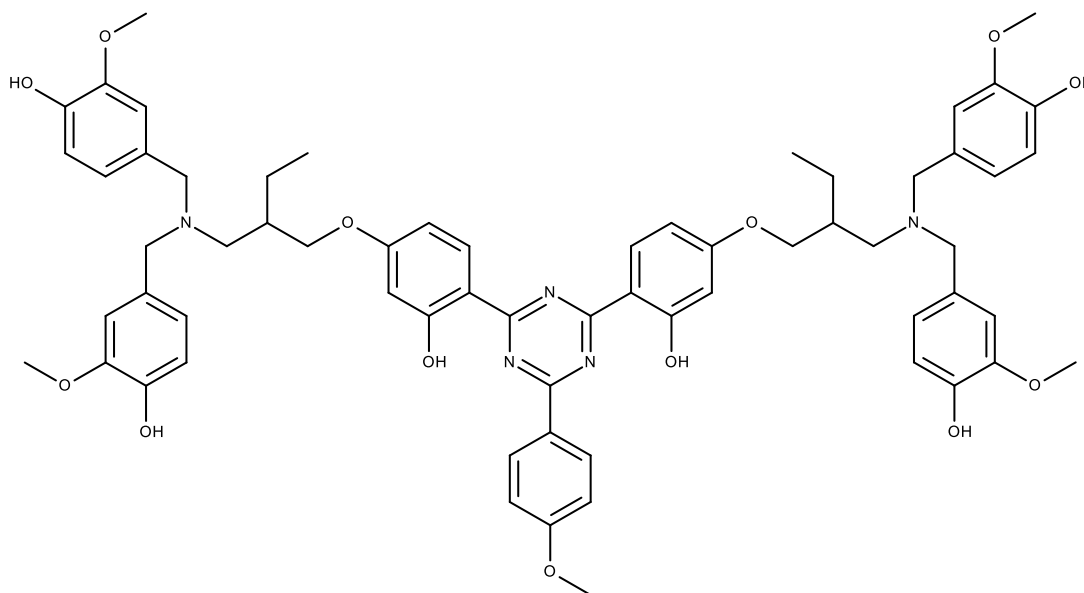
7.2.31. Synthesis of 5-(2-[[bis([3-methoxy-4-(prop-2-en-1-yloxy)phenyl)methyl]amino]methyl]butoxy)-2-[4-[4-(2-[[bis([3-methoxy-4-(prop-2-en-1-yloxy)phenyl)methyl]amino]methyl]butoxy)-2-hydroxyphenyl]-6-(4-methoxyphenyl)-1,3,5-triazin-2-yl]phenol (N0256-38-1):



A mixture of 4-[4-(2,4-dihydroxyphenyl)-6-(4-methoxyphenyl)-1,3,5-triazin-2-yl]benzene-1,3-diol (17.0mg, 0.040mmol) and potassium carbonate (11.65mg, 0.080mmol) in DMF (0.500mL) was heated to 80°C with stirring. 2-(Bromomethyl)-N,N-bis[(3-methoxy-4-prop-2-enoxyphenyl)methyl]butan-1-amine (52.44mg, 0.100mmol) dissolved in DMF (0.50mL), was slowly added dropwise over 30 minutes. After the addition was complete, stirring at 80°C was continued for 1 h. Ice water and ethyl acetate were added and the organic phase was separated, washed with brine and dried over sodium sulfate and then evaporated to afford crude target product that was used directly in the next step. 5-(2-[[bis([3-methoxy-4-(prop-2-en-1-yloxy)phenyl)methyl]amino]methyl]butoxy)-2-[4-[4-(2-[[bis([3-methoxy-4-(prop-2-en-1-yloxy)phenyl)methyl]amino]methyl]butoxy)-2-hydroxyphenyl]-6-(4-methoxyphenyl)-1,3,5-triazin-2-yl]phenol (78 mg, 0.061 mmol).

LC-MS: m/z = 1278.78 [M+H]⁺, 1.20 min.

7.2.32. Synthesis of 5-[2-({bis[(4-hydroxy-3-methoxyphenyl)methyl]amino}methyl)butoxy]-2-(4-{4-[2-({bis[(4-hydroxy-3-methoxyphenyl)methyl]amino}methyl)butoxy]-2-hydroxyphenyl}-6-(4-methoxyphenyl)-1,3,5-triazin-2-yl}phenol (N0256-39-1):



To a stirred solution of 5-(2-({bis({[3-methoxy-4-(prop-2-en-1-yloxy)phenyl]methyl})amino]methyl}butoxy)-2-({4-[4-(2-({bis({[3-methoxy-4-(prop-2-en-1-yloxy)phenyl]methyl})amino]methyl}butoxy)-2-hydroxyphenyl]-6-(4-methoxyphenyl)-1,3,5-triazin-2-yl}phenol (50.0mg, 0.040mmol) in anhydrous methanol was added a catalytic amount of tetrakis(triphenylphosphine)palladium(0) (13.56mg, 0.010mmol) under a nitrogen atmosphere. The solution was stirred for 5 min., and potassium carbonate (64.86mg, 0.470mmol) was added. The reaction was run overnight. Volatiles were removed under vacuum and the residue was treated with 1M aqueous citric acid solution. The aqueous phase was extracted with CH₂Cl₂. The combined organic layers were dried over Na₂SO₄, filtered, concentrated and purified by preparative HPLC (Liquid Chromatography-Mass Spectrometry Method A) to afford the target compound 5-[2-({bis[(4-hydroxy-3-methoxyphenyl)methyl]amino}methyl)butoxy]-2-(4-{4-[2-({bis[(4-hydroxy-3-methoxyphenyl)methyl]amino}methyl)butoxy]-2-hydroxyphenyl}-6-(4-methoxyphenyl)-1,3,5-triazin-2-yl}phenol (5 mg, 0.004 mmol, 11.43% yield).

LC-MS: $m/z = 1118.0 [M+H]^+$, 1.01 min.

^1H NMR (500 MHz, Methanol- d_4) δ 0.90 (br t, $J = 7.2$ Hz, 6 H), 1.35 - 1.54 (m, 4 H), 1.93 (br s, 2 H), 2.27 - 2.61 (m, 4 H), 3.32 - 3.38 (m, 4 H), 3.51 - 3.65 (m, 4 H), 3.73 - 3.88 (m, 2 H), 3.78 (s, 12 H), 3.85 (s, 3 H), 3.92 - 4.03 (m, 2 H), 6.20 - 6.46 (m, 4 H), 6.67 - 6.81 (m, 8 H), 6.87 - 6.93 (m, 4 H), 6.99 (br d, $J=7.6$ Hz, 2 H), 8.05 - 8.31 (m, 4 H).

^{13}C NMR (101 MHz, DMSO- d_6) δ ppm 147.60, 147.45, 145.20, 130.20, 130.00, 121.20, 114.00, 112.00, 107.90, 101.00, 69.00, 58.50, 54.80, 54.60, 54.30, 37.70, 22.40, 10.20.

7.3 Antibiotic susceptibility testing protocol

7.3.1. Antimicrobial agents preparation

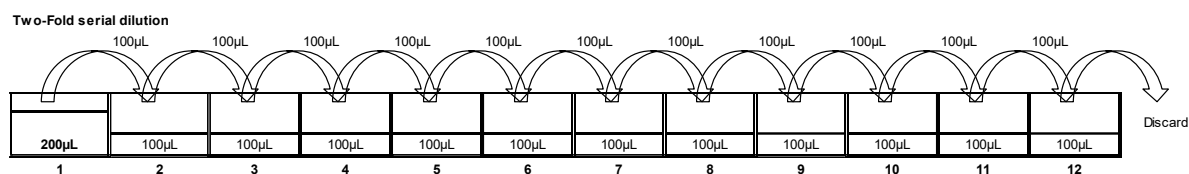
All reference antibiotics were handled according with the Material Safety Data Sheets (MSDS). All the NCEs, which have no MSDS were treated as belonging to Occupational Exposure Band 4 (OEB 4) class.

The compounds stock solutions were prepared at concentrations of at least 1000 µg/ml using the appropriate solvents as indicated in M100S-27th Edition - Table 6A (CLSI).

All the compounds were dissolved at 100X the desired highest concentration in the appropriate solvent.

- Meropenem was dissolved in MilliQ water at 1,600µg/mL to have a final test concentration of 16µg/ml.
- NCEs were dissolved in dimethyl sulfoxide (DMSO) at 12,800µg/ml to have a final test concentration of 128µg/ml.

Twelve serial doubling dilutions were performed (in DMSO) transferring 100 µL of one well to the following one with a multichannel pipette



1µL of each well was transferred into round bottom 96-well plates using Tecan Fluent.

Each plate has growth-control wells and sterility-check wells (100 µL of appropriate solvent).

7.3.2. Medium

The following medium were used:

Cation-adjusted Mueller-Hinton broth (CaMHB) for susceptibility testing of common isolates* (*E. coli*, *K. pneumoniae*, *A. baumannii*, *P.aeruginosa*, *S. aureus*, *E. faecalis*, *S. cerevisiae*)

Cation-adjusted Mueller-Hinton broth (CaMHB) + 2.5% to 5% lysed horse blood (LHB) for Fastidious Organisms (*Streptococcus spp*)

Haemophilus Test Medium (HTM) for *Haemophilus spp*.

*See Appendix C. Conditions for Dilution Antimicrobial Susceptibility Tests, CLSI M7-A11.

7.3.3. Inoculum preparation

The inoculum was prepared by making a direct saline suspension of isolated colonies selected from an 18 to 24 hours agar plates.

The suspension was adjusted to achieve a turbidity equivalent to a 0.5 McFarland turbidity standard (1 to 2 x10⁸ Colony Forming Units (CFU) and diluted 200-fold within 15 minutes in broth.

100 µL of the broth dilution was dispensed in each well plate to have a final concentration in the plate of ~5x10⁵ CFU/mL.

The plates were incubated at 35±2 °C in ambient air for 20 hours.

7.3.4. Determination of MIC End Points

MIC is the lowest concentration of antimicrobial agent that completely inhibits growth of the organism in the microdilution wells as detected by the unaided eye. Viewing devices intended to facilitate reading microdilution tests and recording of results may be used as long as there is no compromise in the ability to discern growth in the well.

Compare the amount of growth in the wells containing the antimicrobial agent with the amount of growth in the growth-control wells used in each set of test when determining the growth end points. For a test to be considered valid, acceptable growth (≥ 2 mm button or define turbidity) must occur in the growth-control well.

The appropriate ATCC strain(s) is/are used in each assay as a quality control to confirm the validity of the results based on the current CLSI breakpoints for each ATCC strain.

7.4 Antioxidant Assays

7.4.1 DPPH (1,1-diphenyl-2-picrylhydrazyl) test

A methanolic solution of DPPH (1.5mL) was added to 0.750mL of test sample solutions (methanol + DMSO) at different concentrations (1, 0.1 mg/mL). The samples were kept in the dark at room temperature. After 30 min, the absorbance values were measured using a Life-Science UV-VIS spectrophotometer (Beckman Coulter™, DU®530, Single Cell Module) at fixed wavelength of 517 nm. A blank sample was prepared adding methanol to a DPPH solution. The percentage of the DPPH radical scavenging is calculated using **Equation 1**.

Equation 1: DPPH radical-scavenging capacity (%) = $[1 - (A_1 - A_2) / A_0] \times 100\%$

Where A_0 was the absorbance of the blank control (without sample), A_1 was the absorbance in the presence of the sample, and A_2 was the absorbance without DPPH.

7.4.2 Ferric Reducing Antioxidant Power (FRAP) assay

FRAP assay is based on the reduction of ferric ions (Fe^{3+}) to ferrous ions (Fe^{2+}) in the presence of TPTZ (2,4,6-tris(2-pyridyl)-s-triazine). This reaction is monitored by measuring the change in absorbance at 593 nm after 10 minutes of incubation in the dark at 37°C. The FRAP analysis reagent was freshly prepared by mixing the following solutions in the reported ratio 10/1/1 (v:v:v): i) 0.1 M pH 3.6 acetate buffer, ii) TPTZ 10 mM in 40 mM HCl, iii) ferric chloride 20 mM.

1.9mL of FRAP reagent was mixed with 0.1mL of sample solution (suitably diluted test article, or solvent when the blank was performed). FRAP values are obtained by comparing the absorbance change at 593 nm in the test sample solution with the absorbance of the blank solution, using a UV-VIS spectrophotometer. Because Trolox was used to effect the calibration curves, the antioxidant activity was expressed in $\mu\text{mol TE/g}$.

7.4.3 Evaluation of filtering parameters of compounds in solution

The absorbance of synthesized compounds was measured between 290-400 nm using a 1 cm quartz cell at intervals of 1 nm using a UV-Vis Spectrophotometer (SHIMADZU UV-2600 240 V). Test compounds were dissolved in dimethylsulfoxide at the concentration of 0.0015 (± 0.0005) % and the absorbance $A(\lambda)$ at wavelength λ is related to the transmittance $T(\lambda)$ by **Equation 2**

$$\text{Equation 2: } A(\lambda) = -\text{Log}[T(\lambda)]$$

Where $T(\lambda)$ is the fraction of incident irradiance transmitted by the sample.

Then, filtering parameters were calculated by applying **Equation 3**, and **Equation 4** described below.

$$\text{Equation 3: } \text{SPF}_{\text{in vitro}} = \frac{\int_{\lambda=290\text{nm}}^{\lambda=400\text{nm}} E(\lambda) \times I(\lambda) \times d\lambda}{\int_{\lambda=290\text{nm}}^{\lambda=400\text{nm}} E(\lambda) \times I(\lambda) \times 10^{-A_0(\lambda)} \times d\lambda}$$

Where $E(\lambda)$ is the erythema action spectrum, $I(\lambda)$ is the spectral irradiance of the UV source, $A_0(\lambda)$ is the monochromatic absorbance of the test sample before UV exposure, and $d\lambda$ is the wavelength step (1 nm).

The wavelength at which the summed absorbance reaches 90% of total absorbance is defined as the critical wavelength (λ_c). Therefore, $T(\lambda)$ were converted into absorbance values $A(\lambda)$ following **Equation 2** and the final Critical Wavelength is:

$$\text{Equation 4: } \int_{290\text{nm}}^{\lambda_c} A\lambda \times d\lambda = 0.9 \int_{290\text{nm}}^{400\text{nm}} A\lambda \times d\lambda$$

Where $A(\lambda)$: monochromatic absorbance calculated from transmittance at wavelength.

7.5 Antiproliferative assay

Cell growth inhibition assays were carried out using the Colo38 human melanoma cell line.⁶⁵ Cell lines were maintained in RPMI 1640, supplemented with 10% fetal bovine serum (FBS), penicillin (100 Units mL^{-1}), streptomycin (100 $\mu\text{g mL}^{-1}$) and glutamine (2 mM) (complete medium). The pH of the medium was 7.2 and the incubation was performed at 37°C in a 5% CO_2 atmosphere. Test compounds were dissolved in 10% MeOH/DMSO to obtain 20mM stock solutions and diluted before cell treatment in 100% MeOH. All the compounds were added at serial dilutions to the cell cultures and incubated for 3 days. Cells were then harvested, suspended in physiological solution, and counted with a Z2 Coulter Counter (Coulter Electronics, Hialeah, FL, USA). The cell number/mL was determined as an IC_{50} after 3 days of culture, when untreated cells are in a log phase of cell growth. Untreated cells were placed in every plate as a negative control.

Acknowledgements

I am most grateful to my supervisor, Professor Manfredini, for his encouragement to start this work and for all his support, kindly guidance, advice, and insightful comments. I want to express my special thanks to my manager Dr. Daniele Andreotti for granting me this possibility and for supporting me in this period. I would like to extend my gratitude to my manager Dr. Colin Philip Leslie, I appreciated his unfailing support and suggestions, and his constructive advice and criticism. His kindness and friendship were, and are, also very precious to me — Thank you!

I want to thank Anna Baldisserotto for her patience and her kind support.

I would like to thank all my colleagues for their support, in particular “Best” for his time, friendly attitude, advice and help in my work. Finally, I am heartily thankful to my family, and especially to my mother for her encouragement and unconditional support. In particular, my dearest thanks are addressed to Stefano for understanding me and my work, and for his love, tireless support and patience.

References

- (1) Gotthardt, I.; Schmutzler, C.; Kirschmeyer, P.; Wuttke, W.; Jarry, H.; Köhrle, J. 4-Methylbenzylidene-Camphor (4MBC) Causes Effects Comparable to Primary Hypothyroidism. *Exp Clin Endocrinol Diabetes* **2007**, *115* (S 1), s-2007-972421. <https://doi.org/10.1055/s-2007-972421>.
- (2) Herzog, B.; Wehrle M.; Quass K. Photostability of UV Absorber Systems in Sunscreens. *Photochem. Photobiol.* **2009**, *85*(4). <https://doi.org/10.1111/j.1751-1097.2009.00544.x>.
- (3) Diffey B. L.; Robson J. A New Substrate to Measure Sunscreen Protection Factors throughout the Ultraviolet Spectrum. *J. Soc Cosmet. Chem.* **1989**, *40*, 127-133.
- (4) Wang, C.; Zhang, J.; Tang, J.; Zou, G. A Sequential Suzuki Coupling Approach to Unsymmetrical Aryl *s*-Triazines from Cyanuric Chloride. *Adv. Synth. Catal.* **2017**, *359* (14), 2514–2519. <https://doi.org/10.1002/adsc.201700260>.
- (5) Wang, C.; Zhang, J.; Tang, J.; Zou, G. A Sequential Suzuki Coupling Approach to Unsymmetrical Aryl *s*-Triazines from Cyanuric Chloride. *Adv. Synth. Catal.* **2017**, *359* (14), 2514–2519. <https://doi.org/10.1002/adsc.201700260>.
- (6) Beck, M. L.; Freihaut, B.; Henry, R.; Pierce, S.; Bayer, W. L. A Serum Haemagglutinating Property Dependent upon Polycarboxyl Groups. *Br. J. Haematol.* **1975**, *29* (1), 149–156. <https://doi.org/10.1111/j.1365-2141.1975.tb01808.x>.
- (7) Mueller, S. O.; Kling, M.; Arifin Firzani, P.; Mecky, A.; Duranti, E.; Shields-Botella, J.; Delansorne, R.; Broschard, T.; Kramer, P.-J. Activation of Estrogen Receptor Alpha and ERbeta by 4-Methylbenzylidene-Camphor in Human and Rat Cells: Comparison with Phyto- and Xenoestrogens. *Toxicol. Lett.* **2003**, *142* (1–2), 89–101. [https://doi.org/10.1016/s0378-4274\(03\)00016-x](https://doi.org/10.1016/s0378-4274(03)00016-x).
- (8) Wang, M.; Li, J.; Rangarajan, M.; Shao, Y.; LaVoie, E. J.; Huang, T.-C.; Ho, C.-T. Antioxidative Phenolic Compounds from Sage (*Salvia Officinalis*). *J. Agric. Food Chem.* **1998**, *46* (12), 4869–4873. <https://doi.org/10.1021/jf980614b>.
- (9) Nohynek, G. J.; Schaefer, H. Benefit and Risk of Organic Ultraviolet Filters. *Regulatory Toxicology and Pharmacology* **2001**, *33* (3), 285–299. <https://doi.org/10.1006/rtp.2001.1476>.
- (10) Addis, P.; Shecterle, L. M.; A. St. Cyr, J. Cellular Protection During Oxidative Stress: A Potential Role for D-Ribose and Antioxidants. *Journal of Dietary Supplements* **2012**, *9* (3), 178–182. <https://doi.org/10.3109/19390211.2012.708715>.
- (11) Brenneisen, P.; Wenk, J.; Klotz, L. O.; Wlaschek, M.; Briviba, K.; Krieg, T.; Sies, H.; Scharffetter-Kochanek, K. Central Role of Ferrous/Ferric Iron in the Ultraviolet B Irradiation-Mediated Signaling Pathway Leading to Increased Interstitial Collagenase (Matrix-Degrading Metalloprotease (MMP)-1) and Stromelysin-1 (MMP-3) mRNA Levels in Cultured Human Dermal Fibroblasts. *J. Biol. Chem.* **1998**, *273* (9), 5279–5287. <https://doi.org/10.1074/jbc.273.9.5279>.
- (12) Brenneisen, P.; Wenk, J.; Klotz, L. O.; Wlaschek, M.; Briviba, K.; Krieg, T.; Sies, H.; Scharffetter-Kochanek, K. Central Role of Ferrous/Ferric Iron in the Ultraviolet B Irradiation-Mediated Signaling Pathway Leading to Increased Interstitial Collagenase (Matrix-Degrading Metalloprotease (MMP)-1) and Stromelysin-1 (MMP-3) mRNA Levels in Cultured Human Dermal Fibroblasts. *J. Biol. Chem.* **1998**, *273* (9), 5279–5287. <https://doi.org/10.1074/jbc.273.9.5279>.
- (13) Haque, T.; Crowther, J. M.; Lane, M. E.; Moore, D. J. Chemical Ultraviolet Absorbers Topically Applied in a Skin Barrier Mimetic Formulation Remain in the Outer Stratum Corneum of Porcine Skin. *International Journal of Pharmaceutics* **2016**, *510* (1), 250–254. <https://doi.org/10.1016/j.ijpharm.2016.06.041>.
- (14) *Clinical Guide to Sunscreens and Photoprotection*.
- (15) Hayakawa, H.; Haraguchi, K.; Tanaka, H.; Miyasaka, T. Direct C-8 Lithiation of Naturally-Occurring Purine Nucleosides. A Simple Method for the Synthesis of 8-Carbon-Substituted Purine Nucleosides. *Chem. Pharm. Bull.* **1987**, *35* (1), 72–79. <https://doi.org/10.1248/cpb.35.72>.
- (16) Xu, G.; Ye, X.; Chen, J.; Liu, D. Effect of Heat Treatment on the Phenolic Compounds and Antioxidant Capacity of Citrus Peel Extract. *J. Agric. Food Chem.* **2007**, *55* (2), 330–335. <https://doi.org/10.1021/jf062517l>.

- (17) Kahn, T.; Bosch, J.; Levitt, M. F.; Goldstein, M. H. Effect of Sodium Nitrate Loading on Electrolyte Transport by the Renal Tubule. *Am. J. Physiol.* **1975**, *229* (3), 746–753. <https://doi.org/10.1152/ajplegacy.1975.229.3.746>.
- (18) Mulani, M. S.; Kamble, E. E.; Kumkar, S. N.; Tawre, M. S.; Pardesi, K. R. Emerging Strategies to Combat ESKAPE Pathogens in the Era of Antimicrobial Resistance: A Review. *Front. Microbiol.* **2019**, *10*, 539. <https://doi.org/10.3389/fmicb.2019.00539>.
- (19) *Houben-Weyl Methods of Organic Chemistry Vol. E 9b/2, 4th Edition Supplement*:
- (20) Jiang, W.-F.; Wang, H.-L.; Li, Z.-Q. Improved Synthesis of 6-(4-Methoxyphenyl)-2,4-Dichloro-1,3,5-Triazine and 2,4-Bis(Resorcinyloxy)-Substituted UV Light Absorbing Derivatives. *J. Chem. Res. (S)* **2008**, *2008* (11), 664–665. <https://doi.org/10.3184/030823408X375142>.
- (21) Lampronti, I.; Martello, D.; Bianchi, N.; Borgatti, M.; Lambertini, E.; Piva, R.; Jabbar, S.; Shahabuddin Kabir Choudhuri, M.; Tareq Hassan Khan, M.; Gambari, R. In Vitro Antiproliferative Effects on Human Tumor Cell Lines of Extracts from the Bangladeshi Medicinal Plant *Aegle Marmelos* Correa. *Phytomedicine* **2003**, *10* (4), 300–308. <https://doi.org/10.1078/094471103322004794>.
- (22) Herzog, B.; Mongiat, S.; Deshayes, C.; Neuhaus, M.; Sommer, K.; Mantler, A. In Vivo and in Vitro Assessment of UVA Protection by Sunscreen Formulations Containing Either Butyl Methoxy Dibenzoyl Methane, Methylene Bis-Benzotriazolyl Tetramethylbutylphenol, or Microfine ZnO. *Int J Cosmet Sci* **2002**, *24* (3), 170–185. <https://doi.org/10.1046/j.1467-2494.2002.00137.x>.
- (23) Demurtas, M.; Baldisserotto, A.; Lampronti, I.; Moi, D.; Balboni, G.; Pacifico, S.; Vertuani, S.; Manfredini, S.; Onnis, V. Indole Derivatives as Multifunctional Drugs: Synthesis and Evaluation of Antioxidant, Photoprotective and Antiproliferative Activity of Indole Hydrazones. *Bioorganic Chemistry* **2019**, *85*, 568–576. <https://doi.org/10.1016/j.bioorg.2019.02.007>.
- (24) Smith, R. J.; Bryant, R. G. Metal Substitutions Incarboxylic Anhydrase: A Halide Ion Probe Study. *Biochem. Biophys. Res. Commun.* **1975**, *66* (4), 1281–1286. [https://doi.org/10.1016/0006-291x\(75\)90498-2](https://doi.org/10.1016/0006-291x(75)90498-2).
- (25) Scipioni, M.; Kay, G.; Megson, I.; Kong Thoo Lin, P. Novel Vanillin Derivatives: Synthesis, Anti-Oxidant, DNA and Cellular Protection Properties. *European Journal of Medicinal Chemistry* **2018**, *143*, 745–754. <https://doi.org/10.1016/j.ejmech.2017.11.072>.
- (26) Novel Vanillin Derivatives: Synthesis, Anti-Oxidant, DNA and Cellular Protection Properties.
- (27) Ouellette, R. J.; Rawn, J. D. Nucleosides, Nucleotides, and Nucleic Acids. In *Organic Chemistry*; Elsevier, 2018; pp 973–1000. <https://doi.org/10.1016/B978-0-12-812838-1.50030-X>.
- (28) Hassner, A.; Stumer, C.; Hassner, A. *Organic Syntheses Based on Name Reactions*, 2nd ed.; Tetrahedron organic chemistry series; Pergamon: Amsterdam ; Boston, 2002.
- (29) Ishizaki, M.; Yamada, M.; Watanabe, S.; Hoshino, O.; Nishitani, K.; Hayashida, M.; Tanaka, A.; Hara, H. Palladium Charcoal-Catalyzed Deprotection of O-Allylphenols. *Tetrahedron* **2004**, *60* (36), 7973–7981. <https://doi.org/10.1016/j.tet.2004.05.097>.
- (30) Martin, J. K.; Luthra, M. G.; Wells, M. A.; Watts, R. P.; Hanahan, D. J. Phospholipase A2 as a Probe of Phospholipid Distribution in Erythrocyte Membranes. Factors Influencing the Apparent Specificity of the Reaction. *Biochemistry* **1975**, *14* (25), 5400–5408. <https://doi.org/10.1021/bi00696a003>.
- (31) Scheele, C. W. (1776). “Examen Chemicum Calculi Urinari” [A Chemical Examination of Kidney Stones]. *Opuscula*. 2: 73. Davies, O.; Mendes, P.;
- (32) Roelandts, R. Shedding Light on Sunscreens. *Clin. Exp. Dermatol.* **1998**, *23* (4), 147–157. <https://doi.org/10.1046/j.1365-2230.1998.00353.x>.
- (33) Fournanier, A.; Moyal, D.; Seit , S. Sunscreens Containing the Broad-Spectrum UVA Absorber, Mexoryl[®] SX, Prevent the Cutaneous Detrimental Effects of UV Exposure: A Review of Clinical Study Results. *Photodermatology, Photoimmunology & Photomedicine* **2008**, *24* (4), 164–174. <https://doi.org/10.1111/j.1600-0781.2008.00365.x>.
- (34) Laufer, S. A.; Domeyer, D. M.; Scior, T. R. F.; Albrecht, W.; Hauser, D. R. J. Synthesis and Biological Testing of Purine Derivatives as Potential ATP-Competitive Kinase Inhibitors. *J. Med. Chem.* **2005**, *48* (3), 710–722. <https://doi.org/10.1021/jm0408767>.
- (35) Conn, G.; Eisler, S. Synthesis and Intramolecular Hydrogen Bonding Networks of 2,4,6-Tri(*o* -Hydroxyaryl)-1,3,5-Triazines. *Org. Lett.* **2011**, *13* (19), 5080–5083. <https://doi.org/10.1021/ol201946f>.

- (36) Butler, R. S.; Cohn, P.; Tenzel, P.; Abboud, K. A.; Castellano, R. K. Synthesis, Photophysical Behavior, and Electronic Structure of Push–Pull Purines. *J. Am. Chem. Soc.* **2009**, *131* (2), 623–633. <https://doi.org/10.1021/ja806348z>.
- (37) Alaqeel, S. I. Synthetic Approaches to Benzimidazoles from O-Phenylenediamine: A Literature Review. *Journal of Saudi Chemical Society* **2017**, *21* (2), 229–237. <https://doi.org/10.1016/j.jscs.2016.08.001>.
- (38) Shaath, N. A. The Chemistry of Ultraviolet Filters. In *Principles and Practice of Photoprotection*; Wang, S. Q., Lim, H. W., Eds.; Springer International Publishing: Cham, 2016; pp 143–157. https://doi.org/10.1007/978-3-319-29382-0_9.
- (39) Rosemeyer, H. The Chemodiversity of Purine as a Constituent of Natural Products. *C&B* **2004**, *1* (3), 361–401. <https://doi.org/10.1002/cbdv.200490033>.
- (40) Benzie, I. F. F.; Strain, J. J. The Ferric Reducing Ability of Plasma (FRAP) as a Measure of “Antioxidant Power”: The FRAP Assay. *Analytical Biochemistry* **1996**, *239* (1), 70–76. <https://doi.org/10.1006/abio.1996.0292>.
- (41) Benzie, I. F. F.; Strain, J. J. The Ferric Reducing Ability of Plasma (FRAP) as a Measure of “Antioxidant Power”: The FRAP Assay. *Analytical Biochemistry* **1996**, *239* (1), 70–76. <https://doi.org/10.1006/abio.1996.0292>.
- (42) González, S.; Fernández-Lorente, M.; Gilaberte-Calzada, Y. The Latest on Skin Photoprotection. *Clin. Dermatol.* **2008**, *26* (6), 614–626. <https://doi.org/10.1016/j.clindermatol.2007.09.010>.
- (43) Imai, K.; Lehmann, H. The Oxygen Affinity of Haemoglobin Tak, a Variant with an Elongated Beta Chain. *Biochim. Biophys. Acta* **1975**, *412* (2), 288–294. [https://doi.org/10.1016/0005-2795\(75\)90043-4](https://doi.org/10.1016/0005-2795(75)90043-4).
- (44) Fischer, E. Ueber das Purin und seine Methylderivate. *Ber. Dtsch. Chem. Ges.* **1898**, *31* (3), 2550–2574. <https://doi.org/10.1002/cber.18980310304>.
- (45) Schwabbauer, M. L. Use of the Latent Image Technique to Develop and Evaluate Problem-Solving Skills. *Am J Med Technol* **1975**, *41* (12), 457–462.
- (46) Nohynek, G. J.; Schaefer, H. Benefit and Risk of Organic Ultraviolet Filters. *Regulatory Toxicology and Pharmacology* **2001**, *33* (3), 285–299. <https://doi.org/10.1006/rtp.2001.1476>.
- (47) Fischer, E. Ueber das Purin und seine Methylderivate. *Ber. Dtsch. Chem. Ges.* **1898**, *31* (3), 2550–2574. <https://doi.org/10.1002/cber.18980310304>.
- (48) Scheele, C. W. (1776). “Examen Chemicum Calculi Urinari” [A Chemical Examination of Kidney Stones]. *Opuscula*. 2: 73. Davies, O.; Mendes, P.
- (49) *Houben-Weyl Methods of Organic Chemistry Vol. E 9b/2, 4th Edition Supplement*:
- (50) Hassner, A.; Stumer, C.; Hassner, A. *Organic Syntheses Based on Name Reactions*, 2nd ed.; Tetrahedron organic chemistry series; Pergamon: Amsterdam ; Boston, 2002.
- (51) Ouellette, R. J.; Rawn, J. D. Nucleosides, Nucleotides, and Nucleic Acids. In *Organic Chemistry*; Elsevier, 2018; pp 973–1000. <https://doi.org/10.1016/B978-0-12-812838-1.50030-X>.
- (52) Laufer, S. A.; Domeyer, D. M.; Scior, T. R. F.; Albrecht, W.; Hauser, D. R. J. Synthesis and Biological Testing of Purine Derivatives as Potential ATP-Competitive Kinase Inhibitors. *J. Med. Chem.* **2005**, *48* (3), 710–722. <https://doi.org/10.1021/jm0408767>.
- (53) Alaqeel, S. I. Synthetic Approaches to Benzimidazoles from O-Phenylenediamine: A Literature Review. *Journal of Saudi Chemical Society* **2017**, *21* (2), 229–237. <https://doi.org/10.1016/j.jscs.2016.08.001>.
- (54) Butler, R. S.; Cohn, P.; Tenzel, P.; Abboud, K. A.; Castellano, R. K. Synthesis, Photophysical Behavior, and Electronic Structure of Push–Pull Purines. *J. Am. Chem. Soc.* **2009**, *131* (2), 623–633. <https://doi.org/10.1021/ja806348z>.
- (55) Conn, G.; Eisler, S. Synthesis and Intramolecular Hydrogen Bonding Networks of 2,4,6-Tri(*o* - Hydroxyaryl)-1,3,5-Triazines. *Org. Lett.* **2011**, *13* (19), 5080–5083. <https://doi.org/10.1021/ol201946f>.

- (56) Scipioni, M.; Kay, G.; Megson, I.; Kong Thoo Lin, P. Novel Vanillin Derivatives: Synthesis, Anti-Oxidant, DNA and Cellular Protection Properties. *European Journal of Medicinal Chemistry* **2018**, *143*, 745–754. <https://doi.org/10.1016/j.ejmech.2017.11.072>.
- (57) Lin, J.-Y.; Selim, M. A.; Shea, C. R.; Grichnik, J. M.; Omar, M. M.; Monteiro-Riviere, N. A.; Pinnell, S. R. UV Photoprotection by Combination Topical Antioxidants Vitamin C and Vitamin E. *Journal of the American Academy of Dermatology* **2003**, *48* (6), 866–874. <https://doi.org/10.1067/mjd.2003.425>.
- (58) Wang, C.; Zhang, J.; Tang, J.; Zou, G. A Sequential Suzuki Coupling Approach to Unsymmetrical Aryl s-Triazines from Cyanuric Chloride. *Adv. Synth. Catal.* **2017**, *359* (14), 2514–2519. <https://doi.org/10.1002/adsc.201700260>.
- (59) Jiang, W.-F.; Wang, H.-L.; Li, Z.-Q. Improved Synthesis of 6-(4-Methoxyphenyl)-2,4-Dichloro-1,3,5-Triazine and 2,4-Bis(Resorcinyloxy)-Substituted UV Light Absorbing Derivatives. *J. Chem. Res. (S)* **2008**, *2008* (11), 664–665. <https://doi.org/10.3184/030823408X375142>.
- (60) Benzie, I. F. F.; Strain, J. J. The Ferric Reducing Ability of Plasma (FRAP) as a Measure of “Antioxidant Power”: The FRAP Assay. *Analytical Biochemistry* **1996**, *239* (1), 70–76. <https://doi.org/10.1006/abio.1996.0292>.
- (61) Xu, G.; Ye, X.; Chen, J.; Liu, D. Effect of Heat Treatment on the Phenolic Compounds and Antioxidant Capacity of Citrus Peel Extract. *J. Agric. Food Chem.* **2007**, *55* (2), 330–335. <https://doi.org/10.1021/jf062517l>.
- (62) Demurtas, M.; Baldisserotto, A.; Lampronti, I.; Moi, D.; Balboni, G.; Pacifico, S.; Vertuani, S.; Manfredini, S.; Onnis, V. Indole Derivatives as Multifunctional Drugs: Synthesis and Evaluation of Antioxidant, Photoprotective and Antiproliferative Activity of Indole Hydrazones. *Bioorganic Chemistry* **2019**, *85*, 568–576. <https://doi.org/10.1016/j.bioorg.2019.02.007>.
- (63) Addis, P.; Shechterle, L. M.; A. St. Cyr, J. Cellular Protection During Oxidative Stress: A Potential Role for D-Ribose and Antioxidants. *Journal of Dietary Supplements* **2012**, *9* (3), 178–182. <https://doi.org/10.3109/19390211.2012.708715>.
- (64) Mulani, M. S.; Kamble, E. E.; Kumkar, S. N.; Tawre, M. S.; Pardesi, K. R. Emerging Strategies to Combat ESKAPE Pathogens in the Era of Antimicrobial Resistance: A Review. *Front. Microbiol.* **2019**, *10*, 539. <https://doi.org/10.3389/fmicb.2019.00539>.
- (65) Lampronti, I.; Martello, D.; Bianchi, N.; Borgatti, M.; Lambertini, E.; Piva, R.; Jabbar, S.; Shahabuddin Kabir Choudhuri, M.; Tareq Hassan Khan, M.; Gambari, R. In Vitro Antiproliferative Effects on Human Tumor Cell Lines of Extracts from the Bangladeshi Medicinal Plant *Aegle Marmelos* Correa. *Phytomedicine* **2003**, *10* (4), 300–308. <https://doi.org/10.1078/094471103322004794>.
- (66) Valdes F.; Brown N.; Morales-Bayuelo A.; Prent-Peñaloza L.; Gutierrez M. Adenosine Derivates as Antioxidant Agents: Synthesis, Characterization, in Vitro Activity, and Theoretical Insights. *Antioxidants* **2019**, *8*(10), 468. <https://doi.org/10.3390/antiox8100468>